UNIVERSITÀ
DEGLI STUDI
DI PADOVA

Sede Amministrativa: Università degli Studi di Padova

Dipartimento di Medicina Molecolare

SCUOLA DI DOTTORATO DI RICERCA IN BIOMEDICINA

INDIRIZZO: MEDICINA MOLECOLARE

CICLO XXVIII

Crosstalk between YAP/TAZ and Cellular Metabolism

Direttore della Scuola: Ch.mo Prof. Stefano Piccolo

Coordinatore d'indirizzo: Ch.mo Prof. Giorgio Palù

Supervisore: Ch.mo Prof. Stefano Piccolo

Co-tutore: Ch.mo Prof. Sirio Dupont

Dottoranda: Dott.ssa Giulia Santinon

Index

PART II

Exploring the link between YAP/TAZ and nucleotide metabolism in oncogene-induced senescence

Summary

The Warburg effect, the metabolic reprogramming of cancer cell toward aerobic glycolysis, occurs as a consequence of transformation carried out by several oncogenes. Aerobic glycolysis represents a metabolism particularly suited for cell growth, because it couples energy production to availability of chemical precursors for the biosynthesis of the main macromolecules (dNTPs, aminoacids and lipids). Metabolic reprogramming is usually considered as a simple phenotypic endpoint that occurs as a consequence of tumor formation. Growing evidences indicate, however, that metabolism on its turn can support oncogenic signaling to foster tumor malignancy. During my PhD, I studied how glucose metabolism regulates gene transcription, and found an unexpected link with YAP/TAZ, key transcription co-factors regulating organ growth, tumor cell proliferation and aggressiveness. Glucose metabolism and a sustained flux of glucose through aerobic glycolysis support YAP/TAZ transcriptional activity, whereas treatments that reprogram cellular metabolism away from aerobic glycolysis induce corresponding reductions in YAP/TAZ activity. Accordingly, glycolysis is required to sustain YAP/TAZ pro-tumorigenic functions: inhibition of glucose metabolism, or knockdown of key enzymes of glycolysis, hampers YAP/TAZ-induced tumorigenic phenotypes in breast cancer cells, such as proliferation, clonogenic activity and self-renewal properties. In addition, YAP/TAZ are required for the full deployment of glucose growth-promoting activity, in keeping with the idea of oncogenic signaling at the service of a metabolic pathway. Mechanistically we found that Phosphofructokinase 1 (PFK1), the enzyme regulating the first committed step of glycolysis, binds the YAP/TAZ transcriptional co-factors TEADs and promote their functional and biochemical cooperation with YAP/TAZ. Strikingly, this regulation is conserved in *Drosophila*, where phosphofructokinase is required for tissue overgrowth promoted by Yki, the fly homologue of YAP/TAZ. Moreover, gene expression regulated by glucose metabolism in breast cancer cells is strongly associated in a large dataset of primary human mammary tumors with YAP/TAZ activation and with the progression toward more advanced and malignant stages. These findings

suggest that aerobic glycolysis endows cancer cells with particular metabolic properties and, at the same time, sustains transcription factors with potent pro-tumorigenic activities such as YAP/TAZ. These results were published in[1] and reviewed in[2,3].

This study highlighted the notion that YAP/TAZ are atypical oncogenic molecules that, rather than being activated by genetic events, lay downstream of metabolic reprogramming. However, which are the genes and cellular mechanisms by which YAP/TAZ sustain cell proliferation remains largely unknown. Recently, extensive gene expression profiling of cancer cells indicate that YAP/TAZ regulate a series of genes and programs linked to cell-cycle regulation, including genes involved in nucleotide metabolism. During the third year of my PhD, I have explored whether YAP/TAZ sustain nucleotide metabolism, and whether this is relevant in the context of oncogene-induced senescence (OIS) and cancer cell proliferation. Preliminary data suggest an important role of nucleotide metabolism downstream of YAP/TAZ for the control of cell proliferation and resistance to cellular senescence.

Summary (Italian version)

L'effetto Warburg, ovvero la riprogrammazione del metabolismo di cellule tumorali verso la glicolisi aerobia, si instaura come conseguenza della trasformazione oncogenica. La glicolisi aerobia rappresenta un tipo di metabolismo particolarmente appropriato per la crescita delle cellule, perché accoppia la produzione di energia alla disponibilità di precursori chimici per la biosintesi delle principali macromolecole (dNTP, aminoacidi e lipidi). La riprogrammazione del metabolismo viene spesso considerata come una semplice conseguenza fenotipica della formazione del tumore. Tuttavia, evidenze crescenti indicano che variazioni nel metabolismo possono esse stesse supportare la segnalazione oncogenica e favorire la malignità tumorale. Durante il mio dottorato, ho indagato come il metabolismo del glucosio regolasse la trascrizione genica, portando alla luce un collegamento inaspettato tra il metabolismo del glucosio e YAP/TAZ, co-fattori trascrizionali chiave per regolare la crescita degli organi, la proliferazione cellulare maligna e l'aggressività dei tumori. Il metabolismo del glucosio e il suo flusso sostenuto attraverso la glicolisi aerobia supportano l'attività trascrizionale di YAP/TAZ, mentre trattamenti che riprogrammano il metabolismo cellulare, riducendo la glicolisi aerobia, inducono una corrispondente riduzione della loro attività. In accordo con i precedenti risultati, la glicolisi è richiesta per sostenere le funzioni pro-tumorigeniche di YAP/TAZ: l'inibizione del metabolismo del glucosio, o la soppressione dell'espressione di enzimi chiave della glicolisi, ostacola fenotipi tumorigenici indotti da YAP/TAZ, tra i quali la proliferazione, l'attività clonogenica e le proprietà di auto-rinnovamento di cellule del cancro al seno. Inoltre, YAP/TAZ sono richiesti affinchè il glucosio promuova a pieno la crescita cellulare, nell'idea di una segnalazione oncogenica al servizio del metabolismo. A livello del meccanismo molecolare, abbiamo scoperto che l'enzima fosfofruttochinasi 1 (PFK1), che regola la prima vera reazione della glicolisi, lega i TEAD, co-fattori trascrizionali di YAP/TAZ, promuovendo così la loro cooperazione funzionale e biochimica con YAP/TAZ. Sorprendentemente, questa regolazione è conservata anche in *Drosophila*, dove la fosfofruttochinasi è richiesta per la crescita abnorme

dei tessuti promossa da Yki, omologo di YAP/TAZ nel moscerino. Inoltre, nelle cellule del cancro al seno, l'espressione genica regolata dal metabolismo del glucosio è fortemente associata all'attivazione di YAP/TAZ e ad una progressione tumorale maligna avanzata. Queste osservazioni suggeriscono che la glicolisi aerobia fornisca particolari proprietà metaboliche alle cellule cangerogene e, allo stesso tempo, sostenga fattori di trascrizione che hanno una potente attività tumorigenica, come YAP/TAZ. Questi dati sono stati pubblicati in[1] e riesaminati in[2,3].

Questo studio sottolinea come YAP/TAZ siano oncoproteine atipiche in quanto, invece di essere attivate da eventi genetici, si collocano a valle di una riprogrammazione del metabolismo. Rimane ancora tuttavia oscuro quali siano i geni e i meccanismi cellulari tramite i quali YAP/TAZ sostengano la proliferazione cellulare. Recentemente, profili di espressione genica, effettuati estensivamente su cellule tumorali, hanno evidenziato che YAP/TAZ regolano un insieme di geni e programmi collegati con la regolazione del ciclo cellulare, inclusi geni coinvolti nel metabolismo dei nucleotidi. Durante il terzo anno del mio dottorato, ho analizzato se YAP/TAZ sostenessero il metabolismo dei nucleotidi, e se questo fosse rilevante nel contesto della senescenza indotta da oncogeni (OIS) e della proliferazione delle cellule tumorali. Dati preliminari suggeriscono un ruolo significativo del metabolismo dei nucleotidi a valle di YAP/TAZ, sia nel controllo della proliferazione che nella resistenza alla senescenza cellulare.

Publications

Elena Enzo*, Giulia Santinon*, Arianna Pocaterra, Mariaceleste Aragona, Silvia Bresolin, Mattia Forcato, Daniela Grifoni, Annalisa Pession, Francesca Zanconato, Giulia Guzzo, Silvio Bicciato, Sirio Dupont. **Aerobic glycolysis tunes YAP/TAZ transcriptional activity.** *EMBO J* 2015 vol. 34 (10), pp. 1349-1370

*: co-first author

Giulia Santinon, Elena Enzo, Sirio Dupont. **The sweet side of YAP/TAZ.** *Cell Cycle* 2015 vol. 14 (16), pp. 2543-2544

Giulia Santinon, Arianna Pocaterra, Dupont Sirio. **Control of YAP/TAZ Activity by Metabolic and Nutrient-Sensing Pathways.** *Trends in Cell Biology* 2015, doi:10.1016/j.tcb.2015.11.004

PART I

Aerobic glycolysis tunes YAP/TAZ transcriptional activity

Introduction

GLUCOSE METABOLISM

Glucose is an essential source of energy and carbon building blocks for animal cells, both considering the cellular and systemic levels. Once it enters in the cell through dedicated transporters, glucose is entrapped in the form of glucose-6-phosphate (G6P) by hexokinase enzymes and primed for subsequent metabolic reactions: G6P can be metabolized through glycolysis and the Pentose Phosphate Pathway (PPP), or it can be stored as glycogen. If glucose is directed to catabolic processes, it can be used either to generate the ribose for nucleotide synthesis and reducing equivalents, through the PPP, or to generate chemical energy and other metabolic intermediates through glycolysis. These glycolytic intermediates provide a carbon source to a number of different anabolic processes, including the Hexosamine Biosynthetic Pathway (HBP), providing precursors for protein glycosylation, aminoacid and lipid precursors. Furthermore, glucose also significantly contributes to fuel the tricarboxylic acid (TCA) cycle and mitochondrial respiration, thereby ensuring the continuous and efficient production of energy in the form of ATP. Glucose and its derivatives are thus partitioned into several biosynthetic pathways, representing one main source of energy and, at the same time, providing essential chemical precursors for the biosynthesis of the main macromolecules required to build a cell. Indeed the regulation of glucose uptake and of its intracellular fate is crucial for cell physiology[4].

GLYCOLYSIS

Glycolysis is a set of metabolic reactions that convert glucose to pyruvate and represents a major entry pathway for carbon atoms into cell metabolism. Glycolysis transforms glucose into chemicals that can be used either as precursors for anabolic processes (see above) and/or to sustain energy production, either

directly during glycolysis or by fuelling oxidative phosphorylation and mitochondrial respiration[4].

The sequence of biochemical reactions can be divided in two major phases: (1) an energy requirement step (consuming two molecules of ATP per glucose molecule) and (2) an energy production step (producing four ATPs per glucose). During the first phase, hexokinase (HK) enzymes phosphorylate glucose, thus entrapping G6P in the cell. G6P is then converted into fructose-6-phosphate (F6P) by phosphoglucose isomerase (GPI). The isomerization step is followed by a second energy-consuming reaction catalysed by phosphofructokinase 1 (PFK1), which converts F6P in fructose-1-6-bisphosphate (F1,6BP). Since G6P and F6P can be redirected to other metabolic processes, like the PPP and the HBP, the reaction carried out by PFK1 is the first truly dedicated step of glycolysis. Given its "gatekeeper" role, PFK1 is one of the most tightly regulated enzymes of glycolysis, being allosterically regulated by metabolites of glycolysis, of the TCA cycle and by the AMP/ATP ratio[5].

F1,6BP is then broken by fructose bisphosphate aldolase enzyme into two three-carbon molecules: dihydroxyacetone phosphate (DHAP) and glyceraldehyde-3-phosphate (G3P); DHAP is rapidly converted into G3P, which fuels the remaining reactions of glycolysis. So, two G3P molecules are produced per glucose, with the net consumption of two ATPs.

During the second phase of glycolysis, G3P is converted to 1,3-bisphosphoglycerate (1,3BPG) by glyceraldehyde 3-phosphate dehydrogenase to allow the production of a higher energy molecule. The reaction requires the reduction of NAD^+ to NADH. In the last steps, two molecules of ATP are produced: one derives from the conversion of 1,3BPG into 3-phosphoglycerate (3PG), the other one from the two-step conversion of phosphoenolpyruvate (PEP) into pyruvate. This step, mediated by the enzyme pyruvate kinase (PK), is regulated by the cell's energy status and regulates the entry of carbon atoms from glycolysis into the TCA cycle[4].

Looking at the whole sequence of glycolytic reactions, two ATP and two NADH molecules are produced per glucose molecule[6].

The glycolytic cascade does not require oxygen availability, while to oxidize pyruvate to carbon dioxide through oxidative phosphorylation (OxPhos), oxygen is absolutely necessary. Aerobic respiration requires pyruvate, the final product of glycolysis, to be imported inside the mitochondria and decarboxylated to acetyl-CoA. Acetyl-CoA is then converted to citrate before entering in the Krebs cycle. The Krebs cycle, also known as TCA cycle, generates NADH and carbon dioxide by oxidating acetyl-CoA. Reducing equivalents in the form of NADH are then used by the electron transport chain, which creates a proton gradient across the inner membrane of the mitochondria. This gradient then supports the energy to generate ATP. The complete catabolism of one glucose molecule via OxPhos can produce, in theory, up to 38 ATP molecules[4].

Under anaerobic or hypoxic conditions, pyruvate is transformed into lactate through lactic acid fermentation to keep glycolysis going, and thus to provide a source of ATP in the absence of efficient mitochondrial respiration. This reaction represents the final step of anaerobic glucose catabolism and it can be observed in skeletal muscles during intense activity, when tissue oxygen concentration is low. Lactate dehydrogenase (LDH) enzyme catalyses the conversion between pyruvate and lactate, regenerating NAD^+ in the same reaction. Glycolysis requires NAD^+ for the conversion of G3P in 1,3BPG, thus LDH has an important role in maintaining the cellular redox state to support the glycolytic cascade[7].

CONTROL OF GLYCOLYSIS

The glycolytic pathway is subjected to several regulatory mechanisms, based both on the availability of specific substrates and on the regulation of key enzymes. Among the ten enzymatic steps of glycolysis, three reactions are essentially irreversible, because of a free energy change that is largely negative. These three steps are: (1) glucose phosphorylation, catalyzed by hexokinases 1 and 2; (2) conversion of F6P in F1,6BP, carried out by PFK1; (3) transfer of phosphate from PEP to ADP, which generates ATP and pyruvate, by pyruvate kinase[4]. During gluconeogenesis, the reverse metabolic pathway that regenerates glucose from glycolytic intermediates, most steps are mediated by the same enzymes active during glycolysis, with the except ion of these three reactions. In these cases,

specific enzymes are activated and mediate the reverse reactions. HK, PFK1 and PK, which mediate the three irreversible and committing steps, are also the main regulatory sites of glycolysis and, among them, PFK1 is critical for the commitment of glucose to the glycolytic pathway[5].

Modulation of PFK1 activity is important to regulate glycolytic levels according to the cell's needs. PFK1 is directly regulated by the energetic status of the cell, since ATP and AMP can inhibit or activate PFK1, respectively. Furthermore, high-energy metabolic intermediates, such as citrate and PEP, that accumulate in conditions of sufficient energy storage, also reduce PFK1 enzymatic function. Another end-product of glycolysis, lactate, can reduce PFK1 activity providing a negative feedback for the glycolytic cascade. This is one reason why cells relying on glycolysis as the main source for energy production secrete lactate, to keep glycolysis active[8].

The most potent positive regulator of PFK1 is fructose-2,6-bisphosphate (F2,6BP), which acts with an allosteric mechanism to increase the affinity of PFK1 for its substrate F6P. F2,6BP is able to bypass the inhibitory effect of ATP and act synergistically with AMP. F2,6BP is produced from F6P, such that F6P availability itself can foster PFK1 activity; F2,6BP is produced by a family of enzymes, the 6-phosphofructo-2-kinase/fructose-2,6-bisphosphatase (PFKFB) family, that can mediate both the production (acting as kinases) or consumption (acting as phosphatases) of F2,6BP. The kinase (PFK2) and phosphatase (FBPase) functions of PFKFBs are encoded within the same protein, and the ratio between the two activities determines the amount of F2,6BP in the cell. In mammals, four genes (*PFKFB1-4*) encode for four different enzymes and, among these, PFKFB3 is the one displaying the most active kinase function. Therefore, PFKFB3 overexpression results in F2,6BP production and, in turn, on glycolysis stimulation. The kinase portion PFK2 can be regulated by hormonal stimuli: insulin and adrenalin signals enhance PFK2 functions, increasing glycolysis. Finally, the levels of F2,6BP are adjusted during the cell-cycle through an E3 ubiquitin ligase[5,8].

NUTRIENT-SENSING MECHANISMS

Nutrient sensing is the ability of a cell to sense and respond to changes in essential metabolic substrates. In the presence of abundant nutrients, these signaling systems usually drive anabolic pathways (i.e. de novo synthesis of macromolecules) to permit cell duplication and/or storage pathways (such as glycogen or fatty-acid synthesis) to conserve resources. Otherwise, lack of nutrients triggers the rapid mobilization of internal stores through catabolic mechanisms such as glycogen break-down, fatty acid oxidation and, in extreme or prolonged starving conditions, autophagy. Cells detect their nutrient status both by directly measuring essential nutrients such as glucose, aminoacids and lipids, and by indirectly sensing the overall energy levels, i.e. the ratio between ATP and ADP (or AMP)[6,9].

Usually, nutrient sensing mechanisms act at two levels: the first is a feedback system that aims at maintaining homeostatic levels of a given molecule, by coordinating its uptake, storage and breakdown. This system typically acts by regulating the activity of key metabolic enzymes and their transcriptional levels, to provide short- and long-term adaptation. The second acts more indirectly, by coordinating the presence or absence of nutrients with other cellular processes, including other metabolic pathways and cell proliferation[9]. Glucose metabolism can influence gene transcription by two main mechanisms, mediating a form of metabolic adaptation to changing glucose levels. In one case, glucose (in its intracellular form of G6P) can directly regulate the subcellular localization of MondoA/ChREBP (carbohydrate-response element-binding protein) transcription factors as a feedback mechanism. Indeed these factors, acting together with their partner Mlx (Max-like protein x), mainly control the expression of enzymes involved in glycolysis and lipogenesis[10,11]. In the second case, glucose metabolism contributes to the overall levels of ATP, and this in turn regulates the activity of AMPK (AMP-activated protein kinase). When cells experience a condition of energy stress (i.e. low levels of ATP availability), AMPK phosphorylates TSC2 (tuberous sclerosis complex 2), promoting the inhibitory activity of TSC1–TSC2 towards the mTOR (mammalian target of rapamycin) complex. By this mechanism, AMPK inhibits anabolic processes and promotes

the activation of alternative catabolic pathways, such as autophagy, to re-establish ATP levels, thus maintaining energy homeostasis[12].

METABOLIC REPROGRAMMING OF CANCER CELLS: THE WARBURG EFFECT

One central difference between normal tissues and cancer cells is the ability of the latter to proliferate without control. Cancer cells display a number of distinctive traits that allow them to proliferate in an uncontrolled way[13]; among these, a prominent one is an altered cell metabolism, centered on a higher rate of energetic and anabolic pathways[4].

In the presence of oxygen, most healthy cells metabolize glucose though oxidative phosphorylation to generate ATP. In the 1920s, the Nobel Prize Otto Warburg observed that cancer cells instead incorporate abnormally high levels of glucose and display a high rate of the lactate production, even in the presence of oxygen[14]. This phenomenon, known as "Warburg effect", is observed because cancer cells generate lactate as principal end-product of glycolysis even if oxygen is available, thus performing "aerobic glycolysis". Cancer cells rely on aerobic glycolysis even if this process is far less efficient than mitochondrial respiration in terms of ATP production (18-fold less), counterbalancing the low ATP yield with very high rates of glucose uptake[7,15]. This observation is still exploited clinically to detect tumors by positron emission tomography using 18F-fluorodeoxyglucose (FDG-PET), an analog of glucose that enters into cells but cannot be metabolized[15].

Initially the energetic disadvantage of aerobic glycolysis seemed paradoxical. However, it later became clear that the functional advantage of this particular metabolism lays on the diversion of glucose-derived intermediates toward several biosynthetic pathways, which are fundamental to sustain the production of new daughter cells. Glycolysis intermediates can indeed provide carbon atoms for the synthesis of nucleotides, aminoacids and lipid precursors, all essential molecules to build new daughter cells. Aerobic glycolysis thus represents a metabolism particularly suited for cell growth and sustained proliferation[4]. Supporting this view, aerobic glycolysis is also naturally observed in non-transformed rapidly dividing cells, such as embryonic tissues and stem cell compartments[6,16].

Furthermore, when placed *in vitro* in the presence of unlimited nutrients (glucose and glutamine), almost any cell type shifts its metabolism from oxidative phosphorylation to aerobic glycolysis, in the so-called Crabtree effect, suggesting this is the preferred metabolism in the presence of nutrients[17].

Aerobic glycolysis is characterized not only by high rates of glycolytic reactions, but also by the unusual production of lactate. Lactate generation maintains low levels of pyruvate, which otherwise inhibits glycolysis, and has an important role in maintaining the redox balance: pyruvate to lactate conversion regenerates NAD^+, necessary to sustain the conversion of G3P in 1,3BPG during glycolysis. Moreover, NAD^+ is essential for nucleotide and aminoacid biosynthesis and many other cellular functions[4]. Lactate freely diffuses from cells into interstitial fluids and blood; recently, it has been proposed that lactate secretion by tumor cells performing aerobic glycolysis can favor tumor invasiveness properties by acting on the microenvironment. For example, lactate stimulates VEGF production by endothelial cells, thus promoting angiogenesis and sustaining migration. Lactate can also act as a mediator of inflammatory reactions, favoring the production of pro-inflammatory cytokines by T-cells and macrophages. Moreover, tumor cells from the more oxygenated regions of a solid tumor can use lactate, produced in more hypoxic regions, as a fuel for oxidative phosphorylation. In turn, this sets glucose free for hypoxic tumor cells[15,18].

MOLECULAR MECHANISMS OF METABOLIC REPROGRAMMING IN CANCER

Uncontrolled cell proliferation observed in cancer cells requires that constitutive pro-proliferation signals (oncogene activation, tumor-suppressor mutation) are coupled with an adaptation of glucose metabolism to fuel cell growth. In cancer cells, the metabolic switch from mitochondrial respiration to aerobic glycolysis is commonly observed upon activation of oncogenes or mutations in tumor suppressors[19]. One example is the c-Myc oncogene, which directly regulates both cell-cycle genes, such as cyclin D, and genes involved in glucose metabolism (i.e. LDH and PK enzymes, glucose transporters). In addition, c-Myc induces addiction to glutamine by increasing the expression of glutamine transporters and

glutamine catabolic enzymes. Glutamine is a fundamental nutrient that can be converted into other aminoacids, TCA intermediates (and thus, energy), or it can be a source of carbons, for fatty acids, and of nitrogen, for nucleotides. Thus, in transformed cells c-Myc generally promotes macromolecule synthesis and energy production required for sustained cell proliferation[20].

Rapid growth of solid tumors can cause cells to experience local low oxygen conditions which trigger adaptive responses to hypoxic environments, mediated by the HIF transcription factors (HIF1 and HIF2). Under normoxia, the α subunit of the HIF1 transcription factor is degraded, while limiting oxygen concentration induces α subunit stabilization and, in turn, activation of target gene transcription. HIF1 activation on one hand induces the expression of genes promoting formation of new blood vessels, such as VEGF, and in parallel adjusts cell metabolism to low oxygen conditions. Indeed, among the genes regulated by HIF, there are glucose transporters, all the main glycolytic enzymes (i.e. HK, PFK1, PK) and the pyruvate dehydrogenase kinase 1 (PDK1) enzyme, which skews pyruvate from oxidation to lactic fermentation. In this way, hypoxic cells reprogram their metabolism toward glycolysis (in this case, anaerobic glycolysis) in order to sustain energy production and cell proliferation[21].

The reprogramming of cell metabolism can occur also as a consequence of mutation in tumor suppressor genes. One of the most famous examples is the tumor suppressor p53. p53 controls the expression of genes related with glucose metabolism and acts by restraining glucose utilization. p53 positively regulates the expression of TIGAR, a FBPase that inhibits PFK1 activity and redirects glucose toward the PPP. As a consequence, mutations of p53 increase aerobic glycolysis[5,22]. In other cases, metabolic enzymes themselves display tumor suppressor functions, as observed for isocitrate dehydrogenase (IDH), fumarate hydratase (FH) or succinate dehydrogenase (SDH), key enzymes of the TCA cycle, which are often found inactivated/mutated in paraganglioma or leiomyosarcoma, respectively. Interruption of the TCA cycle and accumulation of intermediate metabolites precipitates these tumors in a para-hypoxic condition, leading to enhanced glycolytic levels[23,24].

Given its central role for glycolysis, it is perhaps not suprising that, among the glycolytic enzymes, PFK1 is often found expressed at high levels in cancer cells,

and cells displaying higher expression of PFK1 are the more aggressive ones, at least in some tumor types[25,26]. Moreover, also PFK2 enzymes, and in particular PFKFB3, are found elevated in human cancers or activated through post-translational modifications and reduced degradation[5]. Collectively, this indicates that glycolysis is a central metabolic pathway, which is required for cancer cell proliferation and tumor progression.

YAP/TAZ TRANSCRIPTIONAL CO-ACTIVATORS

Yes-associated protein (YAP) and transcriptional coactivator with PDZ-binding motif (TAZ, also known as WWTR1) are two orthologous mammalian transcriptional coactivators that shuttle between the cytoplasm and the nucleus to regulate gene transcription. In the nucleus, they act mainly in combination with the TEAD/TEF family of DNA-binding transcription factors (TEAD1/2/3/4)[27]. The TEAD family is widely expressed in embryonic and adult tissues, providing a wide potential for YAP/TAZ responsiveness[28].

YAP/TAZ: sensors of multiple inputs

YAP/TAZ were discovered as downstream transducers of the Hippo pathway, an evolutionary conserved tumor suppressor signaling cascade that plays important roles in the control of tissue and organ size. The Hippo pathway was revealed through genetic screens in *Drosophila*; this identified a number of downstream effectors that are highly conserved in mammals. Genetic alterations in components of this signaling cascade lead to aberrant organ overgrowth, due to increased cell proliferation and decreased apoptosis[28]. In its basic formulation, the mammalian pathway operates as follows: MST1/2 (Macrophage Stimulating 1/2) kinases, in association with the regulatory subunit WW45-SAV (Salvador), phosphorylate and activate the LATS1/2 (Large Tumor Suppressor) kinases, which associate with their cofactors MOB1A/B (Mps One Binder 1A/B). MST1/2 and LATS1/2 are homologous to *Hpo* and *Wts Drosophila* kinases, respectively[28,29]. Activated LATS1/2, helped by MOB1A/B factors, phosphorylate YAP and TAZ at multiple residues (S61, S109, S127, S164, S381 for human YAP, and S66, S89, S117, S311 for human TAZ). LATS1/2-mediated

phosphorylation inhibits YAP/TAZ activity through at least two different mechanisms: ubiquitination-dependent degradation and binding to 14-3-3 proteins[28,30]. Several upstream regulators of the Hippo pathway have been identified, including NF2/Merlin, an important inhibitor of YAP/TAZ. In recent years, however, several variations on this basic signaling module have been reported, including LATS-independent phosphorylation of YAP/TAZ, MST-independent activation of LATS, and phosphorylation-independent modalities of YAP/TAZ control[31].

A surge of publications in the last decade identified YAP/TAZ as downstream effectors of several inputs, including apico-basal cell polarity, epithelial-to-mesenchymal transition (EMT), Wnt and other growth factor signaling cascades. Moreover, one of the most fascinating aspects of YAP and TAZ biology was the discovery that YAP/TAZ act as nuclear transducers of mechanical inputs such as extracellular matrix (ECM) stiffness, cell shape and cytoskeletal tension[31,32]. Thus, structural elements that originate at the tissue level, such as adhesion of a cell to its surrounding ECM, cell-cell junctions and the tensional forces of the cytoskeleton that keep cells, tissues and organs in a certain shape[33], by acting on YAP/TAZ activity, can inform individual cells about properties of the tissue in which they are embedded.

Recently, YAP/TAZ activity was also connected to the cell metabolism by the identification of the mevalonate pathway as a required input for YAP/TAZ activity *in vitro*. Mevalonate metabolism is indeed required for RHO membrane localization and activity, which in turn is required and sufficient for YAP/TAZ activity in a LATS-independent manner[34].

Thus, the emerging picture is that YAP/TAZ act as integrators of a series of converging cellular and tissue-embedded cues to determine cell behaviour in a coherent and coordinated manner.

YAP/TAZ functions in normal tissues

YAP/TAZ factors can regulate cell proliferation in many tissues and organs. This is underscored by the seminal observation that knockout of Hippo genes or activation of YAP in mammalian tissues (such as liver, heart and skin) cause tissue hyperplasia and organ overgrowth. Conversely, genetic deletion of YAP

from several fetal tissues results in impaired cell proliferation. During development, full YAP knockout results in embryonic lethality, further worsened by the combined YAP and TAZ knockout[28,29,35]. These observations, together with the finding that YAP/TAZ are broadly required for proliferation of cells *in vitro*, led to the idea that YAP/TAZ are general required factors for cell proliferation[29,36,37]. This idea was however recently challenged by the finding that in mouse some adult tissues, including the intestine, can survive in the absence of YAP and TAZ[38,39]. Thus, it is possible that YAP/TAZ are key for proliferation upon tissue damage, during regeneration or during tumor progression, but not in normal physiological conditions, at least in the adult.

YAP/TAZ activity is increased in cancer cells and required for tumor development

All available data point to a powerful tumor-promoting activity of YAP/TAZ. In line with a tumorigenic role, YAP and TAZ are found overexpressed or amplified in several human cancers, such as lung, pancreas, liver, oral squamous-cell carcinomas and breast cancer. Experimentally, overexpression of YAP is sufficient to induce cell hyperplasia and tumorigenesis, either alone or in combination with other oncogenes[28,29,35]. Finally, recent data indicate that YAP/TAZ are strongly required for experimental tumorigenesis in the intestinal epithelium and in the skin, and that YAP expression can substitute one of the most powerful oncogenes, Ras, in sustaining pancreas cancer development[40]. These findings, together with the observation that YAP/TAZ are not required in at least some adult normal tissues, indicate that inhibiting YAP/TAZ activity might be an ideal target to harm cancer cells. Moreover, a common theme in many of recent studies is that much of the functions of YAP/TAZ are mediated by TEADs, such that disruption of the YAP/TAZ-TEAD protein–protein complex is considered an important way to disable YAP/TAZ activity[41,42].

Rationale

The reprogramming of cell metabolism toward aerobic glycolysis is a hallmark of cancer, indicating that aerobic glycolysis provides a selective advantage that favors cancer cell growth. According to current views, metabolic reprogramming is considered as a simple phenotypic endpoint that occurs as a consequence of oncogene activation and tumor formation. Increasing evidence however indicates that metabolic pathways also incorporate signaling mechanisms that inform and coordinate other cellular functions, including nuclear gene transcription and epigenetics. In this manner, metabolic pathways can even play causative roles in regulating cell behavior, in addition to their core biochemical functions[7,12,19,43].

Our study explored the possible links between glucose metabolism and gene transcription, starting from the hypothesis that known transcriptional pathways, relevant for cancer cell proliferation and aggressiveness, might "sense" aerobic glycolysis. In this way, metabolism and gene transcription should be coordinated to promote cancer cell proliferation. We started our analysis by performing a genome-wide microarray profiling to obtain a list of genes regulated by glucose. Bioinformatic analyses showed that YAP/TAZ target genes are positively regulated by glucose metabolism. We then validated that inhibition of glucose metabolism hampers YAP/TAZ-induced *in vitro* tumorigenic phenotypes in breast cancer cells, including proliferation, clonogenic activity and promotion of self-renewal properties. This regulative axis is strikingly conserved in *Drosophila*, where inhibiting glycolysis blunts tumorigenic clonal expansion induced by Yorkie, the homologue of YAP/TAZ. Finally, and in keeping with the idea of oncogenic signaling at the service of a metabolic pathway, growth/survival promoted by glucose require YAP/TAZ activity in human cancer cells.

Results

GLUCOSE METABOLISM REGULATES YAP/TAZ ACTIVITY

To analyze the link between glucose metabolism and gene transcription, we asked whether glucose metabolism could regulate known signaling pathways relevant for embryonic development, adult tissue homeostasis and disease. For this, we performed a genome-wide microarray expression profiling and compared cells growing in high glucose (which favors aerobic glycolysis due to the Crabtree effect) with cells treated for 24h with 2-deoxy-glucose (2DG, 50mM), a widely used competitive inhibitor of glucose metabolism acting at the level of hexokinase[44]. In this way we obtained a list of genes regulated by glucose metabolism. The underlying idea is that, if glucose regulates the activity of a transcription factor, the target genes of this factor will be regulated by glucose. The dose of 2DG used in this experiment is commonly used in cell cultures to block glucose metabolism and was sufficient to inhibit aerobic glycolysis and to increase mitochondrial respiration in our cells, as measured with an extracellular flux analyzer (see below), and to inhibit cell growth.

We then performed a gene set enrichment analysis (GSEA), searching for more-than-random correlations between the genes regulated by 2DG (either up- or down-regulated) and those contained in a collection of gene signatures denoting activation of transcription factors and signaling pathways. Since most of these signatures were derived from mammary cell lines, we performed the experiments in MDA-MB-231 breast cancer cells and MCF10A mammary epithelial cells. Several signatures appeared regulated, either up or down, upon 2DG treatment, in line with the profound effects of glucose on cell behavior. For instance, genes regulated by Notch or TGFβ were enriched upon inhibition of glucose metabolism, while E2F and Myc target genes were positive correlated with glucose. Among others, the signature indicating activation of YAP/TAZ was the most significantly overrepresented within the genes inhibited by 2DG treatment in both cell lines, whereas the genes repressed by YAP were enriched among the genes activated by 2DG (Fig. 1A) This was also confirmed by monitoring the

overall levels of the YAP/TAZ signatures in our microarrays, which was consistently downregulated upon inhibition of glucose metabolism (Fig. 1B). Of note, basal levels of YAP/TAZ target genes were higher in the cell line displaying higher glycolysis/respiration ratio, i.e. in MDA-MB-231 cells (Fig. 1C).

Our GSEA analysis suggested a link between glucose and YAP/ TAZ, but did not inform us about what is upstream and what is downstream. We initially investigated whether YAP/TAZ regulate glucose metabolism by monitoring aerobic glycolysis and mitochondrial respiration levels in mammary epithelial cells expressing activated TAZ. Even if TAZ activation is per se sufficient to endow these cells aggressive traits *in vitro* and *in vivo*[45], we did not observe notable changes in glycolysis or respiration (Fig. 1D). Moreover, by surveying microarrays obtained by activation or inhibition of YAP/TAZ in multiple cellular systems[27,46,47], we failed to observe consistent regulation of glucose transporters or glycolytic genes that are instead typically induced by oncogenes[15,20]. Thus, YAP/TAZ are not obvious inducers of aerobic glycolysis.

In order to validate our bioinformatics analysis, we then tested whether glucose metabolism regulates YAP/TAZ. For this, we treated MDA-MB-231 cells, displaying high basal YAP/TAZ activation, with 2DG or Lonidamine (another widely used inhibitor of hexokinase[44]) for 24h. To directly monitor YAP/TAZ transcriptional activity, we transfected cells with the luciferase reporter 8XGTIIC-lux, based on TEAD-responsive elements and whose dependence on YAP/TAZ has been previously checked ([31] and Fig. 2A). As shown in Fig. 2A, these treatments inhibited YAP/TAZ activity, whereas treatment with OligomycinA, an inhibitor of mitochondrial respiratory chain, did not inhibit YAP/TAZ activity. This confirmed our initial findings, but also suggested a regulation not generically linked to energy metabolism. In line with a specific inhibition, the effect of 2DG was reversible (Fig. 2A) and was not caused by general inhibition of glycosylation (Fig. 2B); this was tested because 2DG could in principle compete for mannose and interfere with N-linked glycosylation[48]. Similar results were obtained with the CTGF-lux reporter (Fig. 2C), based on the natural human *CTGF* promoter, a well established YAP/TAZ target[27,29,49]. Moreover, we observed similar results in the highly glycolytic Hs578T breast cancer cells (Fig. 2D) and in the HepG2 hepatocellular carcinoma cells (Fig. 2E), indicating a mechanism conserved in

different cell lines. Finally, a reporter for the Notch pathway and a reporter driven by the CMV promoter were not inhibited, ruling out generic effects of 2DG treatment on gene transcription (Fig. 2F and 2G). Collectively, these data confirmed that inhibition of glucose metabolism inhibits YAP/TAZ activity.

Glucose inhibition induces a fast adaptation of cellular metabolism and then secondarily induces other cellular responses, including growth arrest; thus, among the genes regulated by glucose, some could be regulated as a direct consequence of glucose inhibition, while others may be indirect targets of growth arrest. An example of the second class are the E2F-regulated genes[50,51] that were highly enriched in our GSEA analysis (Fig. 1A, E2F3 signature); indeed, we found by luciferase assays that E2F activity is inhibited by 2DG and also by inducing growth arrest through expression of established CDK inhibitors (p21/CDKN1A, p16/CDKN2A, p27/CDKN1B) (Fig. 3A top). In contrast, CDK inhibitors do not inhibit YAP/TAZ activity (Fig. 3A bottom). Thus, growth arrest and/or E2F inhibition is not sufficient to explain YAP/TAZ inhibition by 2DG.
To test the idea of a direct/proximal effect of glucose metabolism on YAP and TAZ activity, we developed a doxycycline-inducible version of the 8XGTIIC-lux reporter, stably integrated in our cells, allowing us to visualize YAP/TAZ responses in a restricted time-window. Cells were supplemented with doxycycline for 4, 6, 8 or 10h to release YAP/TAZ-dependent transcription, and compared with cells treated also with 2DG. As shown in Fig. 3B, 2DG treatment inhibited YAP/TAZ at the earliest time points, indicating a rapid response. Importantly, we observed a reduced YAP/TAZ activity also in cells cultured in absence of glucose (Fig. 3C). Similar results were obtained in HepG2 (Fig. 3D) and in MCF10A-MII cells (Fig. 3E-G). This observation is thus compatible with a direct regulation of YAP/TAZ activity.

To validate further the link between glucose and YAP/TAZ, we checked whether endogenous target genes inhibited by 2DG were coherently regulated also upon knockdown of YAP/TAZ. To select candidate co-regulated genes, we compared microarray profiling of genes regulated by 2DG with microarrays of cells depleted of YAP/TAZ by two independent couples of siRNAs, previously carried out in our laboratory in the same cellular lines (MDA-MB-231 and MCF10A). Out of

this analysis, we could identify several probes that were similarly co-regulated (either up or down) by glucose and by YAP/TAZ in both cell lines. Among the strongest co-regulated microarray probes in MDA-MB-231 cells, we successfully validated a series of transcriptional targets by qPCR, concordantly repressed or activated by 2DG and YAP/TAZ knockdown, including the established YAP/TAZ targets *HMMR*, *TK1* and *RRM2*[52,53] (Fig. 4A). Noteworthy, the same target genes were also regulated by 2DG treatment and YAP/TAZ knockdown in another breast cancer cell line, Hs578T (Fig. 4B). This indicates that a portion of the genes regulated by 2DG is also regulated by endogenous YAP/TAZ. Other YAP/TAZ targets, such as *CTGF* or *ANKRD1*, were not regulated, likely due to compensating parallel inputs. Interestingly, Gene Ontology analysis indicates that the genes co-regulated by glucose and YAP/TAZ are particularly related to cell cycle control and to DNA synthesis, repair and metabolism (Fig. 4C), in keeping with the validation of *TK1*, *TYMS*, *RRM2* (required for nucleotide biosynthesis) and *CDC* (Cell Division Cycle) factors shown above.

Collectively, these results indicate that YAP/TAZ transcriptional activity is sustained by glucose metabolism.

YAP/TAZ ACTIVITY IS REGULATED BY GLYCOLYSIS

We then asked which metabolic pathway fueled by glucose was mainly responsible for YAP/TAZ regulation. Once entrapped in the cell in the form of G6P, glucose can redirect into various metabolic pathways, such as PPP, glycolysis and HBP. Both glycolysis and HBP require the conversion of G6P into F6P by the enzyme GPI (Fig. 5A). To test if GPI was involved in YAP/TAZ regulation, we depleted cells of endogenous GPI with two independent siRNAs, and found this was sufficient to recapitulate the effects of 2DG treatment (Fig. 5B-C). This result excluded the PPP as the main regulator of YAP/TAZ downstream of glucose.

Downstream of GPI, F6P can be used either by PFK1 in the glycolytic cascade or by glucosamine-fructose-6-phosphate transaminase (GFPT), the first enzyme of HBP. To test a potential involvement of the HBP, we used two strategies: first, we blocked the activity of GFPT by treating cells with 6-diazo-5-oxo-L-norleucine

(DON) or O-diazoacetyl-L-serine (AZS) for 24h, at doses commonly used in cancer cells[26,54,55]. Second, we tested if the major pathway fed by the HBP, i.e. protein glycosylation, was involved in the regulation of YAP/TAZ; for this we supplemented N-Acetyl Glucosamine (GlcNAc) in the culture medium, which is sufficient to reactivate glycosylation in absence of glucose[54,55]. However, neither DON or AZS treatments inhibited YAP/TAZ activity (Fig. 5D), nor GlcNAc rescued YAP/TAZ inhibition by 2DG (Fig. 5E). Altogether, this made unlikely that the HBP and protein glycosylation are major regulators of YAP/TAZ; this also suggested glycolysis as the key metabolic pathway regulating YAP/TAZ.

To verify this hypothesis, we then sought to modulate glycolytic levels and see whether this was sufficient to modulate YAP/TAZ activity. For this, we cultured cells for one week in the presence of galactose instead of glucose: in this condition aerobic glycolysis is less favorable and cells shift their metabolism toward oxidative phosphorylation to sustain efficient ATP production[17,56–58]. We first checked glycolysis levels in cells cultured in galactose by measuring extracellular acidification rate (ECAR – an indirect measure of lactate production, and thus of aerobic glycolysis) and oxygen consumption rate (OCR – a direct measure of mitochondrial respiration). As expected, we observed a strong decrease in ECAR and a substantial increase in OCR, confirming the metabolic shift from aerobic glycolysis to oxidative phosphorylation in cells cultured in galactose (Fig. 6A-D). We then measured YAP/TAZ activity in these different cell populations, by using the stably integrated YAP/TAZ luciferase reporter system described above. Strikingly, cells with reduced glycolysis displayed a corresponding reduction of YAP/TAZ activity; moreover, adding back glucose to galactose-fed cells during the last hours of the experiment was sufficient to rescue YAP/TAZ activity (Fig. 6E-F), in line with a rapid response of YAP/TAZ to glucose shown before.

To further test the connection between glycolysis and YAP/TAZ we used UOK262 kidney cancer cells, which are highly glycolytic because of a mutation of the fumarate hydratase (FH) enzyme of the TCA cycle, and their FH-reconstituted counterpart, which have reduced glycolysis as they restore mitochondrial respiration[59,60]. By luciferase assay we found a downregulation of

YAP/TAZ activity in UOK262 upon reconstitution of the FH enzyme (Fig. 6G), in line with our hypothesis.

These results collectively support the notion that glycolysis plays a key role in the regulation of YAP/TAZ by glucose metabolism.

EXPLORING THE MECHANISMS OF YAP/TAZ REGULATION

To understand how glycolysis could regulate YAP/TAZ we initially tested the involvement of known YAP/TAZ regulators, such as the Hippo kinase cascade[28,61], the mevalonate pathway[34,52], or key molecules involved in nutrient-sensing pathways, such as AMPK and mTOR[12,62].

YAP/TAZ regulation by glucose metabolism is independent on Hippo signaling and mevalonate

The best-known regulation of YAP/TAZ occurs by inhibitory phosphorylation from the LATS1/2 kinases, downstream of the Hippo pathway. We thus reasoned that glucose metabolism could keep LATS1/2 inhibited, in turn promoting YAP/TAZ activity. To directly test this hypothesis we depleted LATS1/2 kinases with two independent sets of siRNAs[32,34] in MDA-MB-231 cells. As shown in Fig. 7A LATS1/2 knockdown was able to completely rescue the inhibition induced by NF2 reconstitution[31], but was not sufficient to rescue the inhibition by 2DG treatment, ruling out an involvement of the Hippo cascade.

We then checked if 2DG treatment could regulate YAP/TAZ acting on mevalonate metabolism. In principle, glycolysis can regulate Acetyl-CoA, which is a precursor of mevalonate metabolism; mevalonate in turn is known to be required for Rho geranylgeranylation, and this is relevant to regulate YAP/TAZ activity[34]. We challenged this pathway by providing cells with non-limiting amounts of mevalonate, but found this was not sufficient to rescue 2DG inhibition (Fig. 7B). As a positive control, mevalonate rescued inhibition caused by Cerivastatin treatment, a small-molecule inhibitor of Acetyl-CoA to mevalonate conversion[34]. In line, 2DG induced a very minor nuclear exclusion when compared to Cerivastatin treatment (Fig. 7C).

YAP/TAZ regulation by glucose metabolism is independent on AMPK/mTOR

To test if AMPK/mTOR nutrient-sensing signaling is involved in the regulation of YAP/TAZ by glucose metabolism, we used two approaches: first, we inhibited mTOR activity in MDA-MB-231 cells cultured in high glucose, a condition with low AMPK and high mTOR activity; second, we blocked AMPK activity upon 2DG treatment, a condition where AMPK is activated. As shown in Fig. 7D-F, neither treatment with the dual mTORC1/2 inhibitor AZD2014[63,64] inhibited YAP/TAZ, nor blockade of AMPK activity with Compound C (a well-established inhibitor of AMPK) treatment or siRNAs transfection rescued them from 2DG. Of note, these treatments efficiently regulated dephosphorylation of the established AMPK/mTOR downstream target ribosomal protein S6[12,62] (Fig. 7D-E) and siRNAs efficiently depleted AMPK levels (Fig. 7F).

PFK1 interacts with TEADs

To gain insights into other possible mechanisms by which glycolysis regulates YAP/TAZ, we explored the YAP interactome. For this, we pulled-down a stably over-expressed form of YAP (FLAG-tagged YAP 5SA mutant) in MCF10A and MDA-MB-231 cells and identified coprecipitating proteins by mass-spectrometry (MS). As shown in Fig. 8A, we isolated several known interactors of YAP, including established cytoplasmic and nuclear complexes[65–67]. We then turned our attention to novel interacting proteins, with particular attention to enzymes involved in glucose metabolism; indeed it has been previously shown that some metabolic enzymes, such as PKM2 for example, can fulfill non-metabolic functions by interacting with transcription factors[43,68]. Among new potential YAP-binding proteins, our attention was immediately retained by the isolation, in both cell lines, of the phosphofructokinase enzyme isoform P (PFK1). This suggested the very interesting possibility that YAP/TAZ might crosstalk with PFK1, and thus with glycolysis.

PFK1 mediates the first committed step of glycolysis and it is a central enzyme for the regulation of glycolysis. Recent reports indicate that cancer cells take control over glycolysis by multiple mechanisms acting, directly or indirectly, on PFK1 activity[4,5,69]. Moreover, PFK1 and PFK2 (i.e. the enzyme feeding F2,6P to

PFK1) expression is elevated in advanced breast tumors[25,26], making PFK1 an interesting candidate to link glucose metabolism and YAP/TAZ activity. To explore the functional relevance of this biochemical observation, we designed two independent siRNA duplexes to target endogenous PFK1 expression (Fig. 8B), and challenged YAP/TAZ activity. Remarkably, knockdown of PFK1 caused inhibition of YAP/TAZ activity in MDA-MB-231 cells, as assayed by using 8XGTIIC-lux and CTGF-lux reporters (Fig. 8C-D). Thus, PFK1 is required to sustain YAP/TAZ activity, and recapitulates the effects of 2DG shown above.

So far, results indicate that PFK1 and glucose metabolism are required to sustain YAP/TAZ transcriptional functions. To dissect the molecular mechanism underlying this regulation, we sought to validate a direct interaction between YAP and PFK1, which was suggested by MS analysis. Co-immunoprecipitation experiments between recombinant FLAG-PFK1 and bacterially expressed YAP failed however to detect any direct binding (Fig. 9A). We then reasoned that co-immunoprecipitation could reveal both direct and indirect YAP binding partners, as suggested by the isolation of NF2 from MCF10A, which indirectly binds to YAP[70]. Given that, our experiments pointed to a direct effect of glucose metabolism on YAP/TAZ transcriptional activity, we thus asked whether this regulation could act at the level of YAP/TAZ-TEADs transcriptional complexes. Surprisingly, as shown in Fig. 9B we could detect a direct binding between recombinant GST-TEAD4 and FLAG-PFK1. Moreover, we were able to detect a binding between PFK1 and TEADs both in lysates from cells expressing MYC-TEAD4 and FLAG-PFK1 (Fig. 9C) and by immunoprecipitating endogenous TEAD1 with endogenous PFK1 (Fig. 9D). We also tested if the interaction of TEADs to PFK1 required the presence of YAP by using the mutated form of TEAD4 Y429H, unable to bind YAP[71], but YAP seemed to be dispensable (Fig. 9C). Finally, we performed immunostainings with two different anti-PFK1 antibodies and found a proportion of the protein localized into the nucleus (Fig. 9E), in line with the interaction with nuclear TEAD proteins. In addition, we revealed PFK1/TEAD1 complexes by using the proximity ligation assay (PLA), a technique enabling in situ quantitative detection of endogenous protein–protein complexes[72], and detected PLA signals corresponding to endogenous

PFK1/TEAD1 complexes in the nucleus (Fig. 9F).

We then explored whether PFK1 enzymatic activity was required for TEAD binding and YAP/TAZ activity. PFK1 activity is potently activated by its allosteric modulator F2,6BP[5,73,74]. F2,6BP levels are regulated by PFK2 enzymes and, among these, the PFKFB3 isoform preferentially promotes the phosphorylation of F6P to F2,6BP, thus stimulating PFK1 activity[8,75,76]. We thus tested if PFKFB3 could promote YAP/TAZ transcriptional activity. As shown in Fig. 9G, transfection of PFKFB3 dose dependently enhanced the activity of the YAP/TAZ/TEAD reporter in HEK293 cells, which typically display low levels of YAP/TAZ activity[77]. Conversely, mutation of five key aminoacid residues of PFK1, required for F2,6BP binding, reduced the binding with TEAD4 (Fig. 9H). Altogether, these results indicate that it is the enzymatically-active pool of PFK1 that binds TEADs and fosters YAP/TAZ activity.

GLUCOSE METABOLISM REGULATES THE INTERACTION BETWEEN TEADS AND YAP/TAZ

Prompted by the finding of a PFK1-TEAD interaction, we next asked whether glucose metabolism regulates the formation of the YAP/TAZ-TEAD complex. Co-immunoprecipitation experiments of endogenous proteins revealed that YAP and TAZ interaction with TEAD1 decreased both upon 2DG treatment and glucose withdrawal (Fig. 10A-G), without leading to quantitative YAP or TEAD1 nuclear exclusion (Fig. 10H and see Fig. 7C). In addition, providing glucose to glucose-starved cells restored the binding between YAP and TEAD1 (Fig. 10F-G). Of note, we obtained similar results by using different antibodies to immunoprecipitate YAP or TAZ, and by repeating the experiment from extracts of MDA-MB231, MCF10A, HepG2 and UOK262 cells, indicating a general phenomenon. Finally, we sought to test the requirement of PFK1 for the binding between YAP and TEAD1, by using both co-immunoprecipitation experiments and PLA detection of endogenous YAP/TEAD protein-protein complexes. As shown in Fig. 10I-J, downregulation of PFK1 inhibited the binding between YAP and TEAD1.

TEADs represent the DNA-binding platform for YAP/TAZ at gene promoters.

We thus selected some genes with known or predicted TEAD binding sites, such as *HMMR*, *TK1*, *CTGF* and *ANKRD1*[27,52,53] and we verified if the recruitment of YAP at these promoters was affected upon 2DG treatment. As shown in Fig. 11A-B, chromatin immunoprecipitation (ChIP) analyses revealed that inhibition of glucose metabolism reduced the binding of YAP to the regulatory regions of its target genes, in line with inhibition of YAP/TAZ-TEAD complexes. Of note, this analysis was carried out based on known targets of YAP/TAZ, such as *CTGF*, *ANKRD1* and *RHAMM*, and also on a novel target, *TK1,* included in the analysis because it is jointly regulated by glucose and YAP/TAZ (see Fig. 4A). By visual inspection we indeed identified two conserved TEAD-binding motifs in the proximal promoter region of the *TK1* gene, which are sufficient to drive YAP/TAZ dependent transcription in luciferase assays (Fig. 11C) and respond to glucose metabolism (Fig. 11D). Collectively, our results suggest that glucose metabolism regulates the stability of YAP/TAZ-TEAD complexes at gene promoters.

To further strengthen the finding that glucose metabolism regulates the ability of YAP/TAZ to interact with TEADs, we reasoned that a TEAD1 isoform (Y406A mutant) unable to bind YAP/TAZ[78] should be insensitive to modulation of glucose metabolism. To test this, we took advantage of the UAS-GAL4 system to compare the activity of TEAD isoforms without interference from endogenous complexes; with this system it was possible to uncouple the basal transcriptional activity of TEAD1 (observed in the Y406A mutant) from YAP/TAZ-induced transcription (observed only with WT TEAD1). As shown in Fig. 11E, 2DG inhibited transcription driven by WT GAL4-TEAD1, but was unable to inhibit the basal activity of the Y406A GAL4-TEAD1 mutant in MDA-MB-231 cells. Moreover, overexpressing PFKFB3 in HEK293 selectively enhanced transcription driven by WT GAL4-TEAD1 (Fig. 11F).

In sum, we thus propose a model in which PFK1 acts as a scaffold protein to promote YAP/TAZ-TEADs interaction and gene transcription.

INTERPLAY OF GLYCOLYSIS, PFK1 AND YAP/TAZ FOR CANCER CELL GROWTH

Data shown so far indicates that YAP/TAZ require glycolysis for full activation. So, we hypothesized that phenotypes induced by YAP/TAZ should be counteracted by inhibiting glucose metabolism.

First we challenged the ability of activated S89A-mutant TAZ to promote self-renewal of MCF10A-MII mammary cells in a previously established mammosphere-forming assay[34,45]. Inhibition of glycolysis by 2DG treatment, or by transfection of PFK1 and GPI siRNAs, potently blocked the effects of TAZ (Fig. 12A-D).

Second, we challenged the ability of YAP to promote anchorage-independent growth in soft agar, another established hallmark of YAP activation[79]. Knockdown of PFK1 by siRNA transfection decreased the basal clonogenic potential of MDA-MB-231 cells, recapitulating the inhibition of YAP/TAZ (Fig. 12E); moreover, blockade of glucose metabolism with 2DG inhibited the growth of colonies experimentally induced by expression of activated YAP-5SA (Fig. 12F).

Third, we took advantage of the fact that YAP/TAZ activity can be inhibited in mammary epithelial cells grown at high confluence, leading to growth arrest, and then locally reactivated by inducing a ‘‘wound’’ in the monolayer, enabling cell proliferation. This happens because cells close to the edge of the wound can stretch and remodel their F-actin cytoskeleton, leading to reactivation of YAP/TAZ[32,80]. As shown in Fig. 12G-H, cells close to the wound, but treated with 2DG, re-entered cell proliferation much less efficiently than untreated cells, indicating that glucose metabolism is required to sustain YAP/TAZ-induced proliferation.

To further extend the functional connections between glucose metabolism and YAP/TAZ we tested if proliferation promoted by glucose would depend, at least to some extent, on YAP/TAZ. In control MDA-MB-231 cells, 48h of nutrient deprivation (glucose and glutamine) induces growth arrest, and supplementing back glucose in the medium restarts proliferation (as measured by BrdU incorporation). Strikingly, upon YAP/TAZ silencing, glucose-induced

proliferation is greatly impaired (Fig. 12I), although not completely as expected from the general (and YAP/TAZ independent) functions of glucose.

We also compared parental UOK262 cells (glycolytic) with FH-reconstituted UOK262 cells (that rely more on mitochondrial respiration[59,60]) for their sensitivity to inhibition of glucose metabolism and of YAP/TAZ. As expected, in clonogenic assays parental UOK262 cells are more sensitive to 2DG (Fig. 12J). In line with our findings, parental cells relying on high levels of aerobic glycolysis were also more sensitive to inhibition of YAP/TAZ activity by verteporfin (VP), a small-molecule that specifically impairs the binding of YAP/TAZ to TEADs[41] (Fig. 12K).

PFK1 is required for YAP/TAZ-dependent growth *in vivo*

Having found that pro-tumorigenic phenotypes and proliferation induced by YAP/TAZ require glucose metabolism, we then asked whether this was relevant also *in vivo*. For this, we used the *Drosophila* model system, in collaboration with Prof. Grifoni (UniBo). *Drosophila* imaginal discs are well-established experimental systems for Yorkie (Yki) activity, the fly homolog of YAP/TAZ: Yki hyperactivation, in the context of a *lethal giant larvae* tumor-suppressor (*lgl*$^{-}$) mutant background[81–83], causes tissue overgrowth[61,84]. As shown in Fig. 13A, silencing of Pfk by RNAi inhibited the growth of Yki-overexpressing cells. Importantly, this was associated also in *Drosophila* with inhibition of Yki transcriptional activity, because we observed decreased expression of DIAP1 and dMyc, established Yki/TEAD target genes in *Drosophila*[85–88], upon Pfk RNAi (Fig. 13B-E). This suggests that Pfk is instrumental for Yki activity during tumorigenic growth of fly larval tissues.

Collectively, our findings indicate that glycolysis is required for the full deployment of YAP/TAZ tumorigenic activities, and that YAP/TAZ mediate a segment of the proliferative effects of glucose metabolism, reflecting regulation of YAP/TAZ transcription downstream of glucose in human cells and fly tissues. Mechanistically we found that glycolysis regulates YAP/TEAD complex formation, which is in line with the requirement of TEAD binding for most YAP/Yki tumorigenic activities, and in particular for the biological assays used

above[27,47,86].

CORRELATION BETWEEN HIGH YAP/TAZ ACTIVITY AND HIGH LEVELS OF A GENE SIGNATURE ASSOCIATED TO GLYCOLYSIS IN PRIMARY HUMAN BREAST CANCERS

YAP/TAZ activation and a shift toward a glycolytic metabolism are commonly observed during tumor progression. This is true in particular for breast cancers, where YAP/TAZ activity is associated with high-grade (G3) tumors and with the cancer-stem-cell (CSC) content of the tumors, reflecting YAP/TAZ requirement for CSC self-renewal and cancer aggressiveness[45,89]. Moreover, mammary tumor-initiating cells and undifferentiated basal-like breast cancers display a shift toward aerobic glycolysis, which in turn is required for their self-renewal ability[90,91]. Given our results for a direct link between glycolysis and YAP/TAZ activity, we sought to test if YAP/TAZ activation specifically associates with glucose metabolism also in primary human mammary tumors.

We first derived a gene expression signature experimentally associated with high glucose metabolism in cells of mammary origin (glucose signature) by selecting the genes that were downregulated by 2DG treatment both in MCF10A and MDA-MB-231 microarrays. We then analyzed a large metadataset collecting gene expression and associated clinical data of more than 3600 primary mammary tumors[45,92], and evaluated how the levels of glucose signature were associated with YAP/TAZ activity. Strikingly, bioinformatic analyses showed that glucose signature is positively and strongly correlated with expression of previously established gene signatures denoting YAP/YAZ activity (Fig. 14A-B); moreover, tumors classified according to high (vs. low) glucose signature also display corresponding high and low activity of YAP/TAZ (Fig. 14C-D).

Prompted by this observation, we tested whether the glucose signature correlates with cancer features previously associated to YAP/TAZ activity, such as tumor grade and the content of CSC[45,89]. As shown in Fig. 14E-G, we indeed found that glucose signature expression levels associated to higher expression of mammary stem cell signatures[93,94], and it was significantly elevated in G3 vs. G1 grade tumors ($p<0.0001$). Remarkably, by univariate Kaplan-Meier survival analysis we also found that tumors expressing high levels of the glucose signature (“High”)

displayed a significant higher probability to develop recurrence when compared to the “Low” group (Fig. 14H). Of note, the higher expression of the glucose signature in G3 tumors, and its ability to stratify patients, was completely lost when we selected from the glucose signature only the genes that were regulated by 2DG but not by YAP/TAZ siRNA (Fig. 14I-J). Collectively, these data indicate that during mammary tumor progression metabolic reprogramming toward aerobic glycolysis is accompanied by elevated YAP/TAZ activity.

Discussion

Cell metabolism and signaling pathways are powerful regulators of cell proliferation and tumorigenesis. A coherent biological response integrates these separate inputs, linking cellular metabolism with pathways that sustain cell growth[13,15]. With this work we propose that glycolysis, besides its core biochemical role, also contributes to regulate the activity of YAP/TAZ; in so doing, glycolysis fuels the proliferative and tumorigenic functions of these powerful oncogenic factors. Blocking glucose metabolism, or shifting cellular metabolism away from glycolysis, impairs YAP/TAZ transcriptional activity and their ability to promote cell proliferation, cancer cell self-renewal and clonogenic abilities *in vitro*, and tissue overgrowth in *Drosophila*. In line with this, growth/survival promoted by glucose incorporates YAP/TAZ activity as downstream effectors.

Mechanistically, we found that phosphofructokinase 1 (PFK1), mediating the first committed step of glycolysis, interacts with the transcription factors TEADs to stabilize their interaction with YAP/TAZ. In so doing, glucose metabolism regulates the recruitment of YAP at target promoters, providing a rationale for the regulation of YAP/TAZ transcriptional activity.

This study highlights some peculiarities of YAP/TAZ. Classical oncogenes such as Ras, Myc and HIFs actively induce metabolic reprogramming toward aerobic glycolysis[15,20], while YAP/ TAZ are instead regulated downstream to changes in glucose and mevalonate metabolism[34]. Since YAP/TAZ are also regulated by cues embedded in the cell microenvironment (Hippo kinase cascade, ECM mechanics, cell-cell adhesion structures, GPCR and Wnt signaling), it is tempting to speculate that this mechanism might represent a way by which cell metabolism and tissue-level information are integrated into a common output. YAP/TAZ also appear different from another transcription factor regulated by glucose, ChREBP/ MondoA: ChREBP mainly regulates expression of metabolic enzymes and thus serves as a feedback transcriptional mechanism to adjust enzyme levels to nutrient availability and to coordinate lipid and glucose metabolism[7,11]; YAP/TAZ instead

incorporate clues from glucose metabolism into cancer cell growth and self-renewal.

LINK BETWEEN GLUCOSE METABOLISM AND YAP/TAZ ACTIVITY IN BREAST CANCER

An increase in glucose uptake and a shift toward aerobic glycolysis are commonly observed in several tumors. This is true for breast cancers, and in particular in mammary tumor-initiating cells (TICs) and undifferentiated basal-like mammary tumors (i.e. those mostly enriched in TICs) that require glycolysis for their self-renewal ability[90,91]. Strikingly, aerobic glycolysis can be even sufficient, at least *in vitro*, to induce malignant phenotypes in breast cancer cells[26]. This parallels with YAP/TAZ activity, which is increased in high-grade (G3 vs. G1) tumors and is functionally required for CSC self-renewal, tumor-seeding ability and aggressiveness[45]. Thus, the link between YAP/TAZ and glucose metabolism appears particularly relevant in breast cancer. Functionally, we showed that aerobic glycolysis is key to regulate YAP/TAZ-induced mammosphere formation and colony-forming ability. Accordingly, we also found that genes regulated by glucose showed a significant enrichment in high-grade tumors, and inversely correlated with disease-free progression in a large dataset of primary human breast cancers, closely overlapping YAP/TAZ activity. Interestingly, different studies identified that a high expression of PFK1 correlates with poor prognosis in primary breast cancers[26]. In line, a small-molecule inhibitor of PFKFB3 showed a striking inhibitory effect on the growth of mammary cancer cells in orthotopic assays[95]. This may indicate that YAP/TAZ activity in breast cancer tumor-initiating cells might be particularly susceptible to therapeutic approaches targeting glycolysis.

Collectively, our and other findings suggest that YAP/TAZ oncogenic activity needs to be coordinated with cell metabolism to efficiently drive cell growth. Infact YAP/TAZ are powerful inducers of proliferation, but this activity would be unleashed only when cells are in the right metabolic conditions to sustain cell growth. This would perhaps assign to cancer cells undergoing metabolic reprogramming (for example in response to oncogene activation, or to hypoxia) a

further selective advantage in terms of proliferation potential, survival, and tumor-seeding ability.

REGULATION OF YAP/TAZ BY AMPK

Recently, other three publications have described a connection between glucose metabolism and YAP/TAZ activity. These groups independently found that activation of AMPK by the use of small-molecule compounds (such as metformin, phenformin or AICAR) induces an increase in YAP phosphorylation at S127, favors YAP localization to the cytoplasm, and inhibits selected YAP/TAZ target genes[96–98]. To explain this common observation, different biochemical mechanisms were proposed: one study provided evidence that AMPK phosphorylates AMOTL1 and increases LATS1 activity, such that AMOTL1 knockdown can rescue YAP nuclear exclusion upon phenformin treatment[96]. In the second study, AMPK directly binds YAP and phosphorylates it mainly on S61 (and also on S94 and T119), but also promotes LATS1/2 activity and YAP S127 phosphorylation[97]. The third publication largely overlapped with the second one, but identified S94 as the major direct AMPK target on YAP[98]. The finding of a direct phosphorylation on S94 is noteworthy because this residue is key for YAP-TEAD interaction[78], providing a direct explanation for the observation that AICAR inhibits YAP-TEAD complex formation. Bringing together all biochemical observations, activation of AMPK can thus induce both direct and LATS-dependent YAP phosphorylation events. As for the functional relevance of the AMPK-YAP axis, DeRan et al. showed that AMPK activation opposes a YAP-driven growth phenotype, acting through S127 phosphorylation[96]. Mo et al. showed instead that AICAR inhibits endogenous YAP target genes and clonogenic activity in LATS1/2 knockout MEFs (i.e. lacking of any S127 phosphorylation)[98], which instead indicates that AMPK works independently of LATS1/2. However, the requirement of AMPK for the regulation of YAP/TAZ by glucose remains unclear in functional terms: direct inhibition of YAP/TAZ by AMPK activators gave inconsistent results depending on the cell line, despite efficient AMPK modulation. Indeed, Wang and colleagues showed a partial rescue of YAP/TAZ activity by using AICAR compound to inhibit AMPK in

HEK293A cells deprived of glucose[97]. In contrast, as shown in Fig. 7E-F, we did not rescue YAP/TAZ inhibition by blocking AMPK activity in MDA-MB-231 cells treated with 2DG, and we could not rescue YAP/TEAD protein-protein interction as well (data not shown). Thus, the possibility exists that regulation of YAP/TAZ by glucose entails multiple parallel mechanisms, included but not limited to AMPK.

It should also be considered that AMPK is not a general and bona-fide tumor suppressor. AMPK is a powerful regulator of autophagy, and the AMPK-autophagy axis plays a dual role in carcinogenesis: in some systems AMPK-autophagy favors cancer cell survival under stress, and can thus have protumorigenic functions[99,100], which are however not easily compatible with a general YAP/TAZ inhibitory role. For example, AMPK is activated in breast cancer cells forming mammospheres in absence of matrix attachment, and this activity is required for anoikis resistance; moreover, in these conditions AMPK activation is sufficient to promote malignant phenotypes, such as loss of polarity and luminal filling, typically promoted by oncogenes[101–103]. Of note, all these phenotypes are hallmarks of YAP/TAZ activation[45,79], suggesting that AMPK and autophagy do not inhibit YAP/TAZ in these systems/conditions.

YAP/TAZ-TEADs PROTEIN COMPLEX

The finding that glucose metabolism intersects YAP/TAZ signaling at the level of TEAD factors underscores the idea that TEADs are central players for the regulation of YAP/TAZ. Indeed, recent findings indicate that disruption of YAP-TEADs interaction may be a promising therapeutic strategy against YAP-driven human cancers[41,42]. This builds along a growing series of evidence indicating the importance of TEADs for YAP/TAZ function, and in particular for their pro-tumorigenic activity.

Both in *Drosophila* and in mammalian systems, TEADs normally interact with transcriptional inhibitors, such as the TGI and VGLL4 Tondu-domain containing proteins, and YAP/TAZ replace these factors to activate gene transcription[42,104]. In future, it will be interesting to understand how these cofactor exchanges are reciprocally regulated, and whether these occur while TEAD factors are on or off

DNA.

PART II

Exploring the link between YAP/TAZ and nucleotide metabolism in oncogene-induced senescence

Introduction

NUCLEOTIDE BIOSYNTHESIS

Deoxyribonucleoside triphosphate (dNTP) metabolism is a fundamental pathway providing the essential substrates for DNA synthesis, both in the nucleus and in mitochondria. As a consequence, the size and composition of deoxyribonucleoside triphosphate (dNTP) pools is tightly regulated during the cell-cycle phases: during S-phase, total dNTP amounts peak roughly 10-fold higher then in G_0/G_1, to support DNA replication. For this, a series of enzymes involved in dNTP biosynthesis are specifically transcribed during S-phase in response to mitogenic stimuli. During the cell's whole life, a smaller amount of dNTPs is produced, which is sufficient for DNA repair and mitochondrial DNA (mtDNA) synthesis[105]. Reflecting the central role of dNTP metabolism, both excessive and defective production of dNTPs can influence DNA replication, including origin choice, fork speed and inter-origin distance. As such, a proper dNTP concentration is one key factor enabling cell progression through the S-phase. Maintenance of the proper dNTP concentration is essential not only to ensure a proper DNA replication and cell proliferation, but play significant roles also to prevent replicative mutagenesis, the stall of DNA replication forks, and the risk of DNA breaks: defects in dNTP metabolism can indeed increase the DNA mutation rate and genomic instability[106–108].

Nucleotides can be generated by two processes: de novo production and the salvage pathway. In the de novo synthesis, glucose and glutamine represent the main sources of carbons and nitrogen to produce nucleotides. The ribonucleoside diphosphate reductase (RNR) enzyme catalyzes the rate-limiting step of the pathway, synthetizing dNTPs de novo from ribonucleotides. The salvage pathway instead enables the recycling of both purine and pyrimidine free rings from turnover of cellular materials, to maintain the proper dNTP concentrations[108].

RNR is a heterotetrameric complex consisting of two large catalytic subunits (RRM1) and two small regulatory subunits (RRM2 or p53R2), and it catalyzes the reduction of each ribonucleoside diphosphate into deoxynucleotides. Because of

its critical importance, RNR is tightly regulated by several mechanisms, including allosteric regulation of the enzymatic complex and modulation of the levels and subcellular localization of its subunits. The transcription of RRM1 and RRM2 is generally promoted when cells enter into the S-phase thanks to activation of E2F factors, resulting in expansion of the dNTP pools[108]. Upon leaving S-phase, these two subunits are expressed at much lower levels. Moreover, the RRM2 is targeted to proteasome-dependent degradation during late mitosis. It is generally considered that the levels of the RRM2 subunit, more than RRM1, are key to control dNTP production during DNA replication: its expression is indeed rate-limiting for RNR activity. *p53R2* is a p53-inducible, DNA damage-responsive gene, which encodes for an alternative subunit to RRM2. The RRM1-p53R2 complex provides dNTPs for DNA repair and mtDNA synthesis[105,107].

SENESCENCE

In 1961 Leonard Hayflick and Paul Moorhead were the first to describe the process of cellular senescence[109]. They observed that normal cells can divide a certain number of times, and then stop dividing. Cellular senescence is defined as a state of permanent cell-cycle arrest. At difference with quiescent cells, senescent cells are incapable of resuming proliferation, even upon mitogenic stimulation[110]. Replicative senescence has been observed in several primary cell types including epithelial, stromal (fibroblasts) and vascular (endothelial) cells. The maximal number of cell divisions that a cell population can perform before undergoing senescence is called the “Hayflick limit”. This limit is tightly linked to shortening of the telomeres that occurs upon repeated cell division cycles, which is thought to function as a molecular clock[111]. Cell populations that normally need to preserve long-term proliferation potential, such as stem cells, usually express high levels of TERT (telomerase reverse transcriptase), the enzyme enabling the elongation of telomeres during S-phase. Cells can enter into a senescent state not only as a consequence of repeated cell divisions, but also as a defense against stressful situations, including non-telomeric DNA damage, oxidative stress, perturbations to chromatin organization, excessive mitogenic signals, such as those produced by oncogene activation that are commonly associated with or

instrumental for cell transformation[110]. Senescence is thus considered a tumor-suppressive mechanism intrinsically limiting the proliferation potential of cells. However, cancer cells loose the ability to undergo cell senescence by several mechanisms, including de novo expression of TERT and mutation of tumor-suppressor genes involved in the activation of the senescent state[110] (see below).

Hallmarks of senescence

Cells undergoing senescence display a series of characteristic traits beyond a stable growth arrest, which include both morphological features (such as cell spreading and a bigger nucleus) and a distinctive pattern of gene expression. Senescent cells display activation of cell cycle inhibitors including the cyclin-dependent kinase inhibitors (CDKIs) p21, p15 and p16[112]. p21 is activated in response to activation of the p53 pathway and, together with p16 and p15, activates pRb (Retinoblastoma) signaling. While p21 and p15 are generally regulated during cell-cycle arrest (for example in response to DNA damage or to anti-mitogenic signaling), the concurrent activation of p16 is considered a hallmark of senescence. Indeed p16 is not only a marker of senescence, but a required element for the establishment of the senescent state[110,113]. Senescent cells also inhibit genes that encode for cell cycle progression factors, including cyclins, CDKs (cyclin-dependent kinases) and origin-recognition factors of the MCM family. At least in part, repression of these pro-proliferative genes is linked to inhibition of E2Fs, a family of transcription factors that specifically promotes the expression of genes involved for G_1/S transition[112,114].

A general marker of senescence, unrelated to cell proliferation regulation, is senescent-associated β-galactosidase (SA-βgal). SA-βgal reflects an increase in lysosomal biogenesis that occurs in senescent cells, leading to the appearance of lysosomal β-galactosidase activity. However, SA-βgal is induced also by stresses, such as cell confluence or oxidative stress[115]. Other phenotypes associated with senescence are the condensation of nuclear heterochromatin into discrete and dense foci, called senescence-associated heterochromatin foci (SAHF), and the general up-regulation of genes encoding for secreted cytokines and growth factors that are defined as SASP (senescence associated secretory phenotype)[110,112]. The function of these secreted proteins is both cell-autonomous, by installing a feed-

forward loop that maintains cell senescence, and non cell-autonomous, by altering the cell microenvironment through remodeling of the extracellular matrix and recruitment of inflammatory cells[116]. Thus, senescence is defined by a series of distinct phenotypes, which are activated and regulated by different signaling pathways acting in parallel. It is also important to note that, among the markers of senescence so far presented, no one is exclusive to the senescent state and thus sufficient to define a senescent phenotype.

Oncogene-Induced Senescence

As anticipated above, a number of different stimuli can induce cellular senescence. These include critically shortened telomeres, DNA damage (especially double strand breaks – DSBs) and oncogene activation[110,112,116]. Oncogene-induced senescence (OIS) is the response of primary mammalian cells to oncogene activation. This paradoxical phenomenon has been mainly observed upon activation of mutated Ras (Hras or Kras) in normal fibroblasts. Ras is a cytoplasmic transducer of mitogenic signals that leads the activation of the MAPK/ERK and PI3K signaling cascades. Accordingly, other upstream or downstream members of the pathway were described to cause senescence when overexpressed or activated, including ERBB2/Neu, RAF and MEK. In this case, senescence is thought to occur in response to excessive mitogenic stimulation, acting as a tumor-suppressor to avoid oncogenic transformation. Findings in mouse cells support this idea: cells cultured in serum-free medium (i.e. with low mitogenic pressure) resist Ras-induced senescence[110,112,114].

Oncogene-induced senescence (OIS) by Ras activation was originally identified in cultured cells[117] and has been a key model system for the study of senescence and of the pathways underlying its development. The relevance of OIS for real tumors is based on several observations, which indicate that senescence indeed plays a key tumor-suppressive role also in human tumors. Senescence markers, including p16 and SA-βgal activation, can be observed in early-stage tumors caused by Ras activation, either in genetically engineered mouse models for cancer or in human primary tumors[117]. For instance, human melanocytes bearing activating mutations of Braf are thought to escape from melanoma formation by forming benign nevi, which contain senescent cells[118]. Moreover, mutation of the locus encoding for

p16INK4a, p15INK4b and *p19ARF* is very often observed in human tumors bearing Ras or Braf activation, is a prerequisite for tumor progression in several genetic mouse models induced by Ras, and is prevalently observed in more advanced tumors, which correlates well with the idea that senescence represents an early barrier for tumor progression[119].

Role of dNTP metabolism in OIS

Upon oncogene activation, the excessive replication rates lead to aberrant DNA replication events, including fork collapse and asymmetric replication forks progression. Stresses during DNA replication in turn lead to activation of the DNA damage response (DDR), which has been shown to be required for OIS induction[120]. DDR indeed activates both the p53/p21 and p16/pRb pathways, thus inducing a stable cell cycle arrest. Recent findings suggest that DNA replication stresses and OIS, observed upon Ras activation, are due to contradictory regulation of dNTP metabolism: while on one hand Ras acts as a mitogen and promotes cell-cycle progression, at the same time it inhibits the transcription of key dNTP metabolism genes, including RRM2[121,122].

Interestingly, dNTP deficiency is required and sufficient, to some extent, for the establishment and maintenance of OIS-associated growth arrest[120–122]. This was shown by the finding that restoration of dNTP levels by exogenous nucleosides addiction or by ectopic RRM2 expression is sufficient to overcome activation of the DDR response and of OIS-associated growth arrest[121].

Rationale

YAP/TAZ are powerful regulators of cell proliferation. Which are the genes and cellular mechanisms by which YAP/TAZ sustain cell proliferation remains largely unknown. Recently, extensive gene expression profiling of cancer cells upon depletion or overexpression of YAP and/or TAZ have been carried out[27,31,47]. Analysis of the genes regulated by YAP/TAZ indicates a widespread regulation of genes and programs linked to cell-cycle regulation, including origin-licensing factors, genes involved in DNA replication and, only to a minor extent, G_1/S cyclin-CDK complexes[1,53], raising the question of how YAP/TAZ regulate cell-cycle progression at the beginning of the S-phase. Among other categories of regulated genes we then noticed the regulation of several genes involved in dNTP metabolism, including key enzymes involved in both the de novo and salvage dNTP synthesis pathways (Fig. 15A). Among these, we previously validated TK1 (thymidine kinase), RRM2, RRM1, TYMS (thymidilate synthase) as bona-fide transcriptional targets of YAP/TAZ. Moreover, these genes are almost invariably contained in the gene signatures used to infer YAP/TAZ activation status in primary tumors by means of bioinformatics analysis such as GSEA[31,45,123], indicating they are part of a core transcriptional program associated to YAP/TAZ driven malignancy. Of note, this regulation appears direct, because recent genome-wide analysis of YAP/TAZ binding sites revealed that YAP/TAZ bind the enhancer of most of these genes[53]. In line, we and others demonstrated by chromatin immunoprecipitation assay that YAP/TAZ bind to the TK1 and RRM2 promoter (Fig.11A-B and [53]). Moreover, as shown in Fig. 11C-D, we found that the isolated proximal TK1 promoter, containing the YAP/TAZ binding site, is responsive to experimental manipulation of YAP/TAZ levels and activity. By RT-PCR or based on published microarray data, we also found that regulation of key dNTP metabolism enzymes occurs in several cellular systems (breast cancer, hepatocellular, mesothelioma, skin cancer), indicating a general mechanism (Fig. 4A-B and [124,125]).

Given these observations, and based on the finding that dNTP metabolism is key not only for cancer cell proliferation, but also to overcome the senescence-

associated growth arrest phenotype[121,122], we asked whether YAP/TAZ, by sustaining dNTP biogenesis, can play a role in preventing OIS and OIS-associated growth arrest. This would help explain why YAP/TAZ activation potently predisposes tumor development in several tissues and why YAP/TAZ activity is required in several set-ups for transformation by oncogene activation. The regulation of RRM2 and dNTP metabolism by YAP/TAZ might thus be central during transformation and tumor initiation, but also in later phases of tumor development, given the continued requirement for DNA building blocks observed in cancer cells and tumors.

Thus, the aim of the experiments presented hereafter is to explore the potential connections between YAP/TAZ activity, dNTP metabolism and OIS.

Preliminary Results

NUCLEOTIDE METABOLISM-RELATED GENES ARE BOTH YAP/TAZ AND RAS TARGETS

The most fundamental trait of senescent cells is growth arrest. Nucleotide metabolism and dNTP levels are crucial in regulating DNA replication and, in turn, cell proliferation. RNR is crucial for dNTP biosynthesis and its regulatory subunit RRM2 is rate-limiting for this process[110]. Recently, Aird and colleagues reported that establishment of the OIS-associated cell growth arrest correlates with and requires downregulation of dNTP metabolism, such that expression of oncogenic Ras in human normal fibroblasts downregulates the expression of dNTP synthesis enzymes, and that sustaining expression of RRM2 can prevent, to a certain extent, OIS-associated DDR and growth arrest[121].

We first asked whether YAP/TAZ regulate expression of dNTP metabolic enzymes not only in transformed cancer cells, but also in primary cells relevant to study OIS. For this, we experimentally manipulated the expression levels of YAP/TAZ in WI38 human fibroblasts by siRNA-mediated knockdown of YAP/TAZ or by retroviral overexpression of an activated form of YAP (YAP 5SA), and monitored expression of RRM2, TK1 and TYMS expression by qPCR. As shown in Fig. 15B, YAP/TAZ positively regulate the expression of dNTP metabolic enzymes in WI38 cells. As a control, expression of activated Ras ($Hras^{G12V}$) inhibited expression of RRM2[121] and also of TK1 and TYMS. In parallel, we validated by qPCR in the same samples other established YAP/TAZ target genes such as *Cyr61*, *ANKRD1* and *AXL*[53,126] (Fig. 15C). Effective regulation of endogenous YAP, TAZ or Ras levels were checked by western blotting or qPCR analysis (Fig. 15D-E). Collectively, these results suggest that YAP/TAZ regulate the transcription of metabolic enzymes involved in dNTP biosynthesis in human primary fibroblasts.

YAP EXPRESSION OVERCOMES RAS-INDUCE SENESCENCE

We next sought to determine whether YAP overexpression is sufficient to restore transcriptional levels of RRM2, TK1 and TYMS in fibroblasts infected with Ras. For this, we generated retroviral constructs enabling co-expression of both Ras and constitutive active YAP (YAP 5SA) from the same plasmid (using an internal ribosome entry site (IRES) sequence; as a control, we generated a Ras-IRES-GFP construct. qPCR analysis of WI38 cells infected with Ras-IRES-GFP or Ras-IRES-YAP 5SA indicates that YAP overexpression is sufficient to reestablish the expression of RRM2, TK1 and TYMS at levels comparable to those present in normal fibroblasts (Fig. 16A), suggesting reactivation of dNTP metabolism. Of note, we observed that not only dNTP metabolic enzymes but also other YAP/TAZ target genes were inhibited upon Ras activation, which was rescued by activated YAP (Fig. 16B). Given that, Ras does not inhibit endogenous YAP and TAZ transcription or translation (Fig. 16C and data not shown), this suggests the possibility that during Ras-induced senescence endogenous YAP/TAZ function is inhibited. We also performed a direct measure of dNTP levels in our cells to assay for effective regulation of dNTP metabolism, and a preliminary experiment indicates this is the case (Fig. 16D).

Does then YAP overexpression rescues only expression of selected genes, or globally interferes with Ras-induced senescence? To answer this question, we monitored by qPCR the expression of established senescence marker genes, such as the CDKIs and cyclins. As shown in Fig. 17A, YAP activation inhibited the expression of p21 and p15 to levels similar to control cells, and increased transcription of cyclin A2, cyclin B1 and cell division cycle associated 7 (CDCA7). By western blotting, we found that YAP expression rescued normal levels of RRM2, cyclin A2 and lamin B (Fig. 17B), the latter being another hallmark of Ras-induced senescence[127]. We instead failed to observe downregulation of p16 (Fig. 17A), despite efficient induction of other senescent-associated phenotypes (see below).

We finally explored if YAP could oppose other hallmarks of senescent cells, such as growth arrest, SA-βgal expression and SAHF formation. As shown in Fig. 17C-E, YAP rescued both Ras-induced growth arrest (as measured by EdU

incorporation assays), SA-βgal expression and SAHF formation, suggesting that YAP expression is sufficient to overcome a large part of senescence phenotypes. Of note, all these phenotypes require the regulation of dNTP metabolism by Ras, further reinforcing the idea that YAP is a relevant regulator of dNTP metabolism.

YAP DEPLETION INDUCES SENESCENT PHENOTYPE

We started our experiments to test whether YAP regulates dNTP metabolism in an experimental set-up, such as OIS, where dNTP metabolism plays a primary functional role. In the course of our analysis, we noted that Ras activation not only inhibit dNTP metabolism, as reported by others[107,108], but also a series of direct and established YAP/TAZ target genes. We thus asked whether YAP inhibition is sufficient to induce senescence in the same cells. For this we depleted WI38 cells of YAP by siRNA transfection, and monitored senescent phenotypes after 5 days, which is the usual time-window required for establishment of OIS upon Ras expression[121] and when YAP protein levels were still clearly downregulated (Fig. 18A). These analysis were performed by transiently transfected siRNA against YAP, whose specificity was previously validated in the lab through a rescue experiment. Perhaps not surprisingly, YAP silencing caused inhibition in cell proliferation (Fig. 18B), as observed in many other cells. However, as shown in Fig. 18C-D, YAP depletion also significantly induced both the SA-βgal activity and SAHF formation. This was accompanied by regulation of senescence markers such as lamin B, cyclinA2 and RRM2, as checked by western blot (Fig. 18A) and by induction of p21 and p16 transcriptional levels (Fig. 18E). These results indicate that in absence of YAP activity, human primary fibroblasts undergo a phenotype strongly reminiscent of cellular senescence.

Discussion and Future directions

Our preliminary results indicate that YAP/TAZ can regulate dNTP metabolism in several cellular systems, and that this regulation is functionally relevant in the context of OIS. Indeed YAP expression in cells undergoing Ras-induced senescence is sufficient to reactivate expression of key dNTP metabolic enzymes whose expression is required and sufficient to oppose OIS. Accordingly, YAP can inhibit a series of phenotypes associated with Ras-induced senescence, including growth arrest, induction of SAHF, increased SA-βgal activity, and regulation of established senescence markers such as CDK inhibitors and cyclins. In future we plan to understand whether regulation of dNTP metabolism is required for the ability of YAP to prevent OIS. For this, we will test whether RRM2 and/or other YAP-regulated enzymes involved in nucleotide metabolism are required for YAP-induced phenotypes.

It also remains to be determined whether YAP can also modulate other phenotypes usually associated to OIS, such as expression of senescence-associated secretory proteins. Given that induction of SASP is considered as a parallel pathway to oncogene-induced growth arrest[112,116], this might indicate us whether YAP intercepts general induction of senescence, or more specifically the pathway(s) regulating growth arrest.

Then we will address the possibility that nucleotide metabolism represents a general subset of YAP/TAZ-induced target genes to promote cell growth and cancer progression. Published evidence indeed suggests that sustained levels of RRM2 are required in transformed cancer cells to support proliferation and oppose the emergence of senescent traits[128]. For this, we will test if inhibition of dNTP metabolic enzymes is sufficient to inhibit YAP/TAZ pro-tumorigenic functions and, if so, whether the expression of RRM2, alone or in combination with other limiting enzymes of the pathway, is able (at least to a certain extent) to rescue proliferation in cells depleted of YAP/TAZ. Moreover, regulation of dNTP metabolism by YAP might underlie the ability of YAP-overexpressing cancer cells and tumors to display increased resistance to chemotherapy involving the use of dNTP metabolism inhibitors, such as gemcitabine[107]. Clearly YAP/TAZ

regulate a wide number of genes involved in DNA replication, cell division and survival, so it is likely that dNTP metabolism will not entirely account for YAP/TAZ pro-proliferation functions.

As a corollary of these experiments, we found that YAP transcriptional targets are widely downregulated upon Ras activation, suggesting that inhibition of YAP activity is part of the mechanisms involved in OIS. In line with this idea, we found that loss of YAP induced the emergence of senescent traits in normal fibroblasts. Based on current knowledge, we will test a series of hypotheses by which Ras could oppose YAP during OIS. One possibility is that Ras might impact YAP/TAZ by inducing LATS activity or other direct post-translational regulatory mechanisms. Another possibility is that activation of pRb during the establishment of senescence, and thus inhibition of E2F factors, might result in inhibition of YAP transcriptional activity; this would be in line with recent findings indicating an intimate relationship between the pRb/E2F and YAP/TAZ activities[40,129].

Materials and Methods

REAGENTS AND PLASMIDS

D-Luciferin, 2-deoxy-D-glucose, Lonidamine, Cerivastatin, DL-mevalonic acid 5-phosphate, DON, AZS, GlcNAc, D-mannose, D-galactose, D-Luciferin, LatrunculinA and Verteporfin were from Sigma. CPRG was from Roche. Coelenterazine was from LifeTechnologies.

8XGTIIC-luciferase plasmid is Addgene 34615. The Renilla luciferase version was derived by subcloning of the promoter region into promoterless pRLuc. CTGF-luciferase was created by amplifying the genomic region corresponding to -225bp from the TSS of the human *CTGF* promoter, containing three TEAD-binding elements and the TATA box, into pGL3b. TK1-luciferase was created by amplifying the genomic region corresponding to -552bp from the ATG of the human *TK1* locus; the two predicted TEAD-binding elements start at -200 and -453. Doxycycline-inducible reporter systems were obtained by subcloning the tet-responsive element from FudeltaGW plasmid upstream of the promoter-luciferase elements into a puromycin-resistant retroviral backbone. rtTA was subcloned from Addgene 19780 into pBABE-hygro. NF2/Merlin plasmid is Addgene 19699. WT and Y429H MYC-TEAD4 plasmids are Addgene 24638 and 33041. WT and F2,6P mutant FLAG-PFK1 isoform P plasmid was subcloned from Addgene 23869. Mutation of the F2,6P allosteric site of PFK1 was carried out based on[73,74] and entails the following mutations: R481A, R576A, R665A, H671A, R744A (reference sequence is NP_002618). PFKFB3 was subcloned from Addgene 23668. Plasmids encoding GAL4 fusions of WT or Y406A TEAD1 are Addgene 33108 and 33034. GST-YAP and GST-TEAD4 plasmids were obtained by standard subcloning. For details on CMV-lacZ, RBPJ-luciferase, 6XE2F-luciferase and UAS-luciferase see[1]. All plasmids were sequence-verified prior to use.

pBABEpuro Hras V12 were from Addgene 39526. pBABEpuro YAP 5SA was generated by subcloning YAP 5SA from pcDNA3[32]. The other retroviral constructs were generated by subcloning IRES-GFP, IRES-YAP 5SA in pBABEpuro Hras V12. pBABEpuro empty vector was used as control retroviral transduction.

siRNA oligos were standard dsRNA oligos with overhanging dTdT from LifeTechnologies. Hereafter, targeted sense sequence of the mRNA:

siRNA	Interfering sequence	siRNA	Interfering sequence
YAP 1	GACAUCUUCUGGUCAGAGA	PFK1 1	GGAGAACCGUGCCCGGAAA
YAP 2	CUGGUCAGAGAUACUUCUU	PFK1 2	CGGGCAACCUGAACACCUA
TAZ 1	ACGUUGACUUAGGAACUUU	LATS1	CACGGCAAGAUAGCAUGGA
TAZ 2	AGGUACUUCCUCAAUCACA	LATS2	CAUACGAGUCAAUCAGUAA
GPI 1	GUUUGGAAUUGACCCUCAA	AMPKa1	CACGAUAUUCUGUACACAA
GPI 2	GCUUGAUGGCAGUGCUCAA	AMPKa2	GAAGUCAGAGCAAACCGUA

siYT1 were used with YAP1 and TAZ1; siYT2 were used with YAP2 and TAZ2; siLATS1/2 were used with LATS1 and LATS2; siAMPKa1/2 were used with

AMPKa1 and AMPKa2. Control siRNAs were Qiagen AllStars Negative Control siRNA or a 1:1:1 mix of Scramble, GFP and Luc* siRNAs, which were used back-to-back, with results comparable to non-transfected cells.

CELL CULTURE, TRANSFECTIONS AND INFECTIONS

MCF10A, MCF10A-MII and MCF10A-MII-TAZ-S89A cells and their empty vector controls[45] were cultured in DMEM/F12 supplemented of 5% Horse Serum, 2mM Glutamine, Insulin, Cholera Toxin, Hydrocortisone and EGF; MDA-MB-231 (STR verified) in DMEM/F12 with 10% FBS and 2mM Glutamine; Hs578T (ATCC) in DMEM with 10% FBS, 2mM Glutamine, Insulin; HEK293 (ATCC) in DMEM with 10% FBS and 2mM Glutamine; HepG2 (ATCC) in MEM with 10% FBS, 2mM Glutamine, NEAA; UOK262 in DMEM with 10% FBS, 2mM Glutamine and 1mM Pyruvate. WI38 human fibroblasts were cultured in MEM with 10% FBS and 2mM Glutamine. Cells were maintained in low oxygen (5%) till infection or transfection. All cells were routiney tested for mycoplasma contaminations with commercial PCR kits (Sigma).
siRNA transfections were done with Lipofectamine RNAi MAX (Invitrogen). Plasmid DNA transfections were done with Transit-LT1 (MirusBio). Retroviral infections were carried out following standard procedures and protocols.
Retroviral particles were prepared by transiently transfecting HEK293gp cells with retroviral vectors together with packaging vector (pMD2-env). Culture medium containing the viral particles was collected and filtered 48h after transfection. Viral infection was performed by incubating target cells with diluted viral supernatant for 24h. Infected cells were selected, 48h after infection, with puromycin.

MAMMOSPHERE ASSAY

Mammosphere assay was carried out by plating 1000 cells for each 24-well, and by plating 4 wells replicates for each sample; primary mammospheres were counted after 6 days. Differences in cell viability at plating were excluded based on TUNEL assays (not shown). Mammospheres were dissociated in trypsin and an equal numer of single cells replated to grow secondary mammospheres.

SOFT AGAR ASSAY

For soft agar assay, we plated 10000 MDA-MB-231 cells in triplicate in 35mm dishes in growth medium containing 0.3% low melting agarose, over a 0.6% agarose layer without cells; colonies were grown for 2 weeks (5SA-YAP expressing cells and their controls) or for 3 weeks (cells transfected with siRNA).

WOUND ASSAY

Wound assay was performed by plating $1.5x10^6$ MCF10A cells in 24-wells containing fibronectin-coated 13mm glass slides; after 24h, the cell monolayer was scratched with a sterile P1000 tip, washed and grown overnight. 2DG was added after washing.
For clonogenic assay, we plated 800 UOK262 cells in a 35mm petri dish, in triplicate; after 10 days colonies were stained with crystal violet, photographed and counted with imageJ software by quantifying the total stained area.

ECAR AND OCR MEASUREMENTS

The XF24 extracellular flux analyzer (Seahorse Bioscience) was used to detect real-time changes in cellular respiration and glycolysis rates. Cells were cultured in standard XF24 plates, by seeding 120000 (MDA-MB-231) or 90000 (MCF10A-MII) cells/well 24h before performing the measures; for experiments with siRNA, cells were transfected, reseeded after 24h, and measured after further 24h. Analysis of the extracellular acidification rate (ECAR) reflects lactate secretion and serves as indirect measure of glycolysis rate; oxygen consumption (OCR) reflects cellular respiration and is directly determined. All measurements were performed following manufacturer's instructions and protocols with at least 4 biological replicates for each condition, and normalized to total protein content as determined by Bradford assays. The analysis was carried out by Dr. Giulia Guzzo (Unipd).

REAL-TIME PCR

Total RNA was extracted using RNeasy Mini Kit (Qiagen) and contaminant DNA was removed by RNase-Free DNase Set (Qiagen). cDNA synthesis was carried out with dT-primed M-MLV Reverse Trascriptase (LifeTechnologies). Real-time qPCR analyses were carried out with triplicate samplings of each sample cDNA on a Rotor-Gene Q (Qiagen) thermal cycler with FastStart SYBR Green Master Mix (Roche) and analyzed with Rotor-Gene Analysis6.1 software. Expression levels are calculated relative to *GAPDH*. Sequences of primers are the following:

Primers for qPCR	sequenses	Primers for qPCR	sequenses
GAPDH	for CTCCTGCACCACCAACTGCT rev GGGCCATCCACAGTCTTCTG	CYP1B1	for TGGCTGCTCCTCCTCTTCAC rev TGGGAATGTGGTAGCCCAAG
YAP	for GCACCTCTGTGTTTTAAGGGTCT rev CAACTTTTGCCCTCCTCCAA	HMMR	for AGCTGAAAGGGAAGGAGGCTG rev CAAGGCTTTGCACCATACTGTCA
TAZ	for GGCTGGGAGATGACCTTCAC rev CTGAGTGGGGTGGTTCTGCT	CTGF	for AGGAGTGGGTGTGTGACGA rev CCAGGCAGTTGGCTCTAATC
GPI	for ACGCCATGCTGCCCTATGAC rev ATGCTGGCCATTGGTCCCTG	ANKRD1	for AGTAGAGGAACTGGTCACTGG rev TGGGCTAGAAGTGTCTTCAGAT
TYMS	for AAACCAACCCTGACGACAGAA rev GTTCACCACATAGAACTGGCAG	Cyr61	for CCTTGTGGACAGCCAGTGTA rev ACTTGGGCCGGTATTTCTTC
RRM2	for CTGGCTCAAGAAACGAGGAC rev GTTTGAACATCAGGCAAGCA	CRIM1	for CCATTGCCTCAGTTGTGGTTC rev TGGTTCCTTTCTTGCAGTCCA
TK1	for TTGTGGCTGCACTGGATGGG rev TCCTTCTCTGTGCCGAGCCT	AXL	for CACCAGCAAGAGCGATGTGT rev CGGTCCTGGGGATTTAGCTC
CDC25A	for AGGGAGGCCACATCAAGGGT rev ACACGCTTGCCATCAGTAGGT	CDCA7	for GTTCGAGGCCAGTTCTGTGG rev AGTCGCACACCGTCCATCTC
AQP3	for TCGTGTGTGTGCTGGCCATT rev AGCCGGAGTTGAAGCCCATG	Cyclin A2	for TTTGATAGATGCTGACCCATACC rev ATGCTGTGGTGCTTTGAGGT
VSIG1	for TGGGGCCTTGATTGGTAGCC rev TGCTTCGCTTTCTCCCCTTGG	Cyclin B1	for CCCCTGCAGAAGAAGACCTG rev AGTGACTTCCCGACCCAGTA
TXNIP	for ATGGGCGGGTGTCTGTCTCT rev TGGCAAGGTAAGTGTGGCGG	p21	for CAGGAGGCCCGTGAGCGATGGA rev ATCAGCCGGCGTTTGGAGTGGT
F3	for TGAAGGATGTGAAGCAGACG rev CCGAGGTTTGTCTCCAGGTA	p16	for CGATGTCGCACGGTACCTG rev TCAATCGGGGATGTCTGAGG
CDCA7	for GTTCGAGGCCAGTTCTGTGG rev AGTCGCACACCGTCCATCTC	p15	for GGACTAGTGGAGAAGGTGCG rev GGTGAGAGTGGCAGGGTCT
FST	for CCGGTGTTCCCTCTGTGATG rev TCCTCTTCCTCGGTGTCTTCC		

LUCIFERASE ASSAYS

For transient transfections, cells were typically plated in 24-well format and luciferase reporter plasmids were transfected with CMV-lacZ to normalize for transfection efficiency based on CPRG (Merck) colorimetric assay, together with plasmids encoding for the indicated proteins; DNA content was kept uniform by using pKS Bluescript. Cells were harvested in Luc lysis buffer (25mM Tris pH 7.8, 2.5mM EDTA, 10% glycerol, 1% NP40). Luciferase activity was determined in a Tecan plate luminometer with freshly reconstituted assay reagent (0.5mM D-Luciferin, 20mM Tricine, 1mM $(MgCO_3)4Mg(OH)_2$, 2.7mM $MgSO_4$, 0.1mM EDTA, 33mM DTT, 0.27mM CoA, 0.53mM ATP). For stable cell lines, cells were plated in 12-well format and treated as indicated before harvesting; normalization was based on total protein content, as measured by Bradford assays. Each sample was transfected at least in two biological duplicates in each experiment to determine the experimental variability; each experiment was repeated independently with consistent results.

DETERMINATION OF INTRACELLULAR dNTP POOLS

100mm dishes plated at 70% of confluence were cooled on ice. Cells were then carefully washed free of medium and extracted with ice-cold 60% methanol. After immersion for 3 min in a boiling water bath the methanolic extract was centrifuged and brought to dryness by centrifugal evaporation. The dry residue was dissolved in 0.2 ml of water and used for assays. We analyzed two aliquots of different size per each sample to ascertain linearity of the assay. The cells remaining after extraction were dissolved in 0.3 M NaOH. The A_{260nm} of the NaOH fraction containing the cellular macromolecules left after pool extraction was used as an index of cell mass[130]. The sizes of the dNTP pools were determined with a DNA polymerase-based assay as in[131] by Dr. Chiara Rampazzo and Dr. Elisa Franzolin (Unipd).

MICROARRAYS AND GLUCOSE SIGNATURES

For microarrays of genes regulated by glucose uptake, cells were plated in 60mm plates, treated with 2DG and harvested after 24h. For YAP/TAZ regulated genes, cells were plated in 60mm plates, transfected with siRNA and harvested 48h after transfection. For each experimental condition, we prepared 4 biological replicates that were processed in parallel. Total RNA was extracted using RNeasy Mini Kit (Qiagen) and contaminant DNA was removed by RNase-Free DNase Set (Qiagen). RNA quality and purity were assessed on the Agilent Bioanalyzer 2100 (Agilent Technologies); RNA concentration was determined using the NanoDrop ND-1000 Spectrophotometer (NanoDrop Technologies). As control of effective gene modulation and of the whole procedure, we monitored the expression levels of established markers (*TXNIP* for 2DG, *CTGF* and *ANKRD1* for YAP/TAZ) by qPCR prior to microarray hybridization. Labeling and hybridization were performed according to Affymetrix One Cycle Target Labeling protocol on HG-U133 Plus 2.0 arrays (Affymetrix). Microarray data are available at Gene Expression Omnibus under accession GSE59232.

All data analyses were performed in R (version 3.0.2) using Bioconductor libraries (BioC 2.13) and R statistical packages. Probe level signals were converted to expression values using robust multi-array average procedure RMA of Bioconductor *affy* package. Differentially expressed genes were identified

using Significance Analysis of Microarray algorithm coded in the *samr* R package. In SAM, we estimated the percentage of false positive predictions (i.e., False Discovery Rate, FDR) with 100 permutations.
To identify genes associated with high glucose uptake in cells of mammary origin (glucose signature), we compared the expression levels of MCF10A and MDA-MB-231 cells grown in high glucose or in the presence of 2DG and selected those probe sets with a fold change ≤ -3 in both MCF10A and MDA-MB-231 comparisons. This selection resulted in 298 probesets downregulated by the presence of 2DG in the culture medium. We then refined this selection eliminating from the glucose signature the genes that were also regulated upon knockdown of YAP/TAZ, i.e. removing 2DG-regulated genes with an FDR ≥ 0.1% in the comparisons between YAP/TAZ depleted MCF10A and MDA-MB-231 cells and their controls.
To functionally annotate genes co-regulated by glucose and YAP/TAZ we consider the Biological Process Gene Ontology (GO) categories of the Database for Annotation, Visualization and Integrated Discovery (DAVID) GO terms were considered significant at a confidence level of 95%.
The analysis was carried out by Prof. Silvio Bicciato and Dr. Mattia Forcato (Unimore).

DROSOPHILA ASSAYS

All the strains were obtained from the Bloomington Stock Center and grown under standard conditions. For Flippase activation, non-overcrowded cultures of 48±6h after egg laying individuals grown at 25°C on standard medium were transferred to a water bath at 37°C for 20 minutes. After additional 72h at 25°C, larvae were dissected for analyses. Genotypes analysed were: *yw,hs-Flp,tub-Gal4,UAS-GFP/w; tub-Gal80,FRT40A/l(2)gl*^{4}*,FRT40A; UAS-yki/+* and *yw,hs-Flp,tub-Gal4,UAS-GFP/w; tub-Gal80,FRT40A/l(2)gl*^{4}*,FRT40A; UAS-yki/UAS-PfkRNAi*.
For immunostainings, larvae were dissected in PBS1X and carcasses were fixed, washed and immunostained following standard methods. Primary antibodies were: rabbit aPKC (Santa Cruz Biotechnology, 1:200), mouse DIAP1 (B. Hay, 1:200) and mouse dMyc (P. Bellosta, 1:5). Secondary antibodies were: anti-mouse Alexa Fluor 555 (Life Technologies) and anti-rabbit DyLight CY5 (Jackson Immunoresearch). Wing discs were isolated, mounted in Vectashield (Vectorlabs) and images were acquired by Leica TCS SP2 confocal microscope. All figures show single, 1mm thick tissue sections.
Clone areas (in pixel^{2}) were measured using ImageJ free software (NIH) on images captured with 90i wide fluorescence microscope (Nikon). Areas of clones grown as multilayers are likely to be underestimated. Discs were scored for clones included in the wing pouch region for a total of 34 discs, and the average clone area was normalized to the wing pouch size.
The analysis was carried out by Prof. Annalisa Pession and Prof. Daniela Grifoni (Unibo).

ANTIBODIES AND MICROSCOPY

Antibodies were FLAG-M2 HRP- or agarose-conjugate (Sigma), YAP/TAZ (sc101199), YAP for IP (Abcam 52771), TAZ for IP (Sigma HPA039557), phospho S127 YAP (CST4911), PFK1 (Abcam 119796, sc130227 or CST5412),

TEAD1 (BD 610922), TEAD1 for IP (Abcam 133533), TEAD4 (sc101184), MYC (sc789), total S6 (CST2217), phospho S6 (CST5364), AMPK (CST2532), GAPDH (Millipore MAB374), Hras (sc-520), RRM2 (sc-10844), p21 (BD 610234), Lamin B (sc-6216), Cyclin A2 (sc-596).
For immunofluorescence, cells were fixed for 10 minutes in 4% PFA, washed in PBS and either stored dried at -80°C or directly permeabilized and processed for immunostaining as described in[31]. Proximity Ligation Assays were performed as indicated by the provider's protocol (OLink Bioscience), after an overnight incubation with primary antibodies following our standard protocol. For PLA, antibodies were YAP (CST4912) and TEAD1 BD and PFK1 sc. pictures were taken at the confocal microscope by selecting the maximal nuclear section. Images were acquired with a Leica SP5 confocal microscope equipped with CCD camera using Volocity software (Perkin Elmer).
For BrdU, cells were fixed and processed according to manifacturer's instructions (BrdU cell proliferation kit, Merck) and images acquired with a Leica DM5000B microscope.

SENESCENCE MARKERS ANALYSIS

Reference time frame for the analyses of senescence markers:
Day 0: cellular selection with puromycin (48h after retroviral infection); Day 6: analysis of senescence markers (% S-phase, SA-βgal, SAHF, p16, p21, p15, cyclin A2, cyclin B1, CDCA7, lamin B).
After the end of the selection cells were plated at low confluence in 13mm dishes. On day 6, cells were incubated with EdU (for analysis of the S-phase) for 1h before fixing them with 3,7% formaldehyde for 15min. Cells were then either left in PBS at 4°C (for few days only) or analyzed according to manifacturer's instructions (Life Technologies).
SA-βgal staining was performed on day 6 as previously described[115].
SAHF were visualized by DAPI staining on fixed cells.

IMMUNOPRECIPITATIONS

For immunoprecipitations, cells were lysed in HPO buffer (50mM Hepes pH 7.5, 100mM NaCl, 50mM KCl, 2mM MgCl2, 1% Triton X100, 0.5% NP40, 5% glycerol) with proteases (Merck) and phosphatases (Sigma) inhibitors, and homogenized by sonication (Diagenode Bioruptor). Extracts of equal total protein content and concentration were then subjected to immunoprecipitation with primary antibodies previously bound to proteinA-conjugated sepharose (GE Healthcare) in 2% BSA. Control IgG for pulldowns with anti YAP and anti TEAD1 rabbit antibodies was anti HA rabbit polyclonal (sc805). After 2,5h of incubation on a rotator at 4°C, beads were washed three times in the same buffer and the purified proteins were boiled in Laemli Final Sample Buffer for western blotting with species-specific secondary HRP-conjugated antibodies (ExactaCruz).
For studies with recombinant proteins, GST-YAP and GST-TEAD4 were produced and purified from bacteria with standard protocols; FLAG-PFK1 and FLAG-TEAD1 were purified from HEK293 transfected lysates by anti-FLAG-M2 immunoprecipitation, followed by elution with 3XFLAG peptide (Sigma). All proteins were dyalised in BC100. Proteins were mixed in HPO buffer with 5% BSA and incubated for 2h at 4°C, followed by another 30 min together with anti-

FLAG-M2 agarose conjugated beads. Beads were washed three times in the same buffer and the purified proteins were boiled in Laemli Final Sample Buffer for western blotting.
For mass-spectrometry of YAP interacting proteins, 50% confluent cultures (150mm dishes) of MCF10A or MDA-MB-231 cells stably expressing FLAG-YAP-5SA were harvested in 1ml HPO buffer and homogenized by sonication. Controls were parental cells. Freshly prepared extracts from two sibling plates were joined and subjected to immunoprecipitation with agarose-conjugated FLAG M2 antibody for 2,5h at 4°C on a rotator. After three washes in the same buffer, immunopurified proteins were eluted by adding 3XFLAG peptide (Sigma) for 30 min at 4°C, in order to reduce aspecific purification of proteins on agarose beads. Eluted proteins were run in a 4-12% MOPS-SDS gel (LifeTechnologies) to separate them from the elution peptides, fixed and stained with colloidal coomassie. The gel was sent to EMBL Proteomic Facility for in gel tryptic digestion and mass spectrometry. Proteins purified with similar frequency from control and FLAG-YAP expressing lysates were considered non-specific background; all other proteins were considered for further analysis.

CHROMATIN IMMUNOPRECIPITETION

Cells were plated in duplicate, using two 150mm dishes for each replicate. After the indicated treatments, cells were crosslinked by adding to the culture medium 1/10 of fresh formaldehyde solution (11% formaldehyde 0.1M NaCl, 1mM EDTA, 0.5mM EGTA, 50mM HEPES pH 7.5) for 10min at RT, followed by quenching with 125mM Glycine for 5 min. After washing in PBS, cells were harvested in PBS with protease inhibitors and pelleted for 5min at 1500rcf at 4°C. Cells were resupended in cold LB1 (10mM NaCl; 1mM EDTA; 50mM; HEPES pH 7.5; 10% Glycerol; 0.5% NP-40; 0.25% Triton-X-100) and incubated for 20min; pelleted and resuspended in LB2 (10mM TRIS pH 8.0; 200mM NaCl; 1mM EDTA; 0.5mM EGTA) and incubated for 10min; pelleted and resuspended in sonication buffer (10mM TRIS pH 8.0; 1mM EDTA; 100mM NaCl; 0.5mM EGTA; 0.1% NaDeoxycholate; 0.5% N-Lauroylsarcosine). Sonication was carried out with a Branson Sonfier 450 to obtain sheared chromatin of 200-600bp fragments. Effective sonication and quantification of the DNA to equalize samples was carried out on 1% of each sample after decrosslinking; this sample was also used as input control for qPCR. The same total amount of sheared chromatin per sample (in the range of 120mg) was supplemented with 1% Triton X100 and subjected to immunoprecipitation o.n. at 4°C with anti-YAP (Abcam) or with control rabbit IgG. ProteinA-dynabeads (LifeTechnologies) were added for 2h after extensive blocking in 0,5% BSA. Washes were (5min each): low salt (0,1% SDS, 2mM EDTA, 1% Triton X100, 20mM Tris pH=8, 150mM NaCl), high salt (500mM NaCl), low salt, high salt, TE + 50mM NaCl. Immunoprecipitated material was eluted from the beads by incubating 20min at 65°C in TE + 1% SDS. Supernatant was decrosslinked o.n. at 65°C, diluted 1:2 in TE, treated 1h at 37°C with RNaseA (0.2mg/ml), followed by 1h at 55°C with ProteinaseK. After phenol-chloroform extraction and ethanol precipitation, DNA was resuspended in water for qPCR analysis. The amount of DNA present in each immunoprecipitate was quantified as the fraction of its input. Sequences of primers are the following:

Primers for ChIP	sequences
CTGF	for TGTGCCAGCTTTTTCAGACG
	rev TGAGCTGAATGGAGTCCTACACA
ANKRD1	for AAAAAGGGCAGTGATGTGGTG
	rev GAAGAGGGAGGGGAGGACAA
HMMR	for TGGAACCAGTGAAGCCGGAAC
	rev CCTGCGAGTTTAGGCTGCCA
TK1	for TGGGCAGGTTAATGCAGCTC
	rev CGGGAACCAGGGGCTTACT
HBB (negative control)	for GCTTCTGACACAACTGTGTTCACTAGC
	rev CACCAACTTCATCCACGTTCACC

OVER-REPRESENTATION GSEA ANALYSIS

Over-representation analysis was performed using Gene Set Enrichment Analysis and gene sets derived from previously published gene signatures. For details see[1] GSEA software was applied on log2 expression data of MCF10A and MDA-MB-231 cells grown in high glucose or in the presence of 2DG. Gene sets were considered significantly enriched at FDR<5% when using Signal2Noise as metric and 1,000 permutations of gene sets. The analysis was carried out by Prof. Silvio Bicciato and Dr. Mattia Forcato (Unimore).

AVERAGE SIGNATURE EXPRESSION AND SIGNATURE SCORES

Average signature expression has been calculated as the standardized average expression of all signature genes in sample subgroups (i.e. 2DG treated/controls; histological grade). Signature scores have been obtained summarizing the standardized expression levels of signature genes into a combined score with zero mean. The values shown in graphs are thus adimensional. The analysis was carried out by Prof. Silvio Bicciato and Dr. Mattia Forcato (Unimore).

COLLECTION AND PROCESSING OF BREAST CANCER GENE EXPRESSION DATA

We started from a collection of 4.640 samples from 27 major datasets comprising microarray data of breast cancer samples annotated with histological tumor grade and clinical outcome. All data were measured on Affymetrix arrays and have been downloaded from NCBI Gene Expression Omnibus (GEO, and EMBL-EBI ArrayExpress).

Prior to analysis, we re-organized all datasets eliminating duplicate samples and re-naming any original set after the medical center where patients were recruited. This re-organization resulted in a compendium (*meta-dataset*) comprising 3.661 unique samples from 25 independent cohorts. The type and content of clinical and pathological annotations of the meta-dataset samples have been derived from the original cohorts.

Since raw data (.CEL files) were available for all samples, the integration, normalization, and summarization of gene expression signals has been obtained applying the procedure described in[132]. Briefly, expression values were generated from intensity signals using a custom-CDF obtained merging HG-U133A, HG-U133AAofAV2, and HG-U133 Plus2 original CDFs and transforming the original CEL files accordingly. Intensity values for a total of 21986 probe sets have been

background adjusted, normalized using quantile normalization, and gene expression levels calculated using median polish summarization (multi-array average procedure, RMA). Clinical information among the various datasets has been standardized as described in[45]. The analysis was carried out by Prof. Silvio Bicciato and Dr. Mattia Forcato (Unimore).

KAPLAN-MEIER SURVIVAL ANALYSIS

To identify two groups of tumors with either high or low glucose signature we used the classifier described in[133], i.e. a classification rule based on the Glucose signature score. Tumors were classified as glucose signature *Low* if the combined score was negative and as glucose signature *High* if the combined score was positive. This classification was applied to expression values of the meta-dataset. To evaluate the prognostic value of the glucose signature, we estimated, using the Kaplan-Meier method, the probabilities that patients would remain free of metastatic. To confirm these findings, the Kaplan-Meier curves were compared using the log-rank (Mantel-Cox) test. P-values were calculated according to the standard normal asymptotic distribution. Survival analysis was performed in GraphPad Prism. The analysis was carried out by Prof. Silvio Bicciato and Dr. Mattia Forcato (Unimore).

STATISTICAL ANALYSIS

Statistical analysis were performed using Prism software (GraphPad Software). Mean values and standard deviations (SD) are shown in graphs that were generated from several repeats of biological experiments, unless otherwise indicated. Immunoprecipitation experiments were performed with n=2 biological replicates for each sample, and repeated at least two times independently with comparable results. The analysis was carried out by Prof. Silvio Bicciato and Dr. Mattia Forcato (Unimore).

Figures

FIGURE 1. Exploring possible links between glucose metabolism and YAP/TAZ activity

A) Over-representation analysis was performed with Gene-Signatures highlighting activation of specific pathways using Gene Set Enrichment Analysis (GSEA) on microarray data obtained from MCF10A or MDA-MB-231 mammary cells untreated or treated with 2-deoxy-glucose (2DG, 50mM) to inhibit glucose metabolism. The normalized enrichment score (NES) is the primary statistic for examining GSEA results; a positive NES (highlighted in red) indicates signatures expressed more in control cells than upon 2DG treatment (i.e. signatures activated when glucose metabolism is on); a negative NES (highlighted in blue) indicates signatures expressed more upon 2DG treatment. The false discovery rate (FDR) is the estimated probability that a gene set with a given NES represents a false positive; we considered signatures to be significantly enriched at FDR<0.05. Gene expression data has been obtained from n=4 biological replicates for each condition.

B) 2DG treatment downregulates the overall levels of the "YAP/TAZ", "YAP", "induced by YAP" and "repressed by YAP" gene signature used in (A) as calculated from microarray data of cells untreated (white bars) or treated with 2DG (black bars). Data are shown as mean ± standard error of the mean (SEM).

C) The plot indicates basal oxygen consumption rate (OCR, indicative of mitochondrial respiration) and extracellular acidification rate (ECAR, indicative of aerobic glycolysis) of MCF10A and MDA-MB-231 cells as measured with an extracellular flux analyzer and normalized to total protein content. Representative results of a single experiment with n=5 biological replicates; 2 independent experiments were consistent.

D) Representative traces of ECAR (left) and OCR (right) performed with an extracellular flux analyzer on monolayers of MCF10A-MII cells. Blue: control cells; red: cells stably expressing activated TAZ-S89A. Representative results of a single experiment with n=5 biological replicates; 2 independent experiments were consistent.
Left: Cells were kept in glucose-free medium and subsequently supplemented with Glucose (10mM), with the ATP synthase inhibitor Oligomycin (0.8mM), with the Glucose inhibitor 2DG (100mM) respectively to enable glycolysis, to measure maximal glycolytic capacity, and to completely inhibit glycolysis.
Right: Subsequent additions of the ATP synthase inhibitor Oligomycin (0.8mM), the uncoupler FCCP (900nM), the electron transport chain (ETC) complex I inhibitor Rotenone (1mM) and the ETC complex III inhibitor antimycin A (1mM) were carried out respectively to measure basal respiration (initial time points), respiration coupled to ATP production in mitochondria, maximal respiratory capacity and non-mitochondrial oxygen consumption.

A

	MCF10A		MDA-MB-231	
Gene Signature	NES	FDR q-val	NES	FDR q-val
YAP-TAZ	12,18	0	8,82	0
INDUCED BY YAP	10,36	0	8,12	0
MUTP53	9,61	0	9,00	0
MYC_b	4,13	0	3,68	0
TCF4	3,84	0	2,74	0
YAP	3,67	0	2,28	0,001
E2F3	3,58	0	3,17	0
MYC_a	3,49	0	2,13	0,003
RAS	2,78	0	-4,68	0
STAMINAL	2,70	0	2,18	0,002
TGFBETA_c	1,88	0,014	-3,30	0
STEM TUMORIGENIC	1,75	0,027	2,35	0
TGFBETA_a	1,53	0,077	-2,59	0,001
WTP53	1,26	0,208	1,24	0,224
SRC	1,15	0,289	-1,28	0,224
HIF	0,80	0,717	-0,97	0,511
WNT	-0,80	0,723	0,96	0,488
ERBB2	-1,04	0,433	-1,01	0,500
BETACATENIN	-1,29	0,210	1,34	0,164
NFKB	-1,51	0,096	-1,37	0,196
SHARP1	-1,62	0,062	-0,89	0,580
STAT3	-1,77	0,033	-2,09	0,008
TGFBETA_b	-2,32	0,001	-2,77	0
NOTCH	-2,59	0	-1,92	0,016
NCID	-2,98	0	-1,30	0,228
REPRESSED BY YAP	-7,90	0	-3,35	0

B

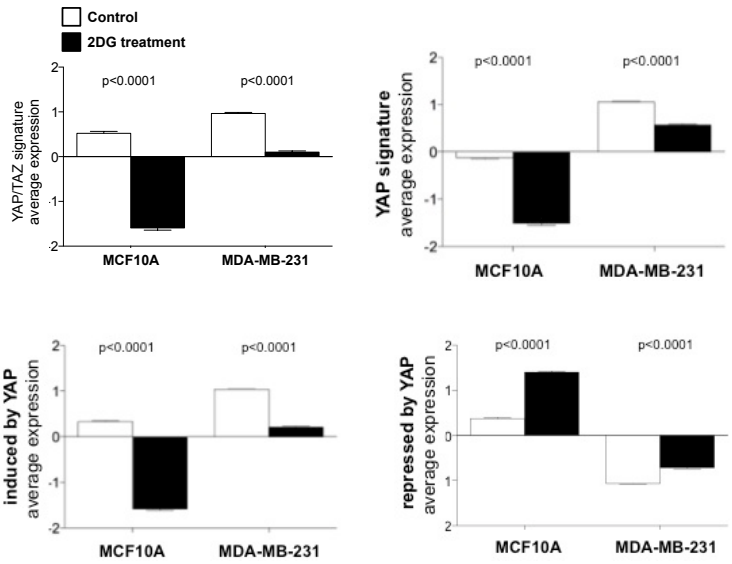

C

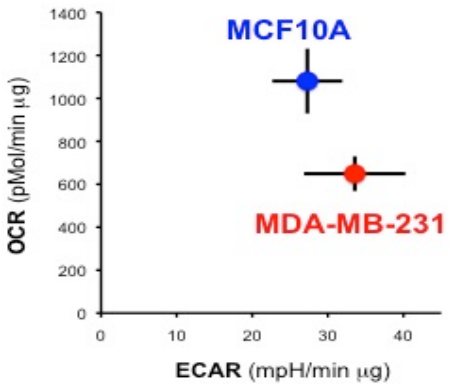

D

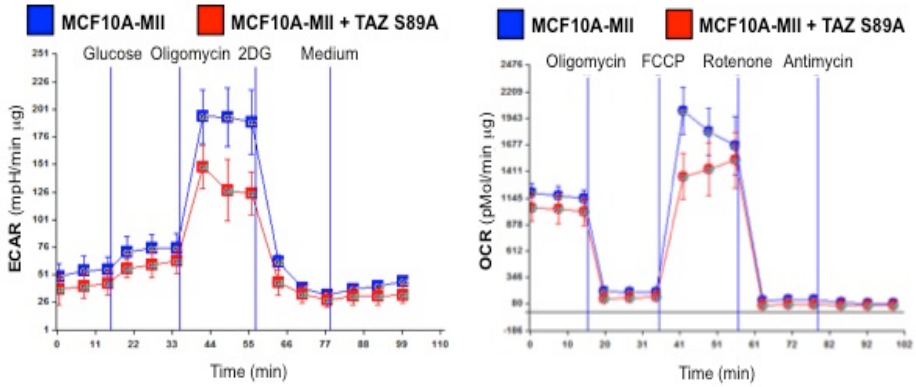

FIGURE 1

FIGURE 2. Glucose metabolism regulates YAP/TAZ transcriptional activity

A) Luciferase assay in MDA-MB-231 breast cancer cells transfected with the synthetic YAP/TAZ reporter 8XGTIIC-lux. Starting on the day after DNA transfection, cells were treated for 24h with the indicated small-molecule inhibitors to block glucose metabolism (50mM 2DG; 1mM Lonidamine, Loni) or with an inhibitor of the mitochondrial respiratory chain (1mM Oligomycin, Oligo). Activity of the reporter is normalized to cotransfected CMV-lacZ, and expressed relative to the cells treated with vehicle only (Co.). Representative results of a single experiment with n=2 biological replicates; 4 independent experiments were consistent.
In the case of 2DG treatment, cells were also released in fresh medium for 24h (fresh medium). Where indicated, cells were also transfected with YAP/TAZ (YT) siRNA. 2 independent experiments were consistent.

B) Luciferase assay in MDA-MB-231 cells treated for 24h with 2DG and/or with Mannose (25mM). Representative results of a single experiment with n=2 biological replicates; 2 independent experiments were consistent.

C) Luciferase assay in MDA-MB-231 cells transfected with the CTGF-luciferase reporter (containing the TEAD-binding region of the natural *CTGF* promoter[27]) and treated for 24h with 2DG, Lonidamine. 2 independent experiments were consistent. Where indicated cells were also transfected with the indicated control (Co.) and YAP/TAZ (YT) siRNAs.

D) Luciferase assay in Hs578T cells and treated with 2DG. Where indicated cells were also transfected with the indicated control (Co.) and YAP/TAZ (YT) siRNAs. Representative results of a single experiment with n=2 biological replicates; 2 independent experiments were consistent.

E) Luciferase assay in HepG2 cells treated with 2DG or Lonidamine to inhibit glucose metabolism. Representative results of a single experiment with n=2 biological replicates; 2 independent experiments were consistent.

F) Luciferase assay in MDA-MB-231 transfected with the Notch-responsive RBPJ-lux reporter alone (Co.) or in combination with increasing doses of constitutively-active Notch plasmid (NΔE, bearing deletion of the extracellular domain) and treated with 2DG. Representative results of a single experiment with n=2 biological replicates; 2 independent experiments were consistent.

G) Luciferase assay in MDA-MB-231 transfected with the 8XGTIIC-Rlux (Renilla-luciferase) or with the CMV-Rlux reporters, and treated with 2DG. Renilla luciferase, at difference with firefly luciferase, is not an ATP-dependent enzyme and therefore its activity is formally insensitive to ATP levels. Representative results of a single experiment with n=2 biological replicates; 2 independent experiments were consistent.

Unless indicated otherwise, error bars represent mean ± SD. * p-value<0,01 relative to control.

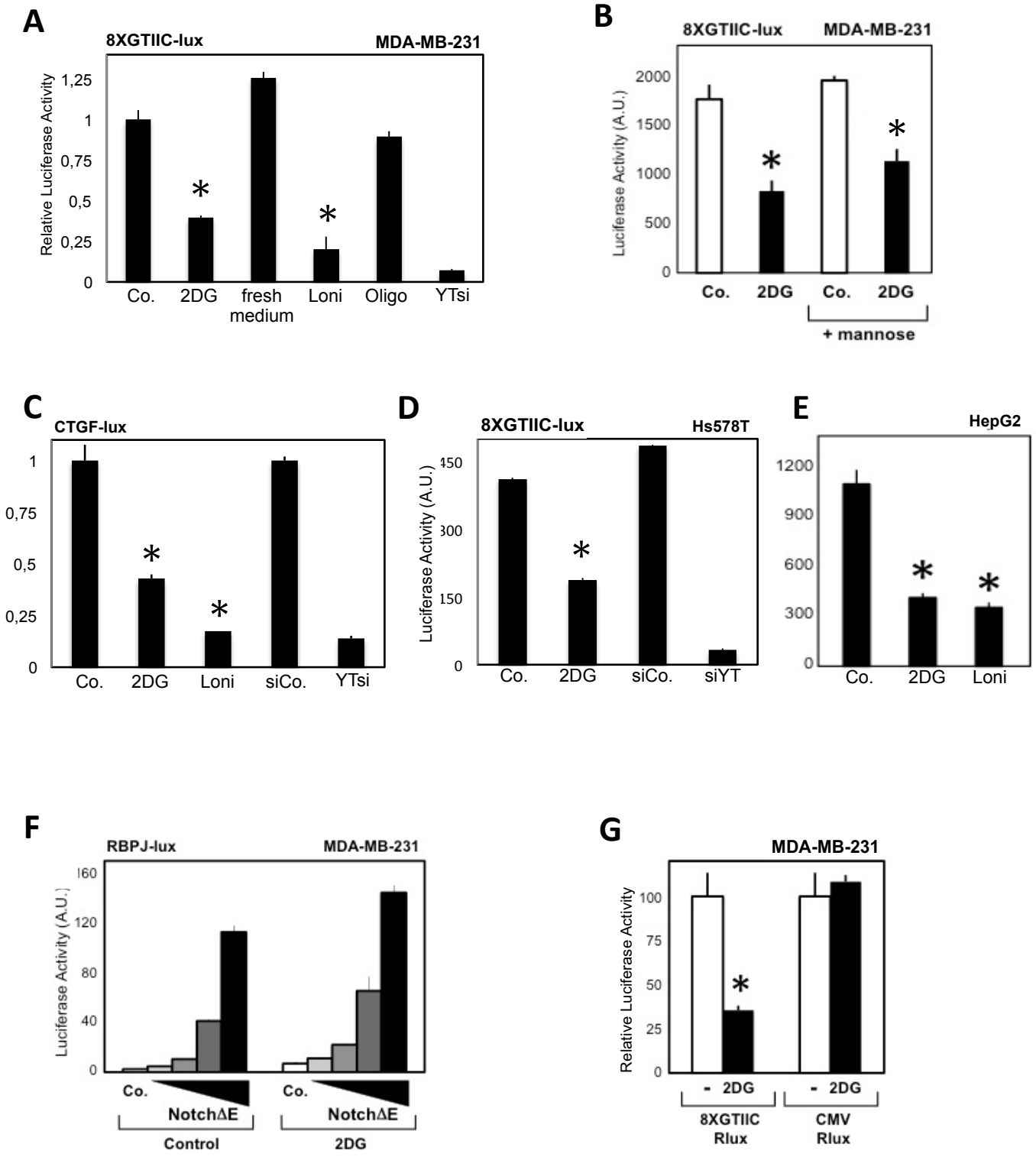
A
8XGTIIC-lux
MDA-MB-231
Relative Luciferase Activity
1,25
1
0,75
0,5
0,25
0
Co.
2DG
fresh medium
Loni
Oligo
YTsi
B
8XGTIIC-lux
MDA-MB-231
Luciferase Activity (A.U.)
2000
1500
1000
500
0
Co.
2DG
Co.
2DG
+ mannose
C
CTGF-lux
1
0,75
0,5
0,25
0
Co.
2DG
Loni
siCo.
YTsi
D
8XGTIIC-lux
Hs578T
Luciferase Activity (A.U.)
450
300
150
0
Co.
2DG
siCo.
siYT
E
HepG2
1200
900
600
300
0
Co.
2DG
Loni
F
RBPJ-lux
MDA-MB-231
Luciferase Activity (A.U.)
160
120
80
40
0
Co.
NotchΔE
Control
Co.
NotchΔE
2DG
G
MDA-MB-231
Relative Luciferase Activity
100
75
50
25
0
- 2DG
- 2DG
8XGTIIC Rlux
CMV Rlux

FIGURE 2

FIGURE 3. Evidence supporting a direct regulation of YAP/TAZ by glucose

A) Luciferase assay in MDA-MB-231 cells transfected with an E2F-responsive reporter (6XE2F-lux) (top) or with the YAP/TAZ reporter (8XGTIIC) (bottom) and treated with 2DG. As expected, co-transfection of plasmids encoding for the CDK inhibitors p16, p21 and p27 inhibits E2F activity, whereas YAP/TAZ activity is not repressed. Representative results of a single experiment with n=2 biological replicates; 2 independent experiments were consistent.

B) Luciferase assay in MDA-MB-231 cells bearing a stably integrated TRE-8XGTIIC-lux reporter. Before harvesting, cells were either left unstimulated (0) or supplemented with doxycycline to release transcription (4, 6, 8 and 10h).
Top: cells were transfected with the indicated control (Co.) and YAP/TAZ (YT) siRNAs for 48h; results indicate that doxycicline-induced transcription is YAP/TAZ dependent.
Bottom: 2DG (100mM) was added together with doxycycline to acutely block glucose metabolism. Representative results of a single experiment with n=2 biological replicates; 3 independent experiments were consistent.

C) Luciferase assay in MDA-MB-231 cells bearing a stably integrated TRE-8XGTIIC-lux reporter. Glucose was removed from the culture medium at the moment of doxycycline supplementation (- Glu). Cells were harvested 24h after treatment. Representative results of a single experiment with n=2 biological replicates; 3 independent experiments were consistent.

D) HepG2 cells were put in medium with (Co.) or without glucose for transfection of the luciferase reporter plasmid; after 36h, cells were either left for another 36h in absence of glucose (- Glu) or refed with glucose (+ Glu). Representative results of a single experiment with n=2 biological replicates; 2 independent experiments were consistent.

E) Luciferase assay in MCF10A-MII cells bearing a stably integrated TRE-CTGF-lux reporter. Cells were transfected with the indicated control (Co.) and YAP/TAZ (YT) siRNAs; after one day cells were either left unstimulated (0) or supplemented with doxycycline to release transcription (24h). Doxycicline-induced transcription is YAP/TAZ dependent. Representative results of a single experiment with n=2 biological replicates; 3 independent experiments were consistent.

F) Luciferase assay in MCF10A-MII cells bearing a stably integrated TRE-CTGF-lux reporter. Cells were left unstimulated (0) or supplemented with doxycycline (6, 8 and 10h of treatment) to release YAP/TAZ-dependent transcription (Co.). 2DG (100mM) was added together with doxycycline to acutely inhibit glycolysis. Representative results of a single experiment with n=2 biological replicates; 3 independent experiments were consistent.

G) Luciferase assay was carried out by removing glucose from the culture medium (- Glu) at the moment of doxycycline supplementation. Cells were harvested 24h after treatment. Representative results of a single experiment with n=2 biological replicates; 3 independent experiments were consistent.

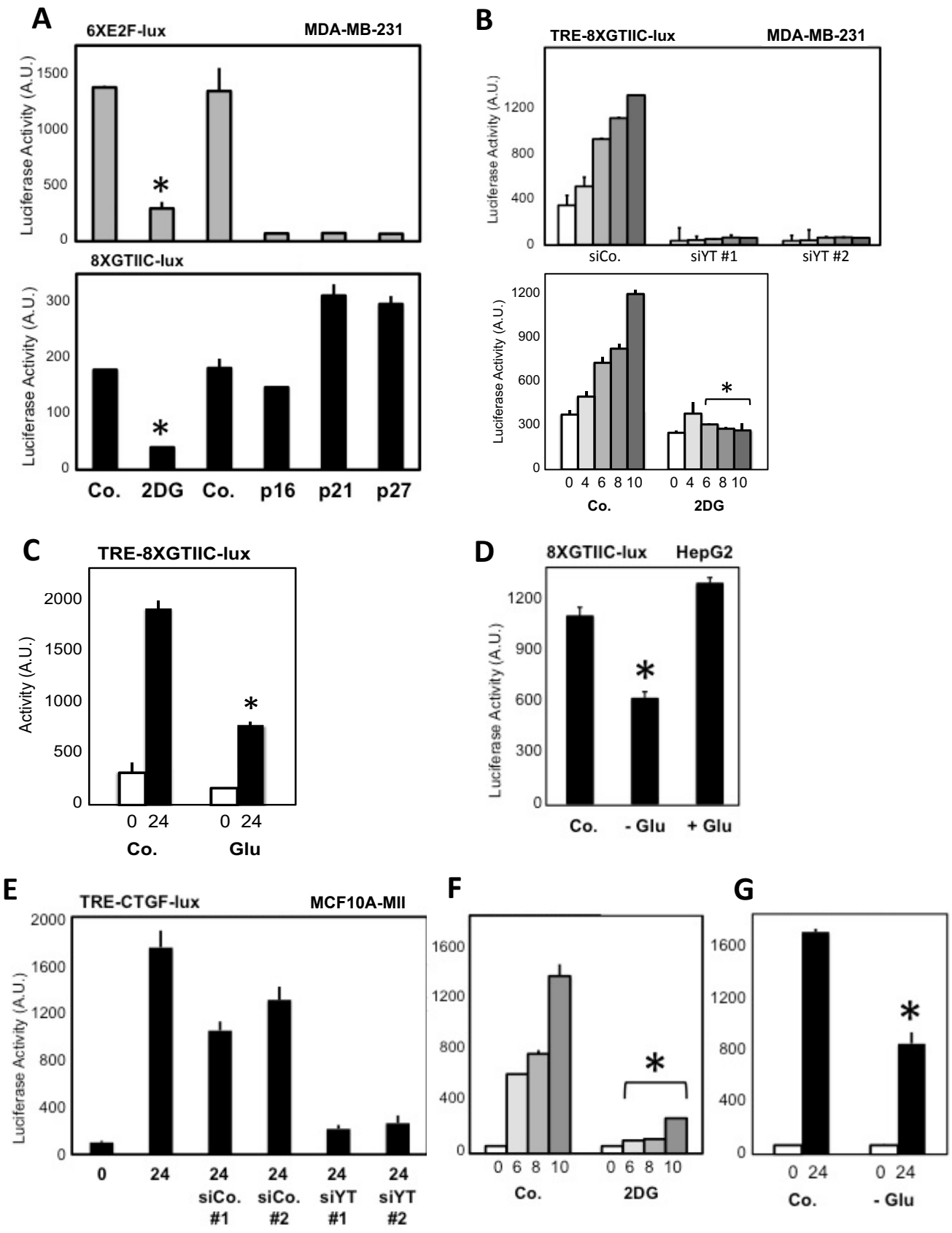
A
6XE2F-lux
MDA-MB-231
Luciferase Activity (A.U.)
8XGTIIC-lux
Co. 2DG Co. p16 p21 p27
B
TRE-8XGTIIC-lux
MDA-MB-231
siCo. siYT #1 siYT #2
0 4 6 8 10 0 4 6 8 10
Co. 2DG
C
TRE-8XGTIIC-lux
Activity (A.U.)
0 24 0 24
Co. Glu
D
8XGTIIC-lux HepG2
Co. - Glu + Glu
E
TRE-CTGF-lux
MCF10A-MII
0 24 24 siCo. #1 24 siCo. #2 24 siYT #1 24 siYT #2
F
0 6 8 10 0 6 8 10
Co. 2DG
G
0 24 0 24
Co. - Glu

FIGURE 3

FIGURE 4. Glucose metabolism and YAP/TAZ regulate a common set of genes important for proliferation

A) YAP/TAZ are required for transcription of 2DG-regulated genes. qPCR for endogenous target genes in MDA-MB-231 cells treated with water (Co.) or with 2DG, or transfected with the indicated siRNAs: control (siCo.), YAP/TAZ mix #1 (siYT1), YAP/TAZ mix #2 (siYT2). Expression levels were calculated relative to *GAPDH*, and are given relative to Co. cells (arbitrarily set to 1). Genes were selected among the probes commonly regulated in microrarray profiling. Both 2DG-induced and 2DG-inhibited genes were coherently regulated by YAP/TAZ knockdown. *YAP1* and *TAZ* levels serve as control for the efficiency of siRNA transfection. *TXNIP* is a positive control for 2DG-regulated transcription[11]. n=4 biological replicates from 2 independent experiments. All differences had p-value<0.01.

B) qPCR for endogenous target genes in Hs578T breast cancer cells treated with water (Co.) or with 2DG, or transfected with the indicated siRNAs: control (siCo.), YAP/TAZ (siYT). Expression levels were calculated relative to *GAPDH*, and are given relative to Co. cells (arbitrarily set to 1). n=4 biological replicates from 2 independent experiments. All differences have p-value<0.01.

C) Enrichment (expressed as –log10(p)) of Gene Ontology (GO) terms among the genes co-regulated by glucose metabolism and YAP/TAZ.

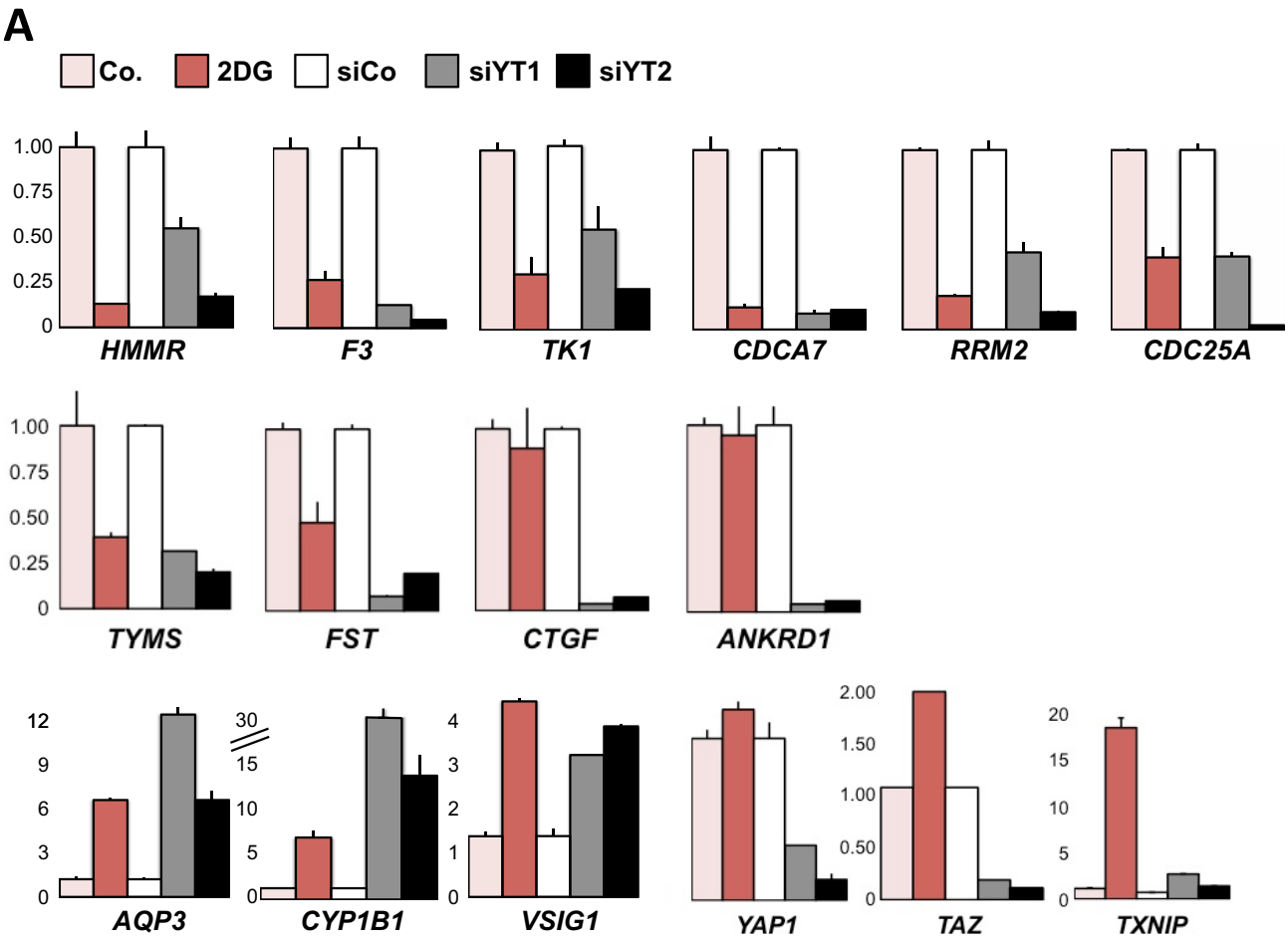
A
Co.
2DG
siCo
siYT1
siYT2
HMMR
F3
TK1
CDCA7
RRM2
CDC25A
TYMS
FST
CTGF
ANKRD1
AQP3
CYP1B1
VSIG1
YAP1
TAZ
TXNIP

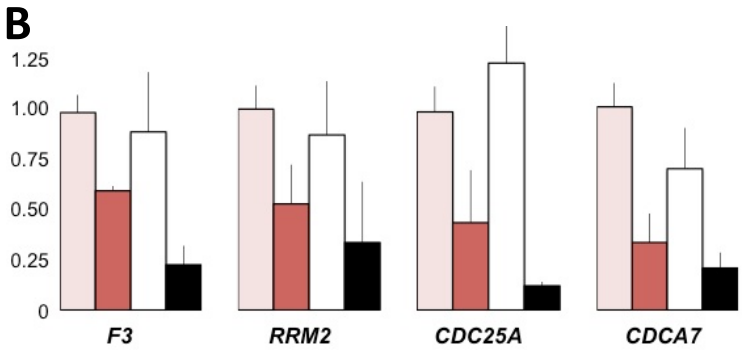
B
F3
RRM2
CDC25A
CDCA7

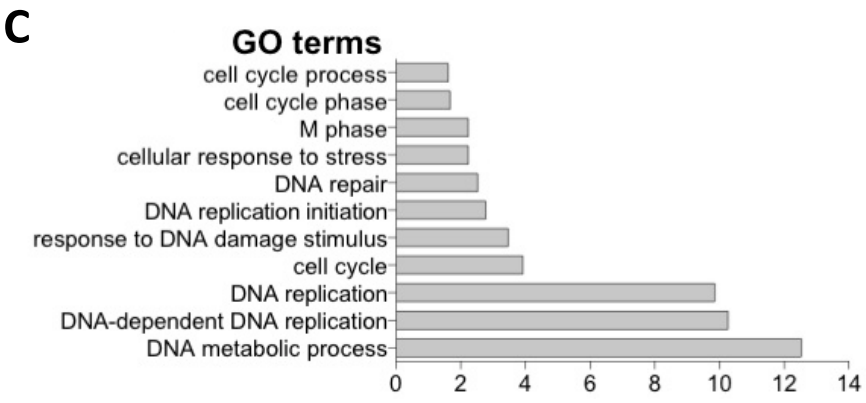
C
GO terms
cell cycle process
cell cycle phase
M phase
cellular response to stress
DNA repair
DNA replication initiation
response to DNA damage stimulus
cell cycle
DNA replication
DNA-dependent DNA replication
DNA metabolic process

FIGURE 4

FIGURE 5. Glycolysis sustains YAP/TAZ activity

A) A simplified scheme indicating the main metabolic routes followed by glucose, the key intermediates and enzymes involved, and the inhibitors used in this study. DON and AZS inhibit the enzyme mediating the first step of the hexosamine pathway[26,54,55]. Colored boxes indicate three pathways fueled by glucose. Dashed arrows indicate downstream intermediates or metabolic pathways.

B) Phosphoglucoisomerase (GPI) is required for YAP/TAZ activity. Luciferase assay in MDA-MB-231 cells transfected with the indicated siRNAs. See (C) for validation of siRNA efficiency. Representative results of a single experiment with n=2 biological replicates; 3 independent experiments were consistent.

C) qPCR for endogenous mRNA levels shows efficient depletion of *GPI* in MDA-MB-231 cells 48h after siRNA transfection. n=4 biological replicates from 2 independent experiments.

D) Luciferase assay in cells treated for 24h with chemical inhibitors of the glucosamine-fructose-6-phosphate transaminase enzyme (GFPT), mediating the first committed step of the hexosamine biosynthetic pathway (HBP). DON (30mM) is 6-diazo-5-oxo-L-norleucine; AZS (30mM) is O-diazoacetyl-l-serine. Doses were as in[26,54]. Control cells (Co.) were treated with the same concentration of vehicle alone (DMSO). Representative results of a single experiment with n=2 biological replicates; 2 independent experiments were consistent.

E) Luciferase assay in MDA-MB-231 cells treated for 24h with 2DG and/or with GlcNAc (30mM). GlcNAc supplementation can rescue protein glycosylation in cells with inhibited glucose metabolism[54], but is unable to rescue YAP/TAZ inhibition. Representative results of a single experiment with n=2 biological replicates; 2 independent experiments were consistent.

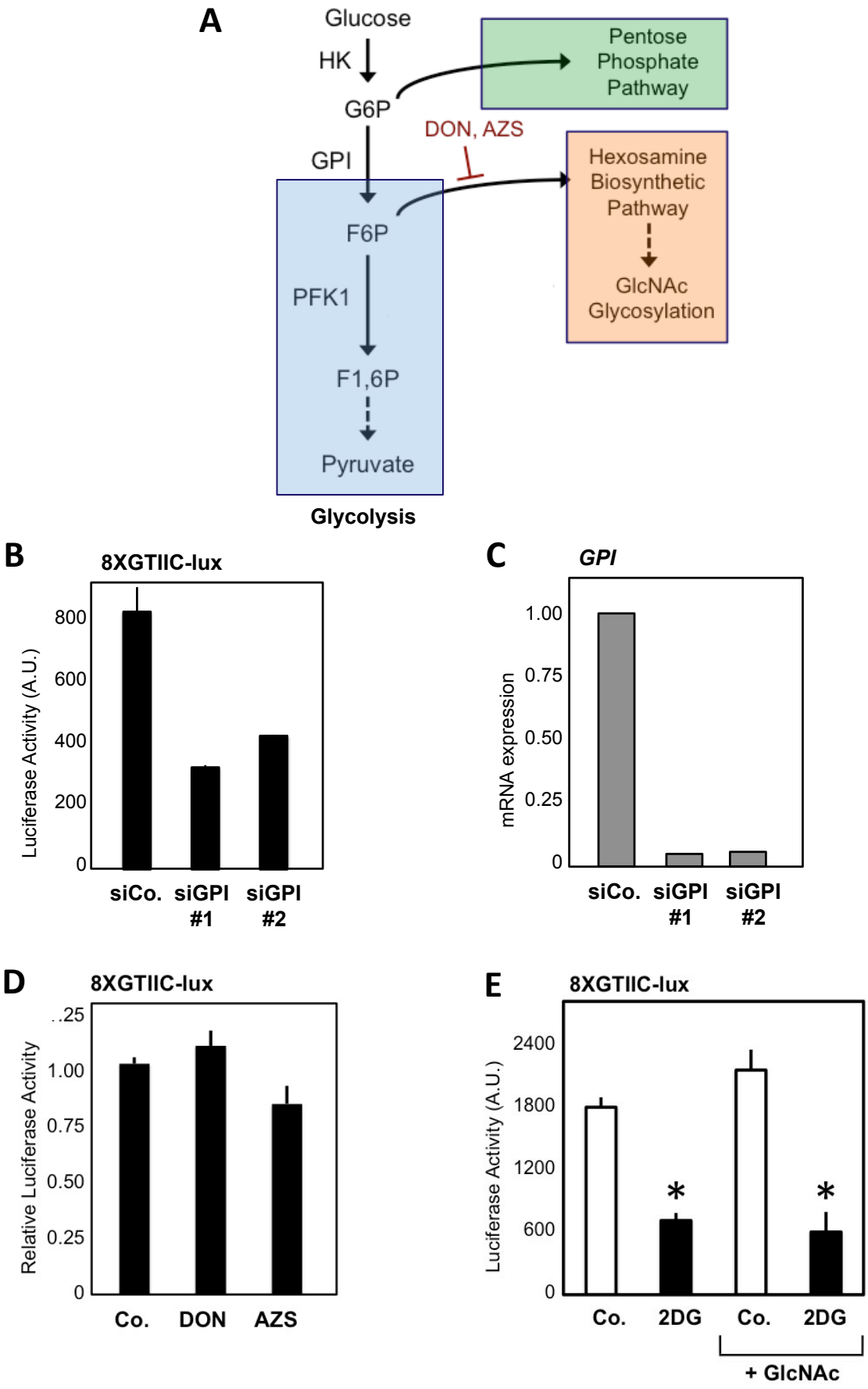
A
Glucose
HK
G6P
GPI
F6P
PFK1
F1,6P
Pyruvate
Glycolysis
Pentose Phosphate Pathway
DON, AZS
Hexosamine Biosynthetic Pathway
GlcNAc Glycosylation
B
8XGTIIC-lux
Luciferase Activity (A.U.)
800
600
400
200
0
siCo.
siGPI #1
siGPI #2
C
GPI
mRNA expression
1.00
0.75
0.50
0.25
0
siCo.
siGPI #1
siGPI #2
D
8XGTIIC-lux
Relative Luciferase Activity
1.00
0.75
0.50
0.25
0
Co.
DON
AZS
E
8XGTIIC-lux
Luciferase Activity (A.U.)
2400
1800
1200
600
0
*
*
Co.
2DG
Co.
2DG
+ GlcNAc

FIGURE 5

FIGURE 6. Modulation of glycolytic levels causes a corresponding variation in YAP/TAZ activity

A) The plot indicates basal oxygen consumption rate (OCR) and extracellular acidification rate (ECAR) of TRE-8XGTIIC-lux MDA-MB-231 cells grown in glucose (red, Glu) or 10mM galactose (blue, Gal). As expected, galactose induces a metabolic shift from aerobic glycolysis to oxidative phosphorylation compared to glucose. Representative results of a single experiment with n=5 biological replicates; 2 independent experiments were consistent.

B) Representative traces of OCR (indicative of mitochondrial respiration) performed with an extracellular flux analyzer on monolayers of MDA-MB-231 cells cultured in glucose (red) or in galactose (blue). Subsequent additions of the ATP synthase inhibitor Oligomycin (0.8mM), the uncoupler FCCP (400nM), the electron transport chain (ETC) complex I inhibitor Rotenone (1mM) and the ETC complex III inhibitor antimycin A (1mM) were carried out. Galactose-fed cells display enhanced respiration and respirator capacity. Representative results of a single experiment with n=5 biological replicates; 2 independent experiments were consistent.

C-D) Representative traces of ECAR (indicative of aerobic glycolysis) performed with an extracellular flux analyzer on monolayers of MDA-MB-231 cells cultured in glucose (red) or in galactose (blue). In (C), subsequent additions of the ATP synthase inhibitor Oligomycin (0.8mM), the uncoupler FCCP (400nM), the electron transport chain (ETC) complex I inhibitor Rotenone (1mM) and the ETC complex III inhibitor antimycin A (1mM) were carried out. Galactose-fed cells display reduced basal and maximal glycolysis levels. In (D), cells were kept in sugar-free medium and subsequently supplemented with Glucose (10mM), with the ATP synthase inhibitor Oligomycin (0.8mM), with the glucose inhibitor 2DG (100mM) and with culture medium. Galactose-fed cells resume to normal or even higher glycolysis levels upon addition of Glucose. Representative results of a single experiment with n=5 biological replicates; 2 independent experiments were consistent.

E-F) Glucose-induced activity of the stably integrated TRE-8XGTIIC-lux reporter in MDA-MB-231. In (E), the activity of the reporter depends on endogenous YAP/TAZ, as shown by siRNA transfection. 2 independent experiments were consistent. In (F), comparison of YAP/TAZ activity in cells grown in glucose (red, Glu), in galactose to induce a shift toward oxidative respiration (blue, Gal), or shifted back to glucose during doxycycline treatment (blue bars with red stripes, Gal + Glu). Cells were treated with doxycycline to release YAP/TAZ-dependent luciferase transcription for 8 or 24h. Galactose-fed cells display reduced glycolysis and downregulate YAP/TAZ activity. Glucose rapidly reactivates glycolysis (D) and YAP/TAZ activity (Gal + Glu). 3 independent experiments were consistent.

G) Luciferase assay in UOK262 kidney cancer cells, bearing mutation of the fumarate hydratase (FH) enzyme of the TCA cycle. FH-reconstituted cells (gray bars) display a reduction of aerobic glycolysis and increased respiration[59]. 2DG treatment (12mM) of parental cells serves as a positive control for inhibition of the glycolysis-YAP/TAZ axis. 2 independent experiments were consistent.

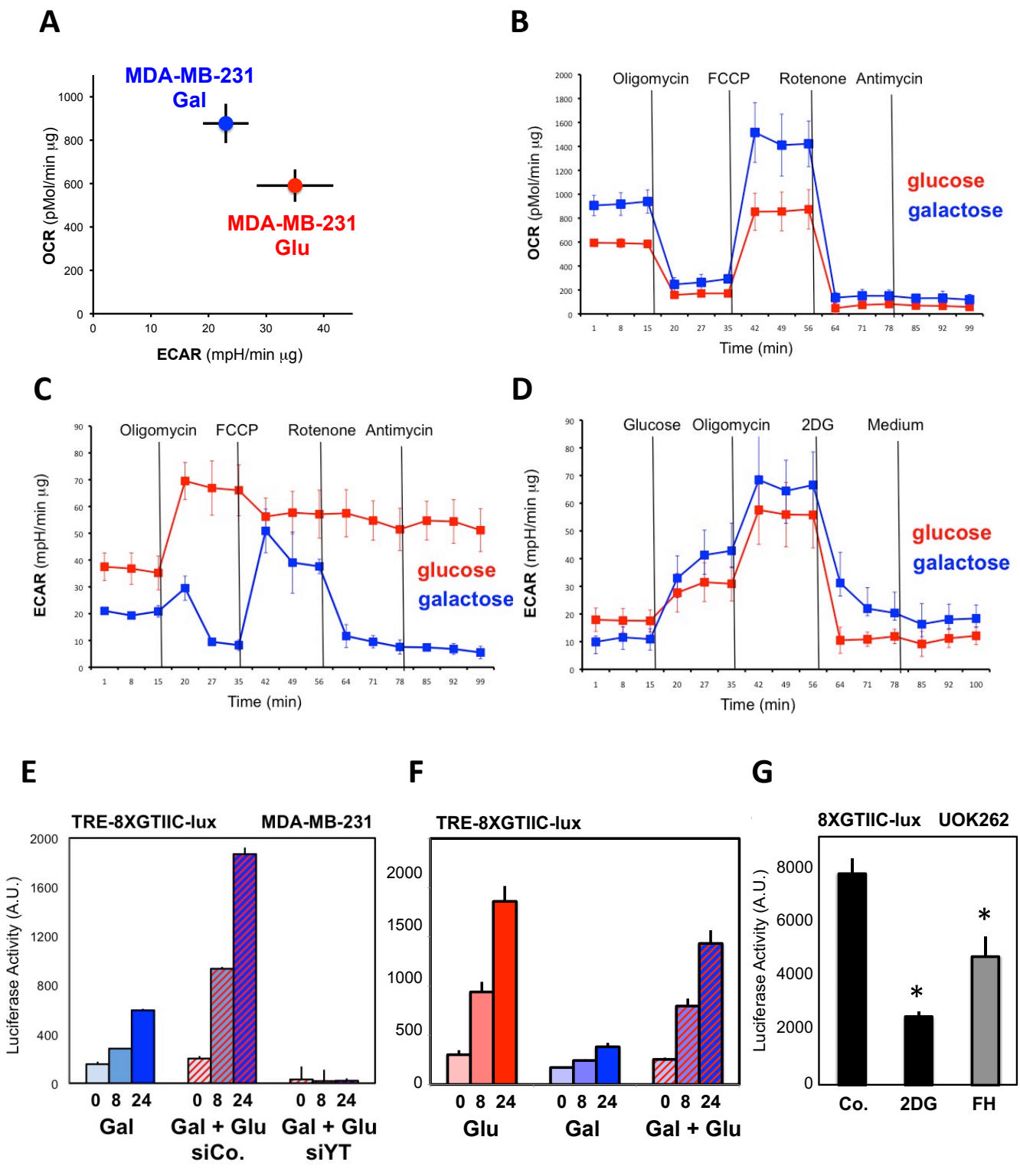
A
MDA-MB-231
Gal
MDA-MB-231
Glu
OCR (pMol/min µg)
ECAR (mpH/min µg)
B
Oligomycin
FCCP
Rotenone
Antimycin
glucose
galactose
OCR (pMol/min µg)
Time (min)
C
Oligomycin
FCCP
Rotenone
Antimycin
glucose
galactose
ECAR (mpH/min µg)
Time (min)
D
Glucose
Oligomycin
2DG
Medium
glucose
galactose
ECAR (mpH/min µg)
Time (min)
E
TRE-8XGTIIC-lux
MDA-MB-231
Luciferase Activity (A.U.)
0 8 24
Gal
Gal + Glu
siCo.
Gal + Glu
siYT
F
TRE-8XGTIIC-lux
0 8 24
Glu
Gal
Gal + Glu
G
8XGTIIC-lux
UOK262
Luciferase Activity (A.U.)
Co.
2DG
FH

FIGURE 6

FIGURE 7. YAP/TAZ regulation by glucose metabolism does not involve known YAP/TAZ regulators or energy-sensing pathways

A) Hippo signaling is not involved in regulation of YAP/TAZ by 2DG. Luciferase assay in cells transfected with control (siCo.) or with an established LATS1/2 siRNA mix (siLATS1/2)[32], and then either treated with 2DG (black bars) or transfected with NF2 expression plasmid to specifically activate the Hippo pathway (green bars). Depletion of LATS1/2 blocked the inhibitory effect of overexpressed NF2, but not of 2DG. Representative results of a single experiment with n=2 biological replicates; 2 independent experiments were consistent.

B) Mevalonate metabolism is not involved in regulation of YAP/TAZ by 2DG. Cells were transfected with the 8XGTIIC-lux YAP/TAZ reporter and treated with 2DG (black bars) or with Cerivastatin (3mM, red bars), an inhibitor of the mevalonate pathway at the level of HMG-CoA reductase. Adding back mevalonate in the culture medium (+ mevalonate, 1mM) rescues YAP/TAZ inhibition from Cerivastatin, but not from 2DG. Representative results of a single experiment with n=2 biological replicates; 2 independent experiments were consistent.

C) Representative confocal immunofluorescence images of YAP/TAZ and nuclei (hoechst) in MDA-MB-231 cells. Cells were treated for 24h with 2DG (100mM) or with Cerivastatin (3μM), as positive control of nuclear exclusion.
Bottom: Quantification of cells shows predominantly nuclear (N), even (N/C) or predominantly cytoplasmic (C) YAP/TAZ subcellular localization. Scale bar: 15μm. n>250 cells were observed for each condition.

D) MDA-MB-231 cells were transfected with the 8XGTIIC-lux reporter and treated for 24h with increasing doses (0.1 - 0.3 - 1mM) of the dual mTORC1/2 inhibitor AZD2014. Representative results of a single experiment with n=2 biological replicates; 2 independent experiments were consistent.
On the right: Western blotting of MDA-MB-231 cell extracts treated with DMSO (Co.) or treated for 24h with AZD2014 (0.1mM; AZD) and probed for phosphorylated-S6 (an established read-out of mTOR inhibition) and total S6 ribosomal protein

E) AMPK, key energy sensor activated upon nutrient starvation, is not involved in regulation of YAP/TAZ by 2DG. Luciferase assay in MDA-MB-231 cells treated for 24h with 2DG (black bars) and/or with Compound-C (30mM), an established inhibitor of AMPK. Representative results of a single experiment with n=2 biological replicates; 3 independent experiments were consistent.
On the right: Western blotting of MDA-MB-231 cell extracts treated for 24 h with 2DG (black bars) and/or with Compound-C (30mM) and then probed for phosphorylated-S6 (a read-out of AMPK activation / mTOR inhibition) and total S6 ribosomal protein.

F) Luciferase assay in MDA-MB-231 cells transfected with AMPKa1/2 siRNAs and treated with 2DG. 2 independent experiments were consistent.
On the right: Western blotting of cell extracts used for luciferase assay, validating AMPKa1/2 siRNAs.

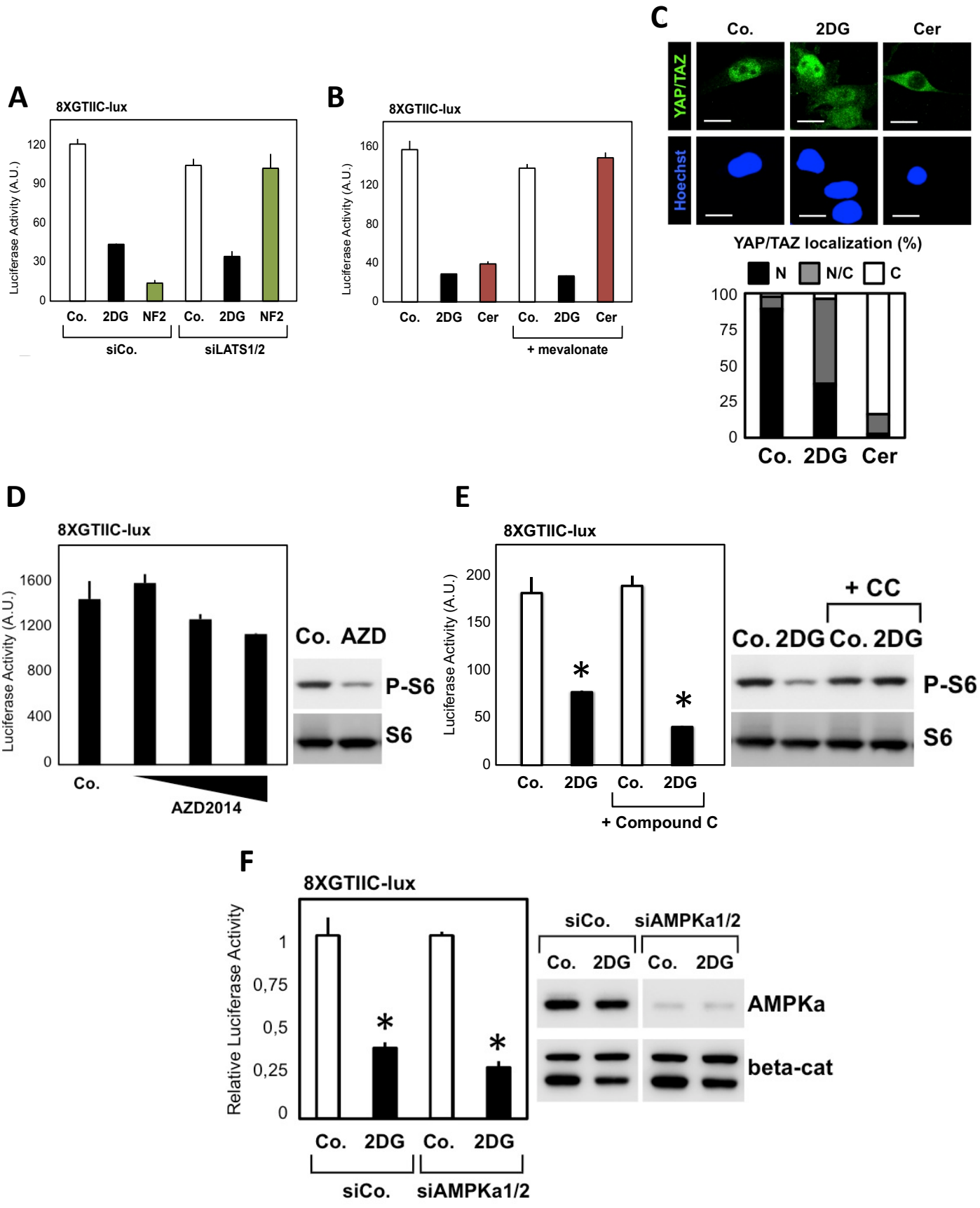
A
8XGTIIC-lux
Luciferase Activity (A.U.)
120
90
60
30
0
Co. 2DG NF2 Co. 2DG NF2
siCo.
siLATS1/2
B
8XGTIIC-lux
Luciferase Activity (A.U.)
160
120
80
40
0
Co. 2DG Cer Co. 2DG Cer
+ mevalonate
C
Co. 2DG Cer
YAP/TAZ
Hoechst
YAP/TAZ localization (%)
N N/C C
100
75
50
25
0
Co. 2DG Cer
D
8XGTIIC-lux
Luciferase Activity (A.U.)
1600
1200
800
400
0
Co.
AZD2014
Co. AZD
P-S6
S6
E
8XGTIIC-lux
Luciferase Activity (A.U.)
200
150
100
50
0
*
*
Co. 2DG Co. 2DG
+ Compound C
+ CC
Co. 2DG Co. 2DG
P-S6
S6
F
8XGTIIC-lux
Relative Luciferase Activity
1
0,75
0,5
0,25
0
*
*
Co. 2DG Co. 2DG
siCo. siAMPKa1/2
siCo. siAMPKa1/2
Co. 2DG Co. 2DG
AMPKa
beta-cat

FIGURE 7

FIGURE 8. Phosphofructokinase regulates YAP/TAZ transcriptional activity

A) Proteomic analysis of YAP binding partners reveals interaction with phosphofructokinase (PFK1). Flag-tagged YAP-5SA stably expressed in MCF10A and MDA-MB-231 cells was immunoprecipitated, and associated proteins identified using mass spectrometry.
Left panel: silver staining of the purified proteins in representative control (Co.) or YAP immunopurifications. Molecular weight markers are indicated. The asterisk indicates the band corresponding to YAP.
Right scheme: The thickness of the lines connecting YAP to its partners is proportional to the number of peptides isolated for each partner. Black proteins (known YAP partners) and PFK1 (in red) were isolated in both cell lines; grey proteins are known regulators of YAP that were only purified from MCF10A cells.

B) Western blotting of MDA-MB-231 cells transfected with the indicated siRNAs and probed with different antibodies detecting endogenous levels of PFK1.

C) Luciferase assay in MDA-MB-231 cells transfected with control (siCo.) or two independent PFK1 siRNAs (siPFK1 #1, #2). Representative results of a single experiment with n=2 biological replicates; 4 independent experiments were consistent.

D) Luciferase assay in MDA-MB-231 cells transfected with the CTGF-lux reporter and with the indicated control (Co.) and PFK1 (P) siRNAs. 2 independent experiments were consistent.

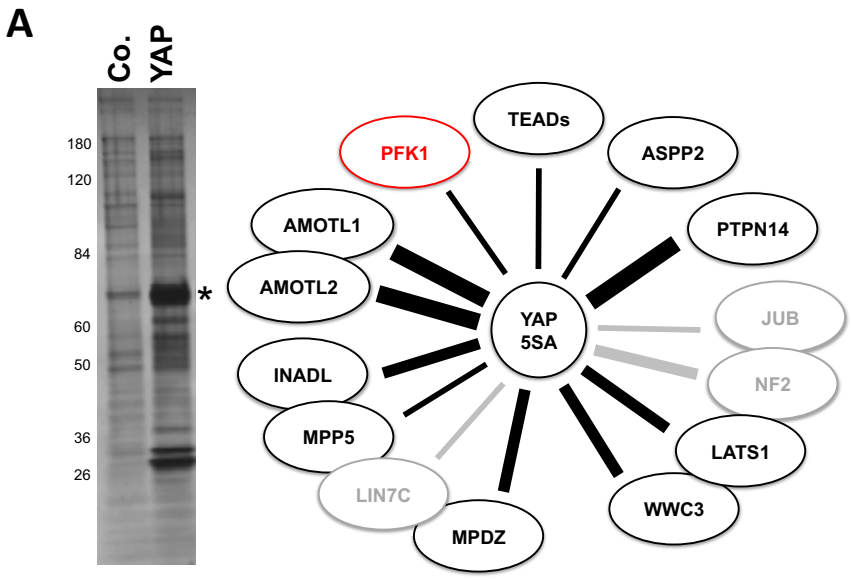
A
Co.
YAP
180
120
84
60
50
36
26
*
PFK1
TEADs
ASPP2
PTPN14
AMOTL1
AMOTL2
YAP
5SA
JUB
NF2
INADL
MPP5
LATS1
LIN7C
WWC3
MPDZ

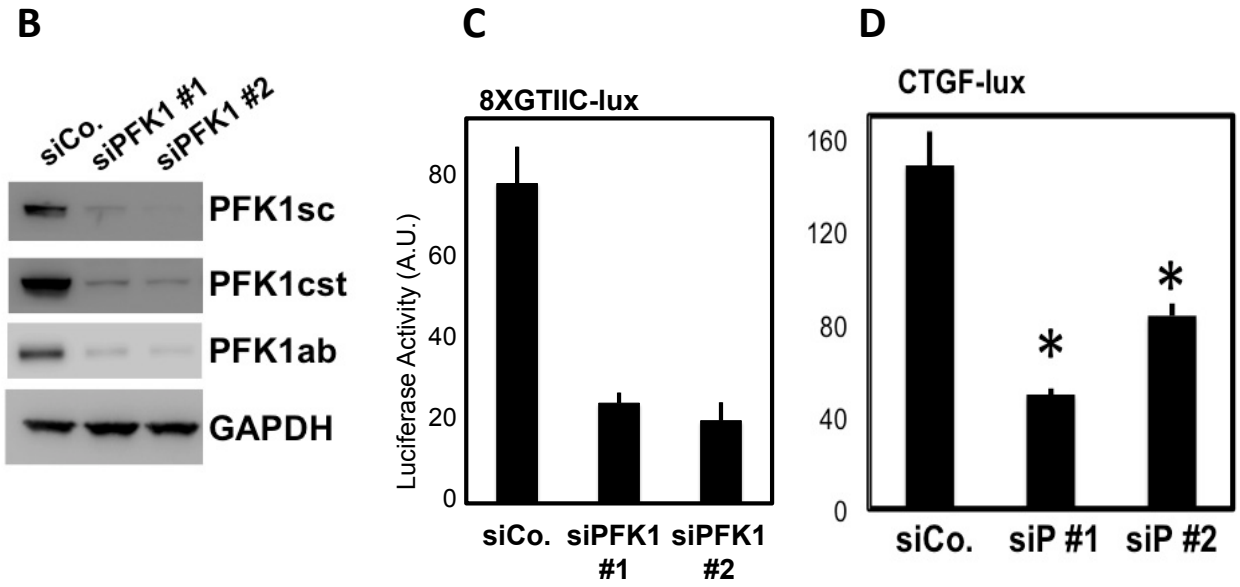
B
siCo.
siPFK1 #1
siPFK1 #2
PFK1sc
PFK1cst
PFK1ab
GAPDH
C
8XGTIIC-lux
Luciferase Activity (A.U.)
0
20
40
60
80
siCo.
siPFK1 #1
siPFK1 #2
D
CTGF-lux
0
40
80
120
160
*
*
siCo.
siP #1
siP #2

FIGURE 8

FIGURE 9. Phosphofructokinase directly interacts with TEADs

A) *In vitro* pull-down assay with purified FLAG-PFK1 and recombinant GST-YAP. GST-YAP was incubated with (first lane) or without (second lane) FLAG-PFK1; as positive control, GST-YAP was incubated with purified FLAG-TEAD1 (right-most lane). Proteins were then subjected to anti-FLAG immunoprecipitation, and purified complexes were probed for coprecipitation of GST-YAP (anti-YAP immunoblot).

B) *In vitro* pull-down assay with purified FLAG-PFK1 and recombinant GST-TEAD4. GST-TEAD4 was incubated with (first lane) or without (second lane) FLAG-PFK1. Proteins were then subjected to anti-FLAG immunoprecipitation, and purified complexes were probed for coprecipitation of GST-TEAD4 (anti-TEAD4 immunoblot).

C) Lysates from HEK293 cells transfected with the indicated proteins were subjected to anti-FLAG-PFK1 immunoprecipitation, and purified complexes were probed for coprecipitation of MYC-TEAD4. Mutation of a key aminoacid required for interaction between TEAD4 and YAP/TAZ (Y429H) did not interfere with PFK1 interaction.

D) MDA-MB-231 cell lysates were immunoprecipitated with anti-TEAD1 antibody, and the precipitating proteins were probed for TEAD1 or PFK1. Immunoprecipitation with an unrelated IgG serves as negative control.

E) Red: Immunofluorescence for endogenous PFK1 with two different primary antibodies in MDA-MB-231 cells. Blue: DAPI serves as nuclear counterstain.

F) Representative confocal images of MCF10A-MII cells subjected to proximity-ligation assay (PLA, in red) by using anti-PFK1 and anti-TEAD1 antibodies. In this assay, two proteins are detected *in situ* with primary antibodies, and the secondary antibodies are conjugated to DNA oligonucleotides instead of fluorophores. Slides are then subjected to DNA ligation and DNA polymerization in the presence of fluorescent-labeled nucleotides: only when the proteins are close to each other the enzymatic reaction takes place, producing discrete sub-nanometer fluorescent dots. Specificity of the assay in detecting nuclear PFK1/TEAD1 proximity was assessed by removing anti-PFK1 or anti-TEAD1 primary antibodies. DAPI serves as a nuclear counterstain. Yellow dashed lines indicate the position of one nucleus in each PLA image. Scale bar: 15μm.

G) Luciferase assay in HEK293 cells transfected with 8XGTIIC-lux reporter and with increasing doses of PFKFB3 expression plasmid. PFKFB3 converts F6P into F2,6BP, a potent allosteric activator of PFK1[134], suggesting that increased PFK1 activity fosters YAP/TAZ activity. 3 independent experiments were consistent.

H) Mutation of the F2,6BP allosteric site of PFK1 negatively regulates its interaction with TEAD4. HEK293 cells were transfected with MYC-TEAD4 and increasing doses of wild-type (WT) or mutated (F2,6P mut) Flag-PFK1 plasmids; cell extracts were immunoprecipitated with anti-FLAG and the coprecipitating MYC-TEAD4 protein was detected by western blotting. Immunoprecipitation in the absence of FLAG-PFK1 (lane 1) serves as a negative control. Quantifications of the TEAD4/PFK1 ratio are provided, relative to lane 2.

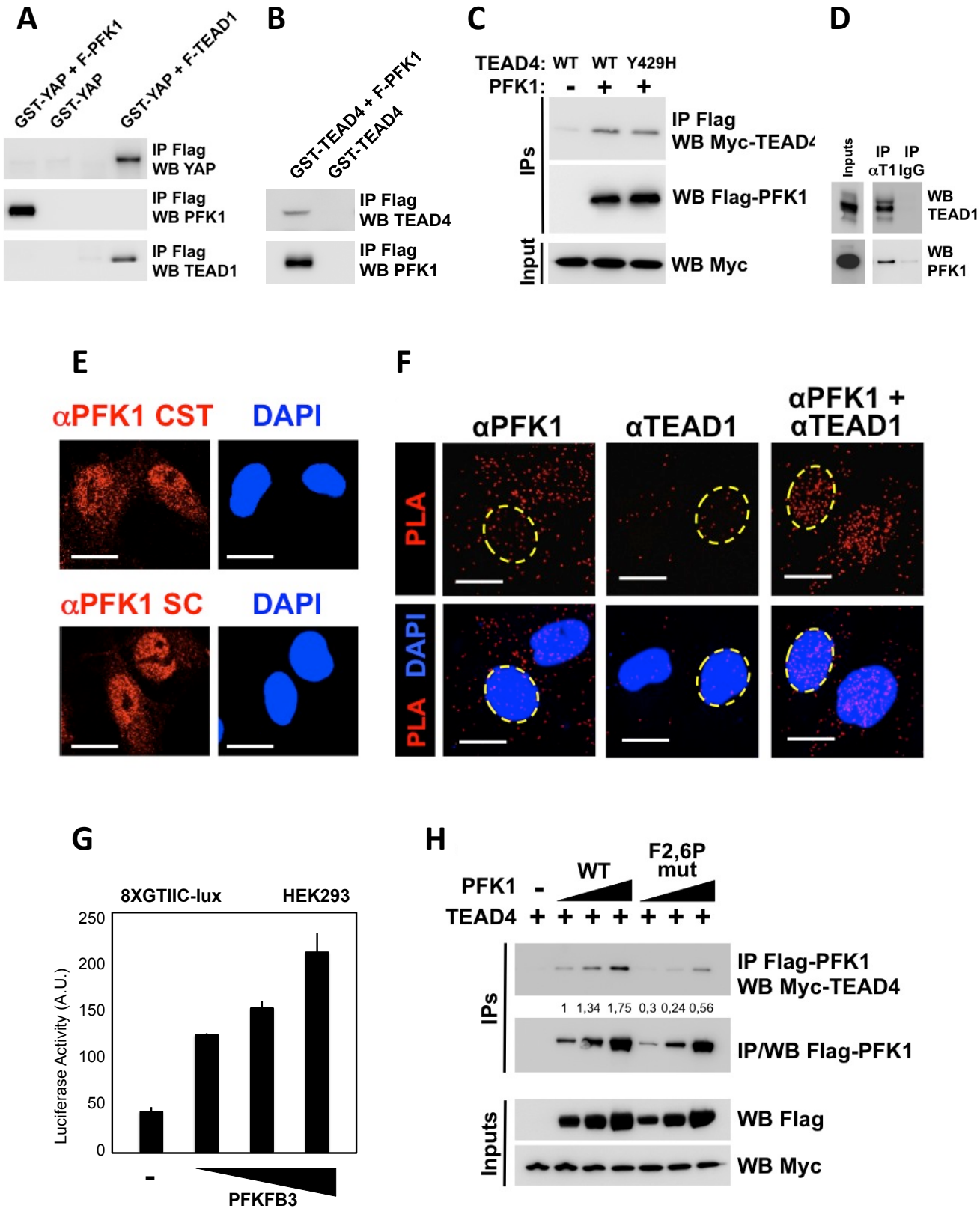
A
GST-YAP + F-PFK1
GST-YAP
GST-YAP + F-TEAD1
IP Flag
WB YAP
IP Flag
WB PFK1
IP Flag
WB TEAD1
B
GST-TEAD4 + F-PFK1
GST-TEAD4
IP Flag
WB TEAD4
IP Flag
WB PFK1
C
TEAD4: WT WT Y429H
PFK1: - + +
IPs
IP Flag
WB Myc-TEAD4
WB Flag-PFK1
Input
WB Myc
D
Inputs
IP αT1
IP IgG
WB TEAD1
WB PFK1
E
αPFK1 CST
DAPI
αPFK1 SC
DAPI
F
αPFK1
αTEAD1
αPFK1 + αTEAD1
PLA
PLA DAPI
G
8XGTIIC-lux
HEK293
Luciferase Activity (A.U.)
250
200
150
100
50
0
-
PFKFB3
H
PFK1 -
WT
F2,6P mut
TEAD4 + + + + + +
IPs
IP Flag-PFK1
WB Myc-TEAD4
1 1,34 1,75 0,3 0,24 0,56
IP/WB Flag-PFK1
Inputs
WB Flag
WB Myc

FIGURE 9

FIGURE 10. Glucose metabolism regulates the interaction between YAP/TAZ and TEADs

A) Glucose metabolism is required for efficient interaction between endogenous YAP and TEAD1 proteins. Extracts of MDA-MB-231 cells treated for 24h with vehicle (-) or with 2DG (+) were subjected to anti-YAP immunoprecipitation; coprecipitating proteins were then analyzed by western blotting to detect TEAD1 interaction. Immunoprecipitation with an unrelated IgG serves as negative control.

B) Same as in (A), but YAP/TAZ were immunoprecipitated with a different antibody (anti-TAZ). Immunoprecipitation with an unrelated IgG (lane 1) serves as negative control.

C-D) Co-immunoprecipitation of endogenous YAP and TEAD1 proteins from extracts of MCF10A (C) or HepG2 (D) cells untreated (-) or treated (+) with 2DG for 24h. Immunoprecipitation with IgG (lane 1) serves as negative control.

E) Co-immunoprecipitation of endogenous YAP and TEAD1 proteins from extracts of UOK262 cells untreated (-), treated with 2DG (15mM) or with Verteporfin (VP, 30mm) for 24h. VP serves as positive control for inhibition of YAP/TEAD1 complexes. Immunoprecipitation with an unrelated IgG (lane 1) serves as negative control.

F) Glucose regulates endogenous YAP/TEAD1 interaction. Co-immunoprecipitations from extracts of MCF10A cells released from contact inhibition by seeding them at low confluence for 36h with glucose (+, lane 2), without glucose (-, lane 3), or cultured without glucose and then refed of glucose (+, lane 4). Immunoprecipitation with IgG (lane 1) serves as negative control.

G) Co-immunoprecipitation of endogenous YAP and TEAD1 proteins from extracts of HepG2 cells cultured for 36h with glucose (+, lane 2), without glucose (-, lane 3), or cultured without glucose and then refed of glucose (+, lane 4). Immunoprecipitation with an unrelated IgG (lane 1) serves as negative control.

H) Representative confocal immunofluorescence images of TEAD1 (green) and nuclei (Hoechst - blue) in MDA-MB-231 cells. Cells were treated for 24h with 100mM 2DG. Hoechst is a nuclear counterstain. Scale bar: 15μm. n>200 cells.

I) Immunoprecipitation of YAP and TEAD1 is reinforced upon glucose supplementation (+), and this requires endogenous PFK1 levels.

J) *In situ* interaction of YAP and TEAD1 is regulated by PFK1 by Proximity Ligation Assay (PLA). Depletion of YAP/TAZ (siYT) or PFK1 with two independent siRNAs (siPFK1 #1, #2) in MCF10A cells reduced the number of nuclear YAP/TEAD1 dots relative to cells transfected with control siRNA (siCo.), suggesting PFK1 is required to stabilize YAP/TEAD1 interaction.
On the left: Representative pictures of MCF10A cells subjected to PLA by using anti-YAP and anti-TEAD1 antibodies. Specificity of the assay in detecting endogenous YAP/TEAD1 proximity was assessed by the expected nuclear localization of the PLA red dots (bottom pictures) and by removing anti-YAP primary antibody (top pictures showing background/aspecific dots). DAPI serves as a nuclear counterstain. Scale bars 15mm.

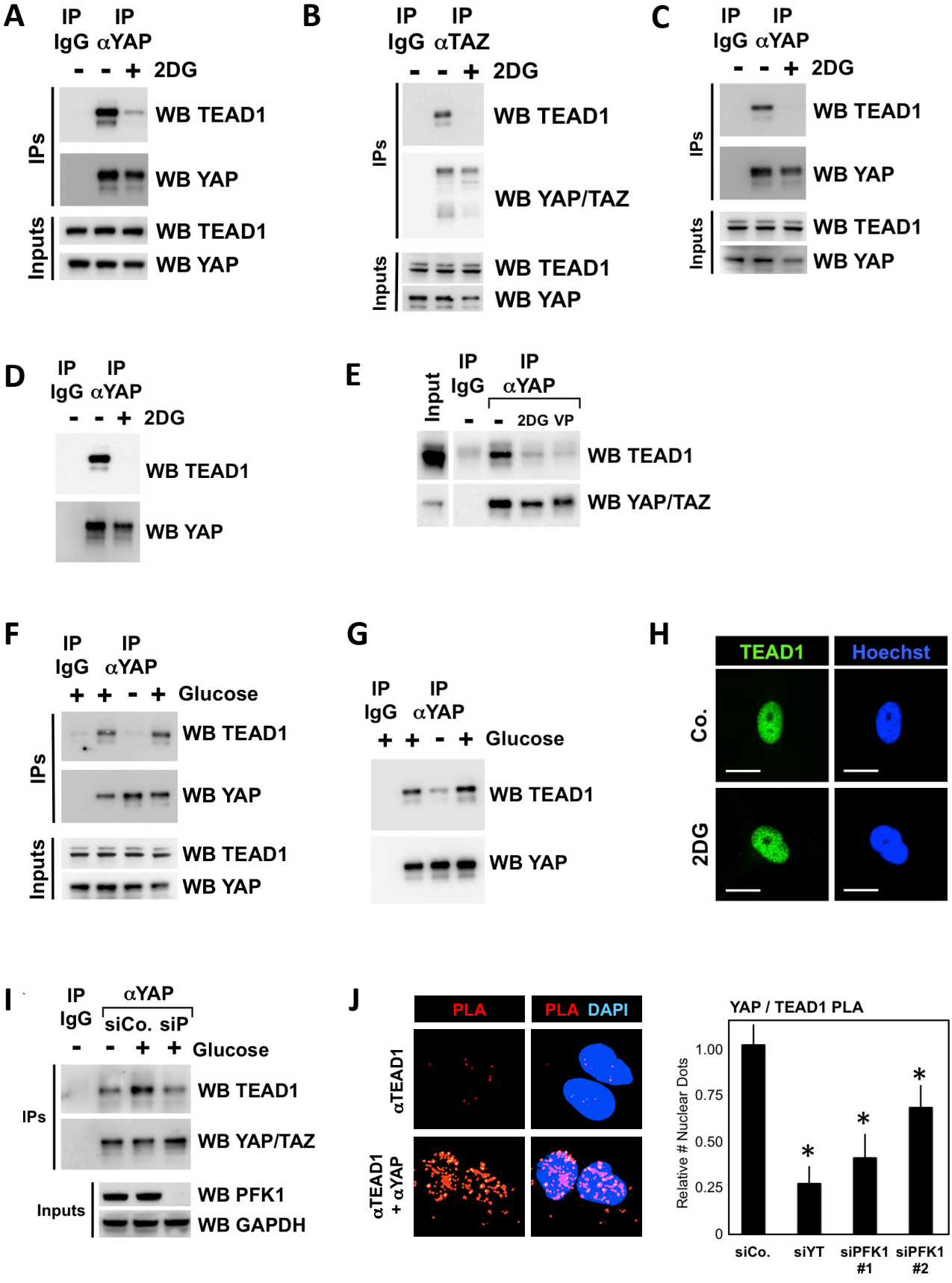
A
IP IgG
IP αYAP
- - + 2DG
IPs
WB TEAD1
WB YAP
Inputs
WB TEAD1
WB YAP
B
IP IgG
IP αTAZ
- - + 2DG
IPs
WB TEAD1
WB YAP/TAZ
Inputs
WB TEAD1
WB YAP
C
IP IgG
IP αYAP
- - + 2DG
IPs
WB TEAD1
WB YAP
Inputs
WB TEAD1
WB YAP
D
IP IgG
IP αYAP
- - + 2DG
WB TEAD1
WB YAP
E
Input
IP IgG
IP αYAP
- - 2DG VP
WB TEAD1
WB YAP/TAZ
F
IP IgG
IP αYAP
+ + - + Glucose
IPs
WB TEAD1
WB YAP
Inputs
WB TEAD1
WB YAP
G
IP IgG
IP αYAP
+ + - + Glucose
WB TEAD1
WB YAP
H
TEAD1
Hoechst
Co.
2DG
I
IP IgG
αYAP siCo. siP
- - + + Glucose
IPs
WB TEAD1
WB YAP/TAZ
Inputs
WB PFK1
WB GAPDH
J
PLA
PLA DAPI
αTEAD1
αTEAD1 + αYAP
YAP / TEAD1 PLA
Relative # Nuclear Dots
1.00
0.75
0.50
0.25
0
siCo.
siYT
siPFK1 #1
siPFK1 #2

FIGURE 10

FIGURE 11. Glucose metabolism regulates the stability of YAP/TEAD transcriptional complexes

A-B) Chromatin immunoprecipitation of MCF10A (A) and MDA-MB-231 (B) cells untreated (Co.) or treated with 100mM 2DG for 24h. Fragmented chromatin from each experimental condition was immunoprecipitated with control IgG or anti-YAP antibodies, and subjected to qPCR to detect the TEAD-binding regions present in the *CTGF*, *ANKRD1*, *HMMR* and *TK1* promoters. Amplification of *Hemoglobin beta* (*HBB*) serves as negative control. Values in Control samples with control IgG were arbitrarily set to 1 and the other values are relative to this. Data are shown as the mean ± SD of two independent experiments.

C-D) Luciferase assays in MDA-MB-231 cells transfected with the TK1-luciferase reporter. By visual inspection, we identified two conserved TEAD-binding motifs in the proximal promoter region of the TK1 gene; this promoter region, when cloned upstream of a luciferase reporter, drives transcription in a manner that is dependent on YAP/TAZ activity (C) and also on glycolysis (D).

E) Luciferase assay in MDA-MB-231 cells transfected with UAS-lux reporter and expression plasmids encoding for in-frame fusions of the GAL4 DNA-binding domain with TEAD1, wild-type (WT) or unable to interact with YAP (Y406A mutant). In this assay, GAL4 provides the DNA-binding platform, while TEAD1 provides transcriptional activation. WT TEAD1 can recruit YAP/TAZ and efficiently promote transcription, while Y406A TEAD1 can only sustain basal transcription[78]. Treatment with 2DG (black bars) inhibited transcription induced by WT TEAD1 but not of the Y406A mutant, in keeping with the observation that 2DG regulates YAP/TEAD1 interaction. LatrunculinA treatment (Lat.A) serves as positive control for inhibition of YAP/TAZ. Representative results of a single experiment with n=2 biological replicates; 2 independent experiments were consistent.

F) Luciferase assay in HEK293 cells transfected as in (E). Co-transfection of PFKFB3, an activator of PFK1 activity, fosters the activity of TEAD1 only when it is able to interact with YAP. Representative results of a single experiment with n=2 biological replicates; 2 independent experiments were consistent.

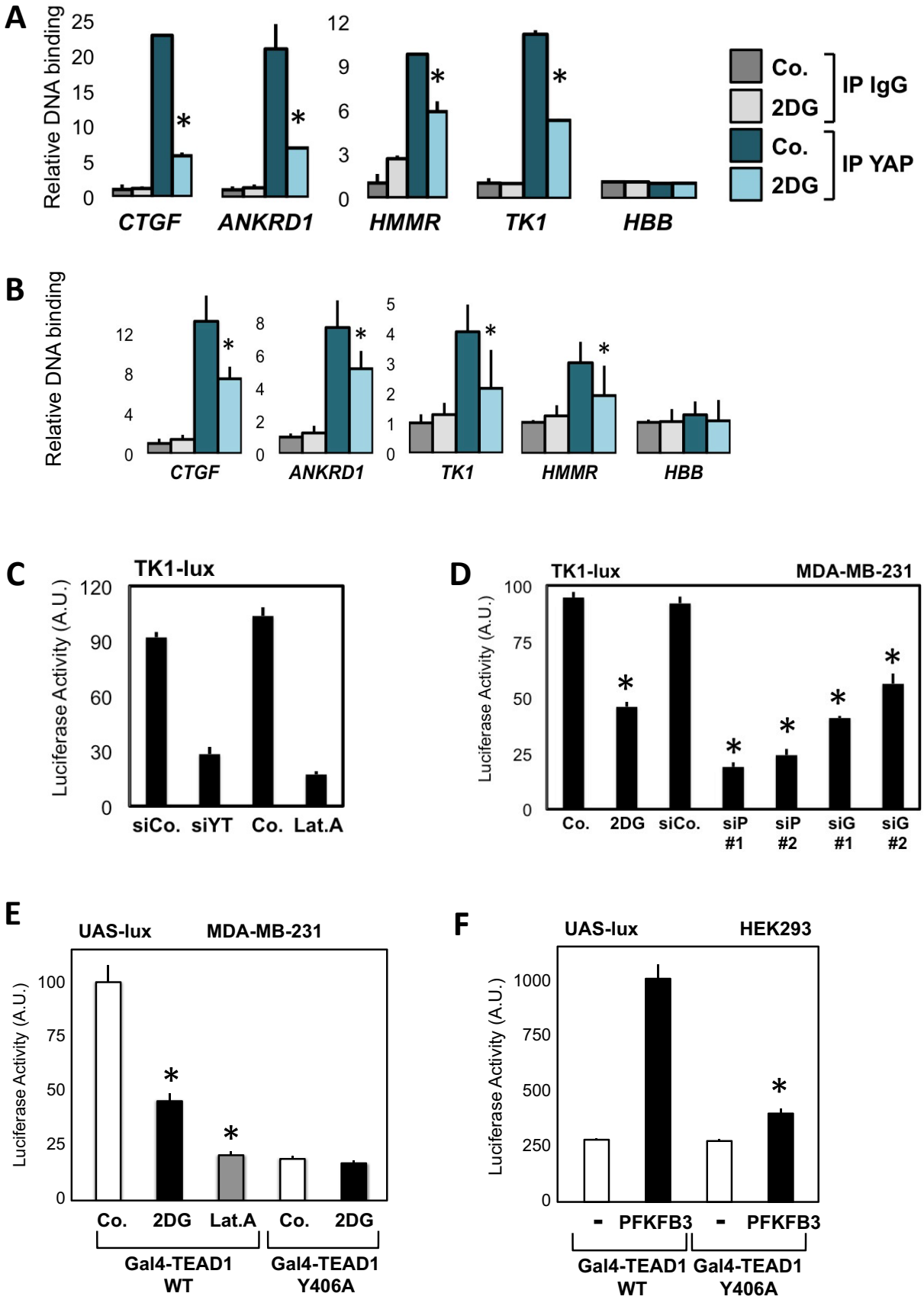
A
Relative DNA binding
25
20
15
10
5
0
12
9
6
3
0
CTGF
ANKRD1
HMMR
TK1
HBB
Co.
2DG
IP IgG
Co.
2DG
IP YAP
B
Relative DNA binding
12
8
4
0
8
6
4
2
0
5
4
3
2
1
0
CTGF
ANKRD1
TK1
HMMR
HBB
C
TK1-lux
Luciferase Activity (A.U.)
120
90
60
30
0
siCo.
siYT
Co.
Lat.A
D
TK1-lux
MDA-MB-231
Luciferase Activity (A.U.)
100
75
50
25
0
Co.
2DG
siCo.
siP #1
siP #2
siG #1
siG #2
E
UAS-lux
MDA-MB-231
Luciferase Activity (A.U.)
100
75
50
25
0
Co.
2DG
Lat.A
Co.
2DG
Gal4-TEAD1 WT
Gal4-TEAD1 Y406A
F
UAS-lux
HEK293
Luciferase Activity (A.U.)
1000
750
500
250
0
-
PFKFB3
-
PFKFB3
Gal4-TEAD1 WT
Gal4-TEAD1 Y406A

FIGURE 11

FIGURE 12. Interplay of glycolysis, PFK1 and YAP/TAZ in cancer cell growth

A-D) Mammosphere assay with MCF10A-MII cells. In (A), retroviral expression of an activated form of TAZ (S89A mutant) increases the efficiency of primary mammosphere formation compared to parental cells (empty-vector infected cells). Treatment of TAZ-expressing cells with 2DG (15mM), depletion of PFK1 (siP) or GPI (siG), impairs the mammosphere-promoting ability of TAZ. n=4 biological replicates; 2 independent experiments were consistent. In (B), representative pictures of S89A-TAZ-expressing mammospheres quantified in (A). In (C), primary mammospheres obtained by seeding parental MCF10A-MII cells transfected with siRNAs for PFK1 (P), GPI (G) or YAP/TAZ (YT). In (D), secondary mammospheres obtained by re-seeding mammospheres obtained from MCF10A-MII-TAZ S89A cells treated with 2DG as (A) or transfected with siRNAs for PFK1 (P) or GPI (G).

E) Depletion of PFK1 (siP) impairs the colony-forming ability of MDA-MB-231 cells in soft agar, recapitulating the requirement for YAP/TAZ (siYT). n=2 biological replicates; 2 independent experiments were consistent.

F) Expression of an activated form of YAP (5SA) strongly promotes the growth of MDA-MB-231 colonies in soft agar, and this is inhibited by 2DG treatment (3mM). Each box signifies the upper and lower quartiles of data (colony size), while the whiskers extend to the minimum and maximum data points.
On the right: representative pictures of colonies. n=2 biological replicates; 4 independent experiments were consistent.

G-H) MCF10A cells were seeded at high density for 48h, leading to YAP/TAZ inhibition and growth arrest (High); scratching the monolayer locally enables cell spreading and activates YAP/TAZ, thus inducing cell proliferation (Wound)[32,80]. Overnight treatment of cells with 2DG (15mM) inhibited such YAP/TAZ-induced proliferation. In (G), the graph reports the quantification of proliferating cells, without or with 2DG. To count cells, we arbitrarily set a 100mm distance from the wound. n=2 biological replicates (>700 cells/replicate); 3 independent experiments were consistent. In (H), representative BrdU stainings and nuclear counterstains (DAPI) of MCF10A cell monolayers in the area abutting the wound.

I) MDA-MB-231 cells were growth-inhibited by glucose withdrawal for 48h (- Glu), and then proliferation was induced by supplementing glucose in the medium for 24h (+ Glu). Culture medium was without glutamine to specifically measure glucose-dependent growth. Quantification of proliferation (by BrdU incorporation), indicates that cells depleted of YAP/TAZ (siYT #1) are unable to efficiently restart proliferation in response to glucose. n=2 biological replicates (>1000 cells/replicate); 3 independent experiments were consistent.

J-K) Clonogenic assay with UOK262 cells. Parental cells (black bars) are highly glycolytic, while their FH-reconstituted counterpart (grey bars) have reduced glycolysis as they can efficiently perform mitochondrial respiration[59]. Cells were grown with titrated doses of 2DG (0.25, 0.5, 1mM) to inhibit glucose metabolism (J), or with VP (0.3, 1, 3 mM) to inhibit the cooperation between YAP/TAZ and TEADs[41] (K). Quantification of colonies after 10 days, relative to untreated cells. n=3 biological replicates; 2 independent experiments were consistent.

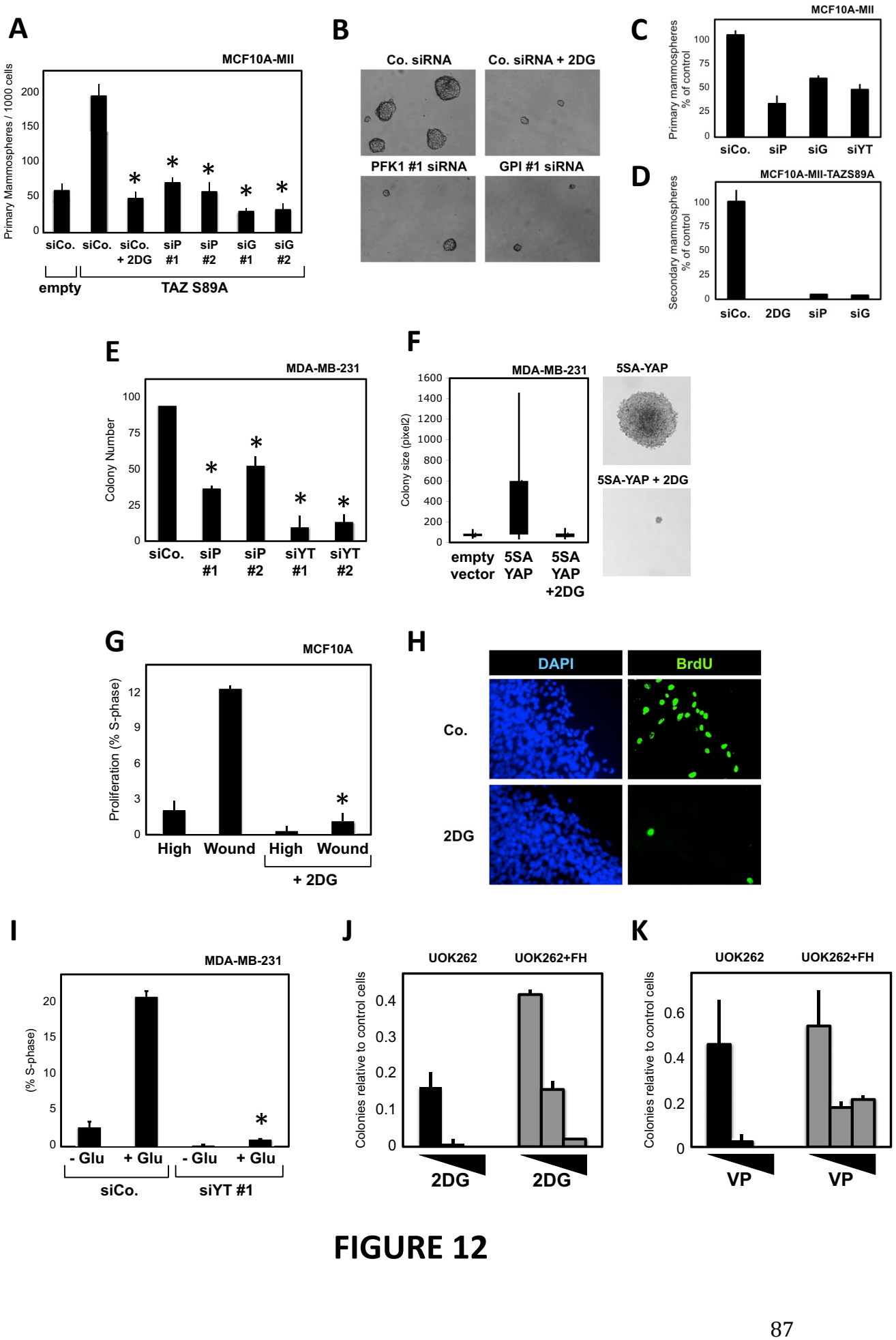
A
MCF10A-MII
Primary Mammospheres / 1000 cells
200
150
100
50
0
siCo.
siCo.
siCo. + 2DG
siP #1
siP #2
siG #1
siG #2
empty
TAZ S89A
B
Co. siRNA
Co. siRNA + 2DG
PFK1 #1 siRNA
GPI #1 siRNA
C
MCF10A-MII
Primary mammospheres % of control
100
75
50
25
0
siCo.
siP
siG
siYT
D
MCF10A-MII-TAZS89A
Secondary mammospheres % of control
100
75
50
25
0
siCo.
2DG
siP
siG
E
MDA-MB-231
Colony Number
100
75
50
25
0
siCo.
siP #1
siP #2
siYT #1
siYT #2
F
MDA-MB-231
Colony size (pixel2)
1600
1400
1200
1000
800
600
400
200
0
empty vector
5SA YAP
5SA YAP +2DG
5SA-YAP
5SA-YAP + 2DG
G
MCF10A
Proliferation (% S-phase)
12
9
6
3
0
High
Wound
High
Wound
+ 2DG
H
DAPI
BrdU
Co.
2DG
I
MDA-MB-231
(% S-phase)
20
15
10
5
0
- Glu
+ Glu
- Glu
+ Glu
siCo.
siYT #1
J
UOK262
UOK262+FH
Colonies relative to control cells
0.4
0.3
0.2
0.1
0
2DG
2DG
K
UOK262
UOK262+FH
Colonies relative to control cells
0.6
0.4
0.2
0
VP
VP

FIGURE 12

FIGURE 13. PFK1 is required for Yki-induced growth in *Drosophila*

A) Clonal expansion induced by overexpression of the YAP homologue Yki in the *Drosophila* wing imaginal disc is restricted by phosphofructokinase (Pfk) RNAi. Panels on the left show pictures of wing imaginal discs bearing clones of cells (marked by GFP) with mutation of the *lethal giant larvae* tumor suppressor gene (lgl^-) and overexpression of Yki (yki^{over}), induced by the MARCM technique[135]. The dotted line indicates the outline of the discs. In this genetic setup, the survival of clones within the wing pouch, i.e. in the distal region of the wing disc, is strictly dependent on Yki activation[81–83]. Upon downregulation of phosphofructokinase, the growth of lgl^-; yki^{over} clones was inhibited, as shown by quantification of clone area ($P<0.0001$, unpaired t-test). In order to obtain consistent observations, only clones included in the wing pouch region were considered for statistical analysis. n=34 discs for each genotype. Scale bars 80mm.

B) Pfk silencing downregulates the Yki target gene DIAP1 in lgl^-; yki^{over} clones. Panels show whole mount immunostainings for DIAP1 protein levels, a hallmark of Yki transcriptional activity[85], on wing imaginal discs of the indicated phenotypes, as in A. GFP identifies mutant cells, growing within an otherwise wild-type tissue. DIAP1 is autonomously upregulated in lgl^-; yki^{over} clones, while it appears downregulated upon Pfk RNAi. This is consistent with a role for Pfk in regulating Yki transcriptional activity. See (D) for similar results obtained with dMyc, another target of Yki[87,88]. Scale bars 20mm.

C) Low magnification pictures of whole wing imaginal discs bearing lgl^-; yki^{over} or lgl^-; yki^{over} *Pfk-RNAi* clones (marked by GFP) and stained for DIAP1 protein. The squares indicate the regions highlighted in (B). Scale bars 80mm.

D) Pfk silencing in lgl^-; yki^{over} cells attenuates dMyc expression in the wing pouch region. Panels show immunostainings for dMyc protein levels, an established target of Yki in the context of clonal expansion[87,88]. GFP identifies mutant cells, growing within an otherwise wild-type tissue. dMyc protein levels are high in lgl^-; yki^{over} clones, and they appear normalized upon phosphofructokinase knockdown (*Pfk-RNAi*). Pictures were taken in the wing pouch region as in (A-B). The dotted line in the lower right panel indicates the borders of the clone, based on GFP signal. Scale bars 20mm.

E) Low magnification pictures of whole wing imaginal discs bearing lgl^-; yki^{over} or lgl^-; yki^{over} *Pfk-RNAi* clones (marked by GFP) and stained for dMyc protein. The squares indicate the regions highlighted in D. Scale bars 80mm.

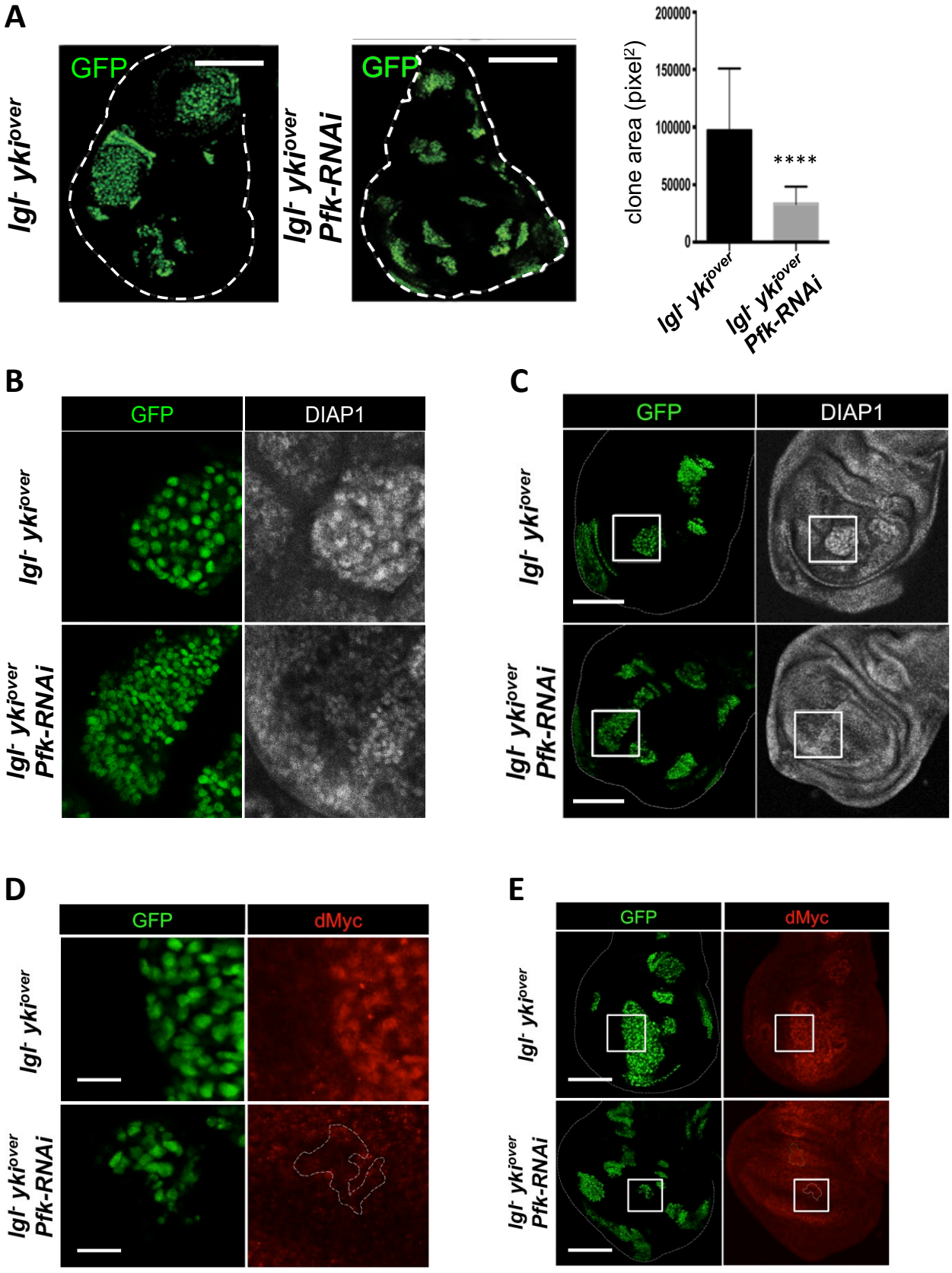
A
GFP
lgl- ykiover
GFP
lgl- ykiover Pfk-RNAi
clone area (pixel2)
200000
150000
100000
50000
0
****
lgl- ykiover
lgl- ykiover Pfk-RNAi
B
GFP
DIAP1
lgl- ykiover
lgl- ykiover Pfk-RNAi
C
GFP
DIAP1
lgl- ykiover
lgl- ykiover Pfk-RNAi
D
GFP
dMyc
lgl- ykiover
lgl- ykiover Pfk-RNAi
E
GFP
dMyc
lgl- ykiover
lgl- ykiover Pfk-RNAi

FIGURE 13

FIGURE 14. YAP/TAZ activity is enhanced in primary human breast cancers displaying high levels of a gene signature regulated by glucose

A-B) Scatter plot (gray dots) and linear regression (red line, slope 0.532) of standardized expression values indicates a positive correlation between a gene signature experimentally associated with active glucose metabolism (Glucose signature) and the "YAP/TAZ" (A) or "induced by YAP" (B) gene signature in a metadataset collecting n=3661 primary human breast cancers. The Glucose signature is composed of the genes downregulated upon 2DG treatment, i.e. requiring active glucose metabolism for their transcription, both in MCF10A and in MDA-MB-231 cells. Pearson r quantifies the linear dependence between the levels of the two signatures. In A: the coefficient of determination is r^2=0.731, p-value<0.0001. In B: r^2=0.477, p-value<0.0001.

C-D) Primary human breast cancers of the metadataset were stratified according to high or low Glucose signature score, and then the levels of the "YAP/TAZ" (C) or "induced by YAP" (D) gene signature score were determined in the two groups. YAP/TAZ activity is significantly higher in tumors with high levels of the Glucose signature, as visualized by box-plot. The bottom and top of the box are the first and third quartiles, and the band inside the box is the median; whiskers represent 1st and 99th percentiles; values lower and greater are shown as circles (p<0.0001, n=3661).

E-F) Primary human breast cancers of the metadataset were classified according to high or low Glucose signature score, and then the levels of the Staminal or Stem tumorigenic signature scores, associated to normal and cancer mammary stem cells, were determined in the two groups. Gene expression associated to mammary stem cells is significantly higher in tumors with high levels of the Glucose signature, as visualized by box-plot (p<0.0001, n=3661).

G) Genes regulated by glucose metabolism (Glucose signature) are elevated in G3 as compared to G1 grade mammary tumors of the metadataset (p<0.0001; G1 vs. G3 unpaired t-test). A similar behavior is observed by using the YAP/TAZ signature[45]. Data are shown as mean ± standard error of the mean (SEM).

H) Kaplan-Meier analysis representing the probability of metastasis-free survival in breast cancer patients from the metadataset stratified according to high or low Glucose signature score. The log-rank test p value reflects the significance of the association between high levels of the glucose signature score and shorter survival. A similar behavior is observed by using the YAP/TAZ signature[45].

I) Genes regulated by glucose metabolism but not by YAP/TAZ (Glucose NOT YT signature) are not expressed at higher levels in G3 grade mammary tumors of the metadataset. Data are shown as mean ± standard error of the mean (SEM).

J) Kaplan-Meier analysis in breast cancer patients from the metadataset stratified according to high or low Glucose NOT YT signature score, which show no differences.

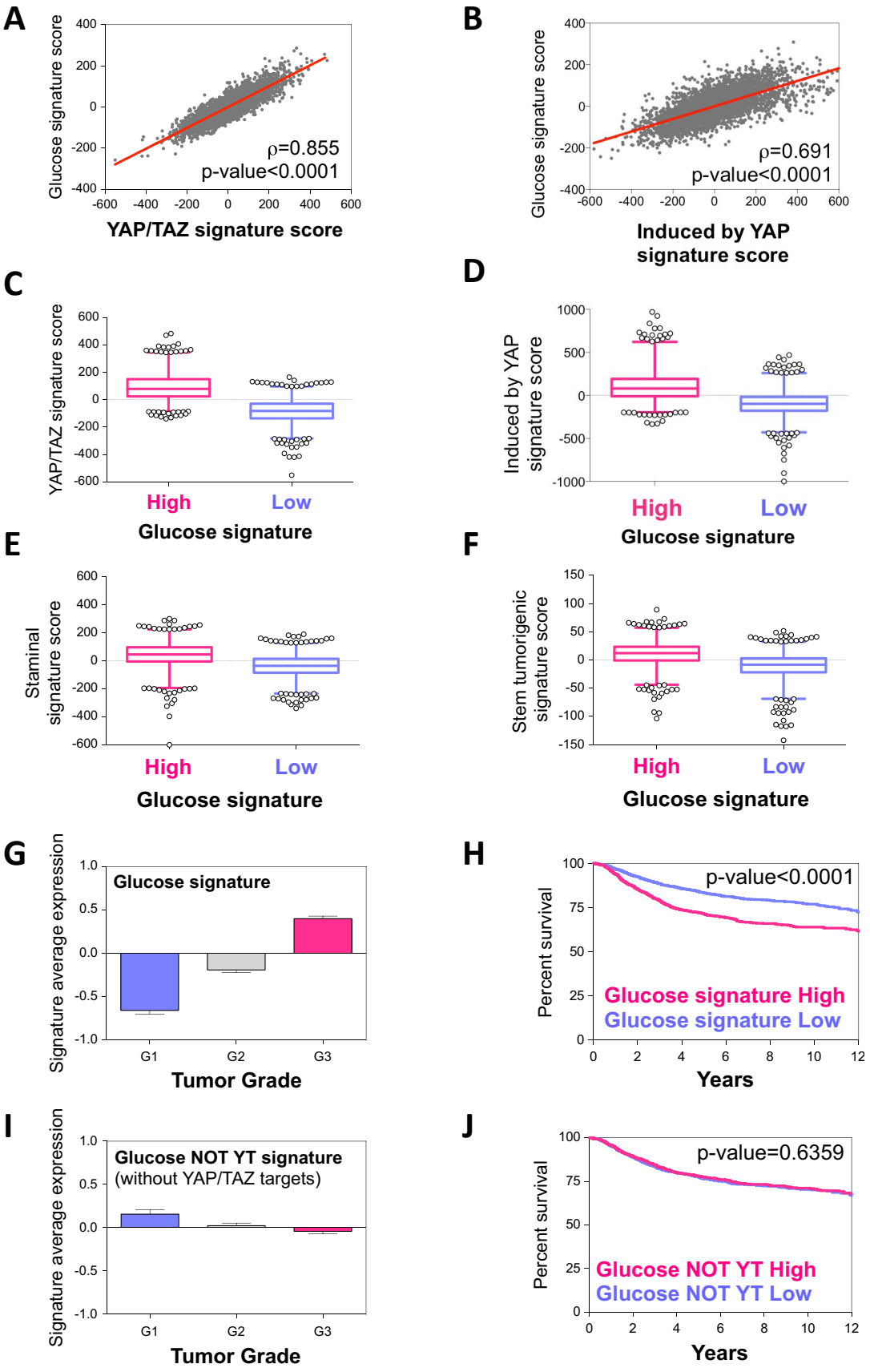
A
Glucose signature score
YAP/TAZ signature score
ρ=0.855
p-value<0.0001
B
Glucose signature score
Induced by YAP signature score
ρ=0.691
p-value<0.0001
C
YAP/TAZ signature score
High
Low
Glucose signature
D
Induced by YAP signature score
High
Low
Glucose signature
E
Staminal signature score
High
Low
Glucose signature
F
Stem tumorigenic signature score
High
Low
Glucose signature
G
Signature average expression
Glucose signature
G1
G2
G3
Tumor Grade
H
Percent survival
p-value<0.0001
Glucose signature High
Glucose signature Low
Years
I
Signature average expression
Glucose NOT YT signature
(without YAP/TAZ targets)
G1
G2
G3
Tumor Grade
J
Percent survival
p-value=0.6359
Glucose NOT YT High
Glucose NOT YT Low
Years

FIGURE 14

FIGURE 15. YAP/TAZ regulate the expression of multiple key enzymes involved in nucleotide metabolism

A) The table shows the list of genes involved in nucleotide metabolism whose expression is inhibited upon YAP/TAZ silencing. We analyzed gene expression profiles carried out in 4 cell lines: MDA-MB-231 (metastatic breast cancer cells)[1], Meso-33 (mesothelioma cells)[125], HepG2 (liver hepatocellular carcinoma cells)[124], HaCaT (keratinocyte cell line)[124]. Coregulated genes were identified by comparing control-siRNA transfected cells with YAP/TAZ-depleted cells. In MDA-MB-231 cells, two independent mix of YAP/TAZ siRNAs were used. The presence of an "x" indicates the gene is dowregulated (at least two fold) upon YAP/TAZ silencing.

B) WI38 primary human fibroblasts cell line were infected with control (Co.), Ras or YAP 5SA-encoding retrovirus, or transfected with the indicated siRNAs: control (siCo.), YAP/TAZ (siYT). Infected cells were examined 6 days from the beginning of the selection, whereas transfected cells were analyzed 48h after the transfection. qPCR for endogenous target genes related with nucleotide biosynthesis showed that the expression of these genes were coherently regulated both by YAP/TAZ knockdown and by YAP overexpression. Ras infection serves as positive control[121,122]. Expression levels were calculated relative to *GAPDH*, and are given relative to Co. cells (arbitrarily set to 1). n=2 biological replicates from 2 independent experiments.

C) Same samples as in (B) but examined for mRNA expression of established YAP/TAZ target genes[53,126]. These genes are YAP/TAZ targets also in WI38 cell line. n=2 biological replicates from 2 independent experiments.

D) Western blot analysis of cell extracts infected as in (B) and probed for YAP or Ras, validating the overexpression.

E) qPCR for endogenous mRNA levels showed efficient depletion of both YAP and TAZ in WI38 cells 48h after siRNA transfection. n=2 biological replicates from 2 independent experiments.

A

Gene symbol	Gene name	MDA-MB-231 siYT 1	MDA-MB-231 siYT 2	Meso-33 siYT	HepG2 siYT	HaCaT siYT
CAD	carbamoyl-phosphate synthetase 2, aspartate transcarbamylase, and dihydroorotase	x	x			x
CTPS1	CTP synthase 1	x	x	x		
DCK	deoxycytidine kinase	x	x	x		
DHFR	dihydrofolate reductase	x	x	x		
DHOD	dihydroorotate dehydrogenase (quinone)	x	x	x		
DTYMK	deoxythymidylate kinase (thymidylate kinase)	x	x	x	x	x
IMPDH2	IMP (inosine 5'-monophosphate) dehydrogenase 2	x	x			
MTHFD	methylenetetrahydrofolate dehydrogenase (NADP+ dependent)	x	x			
NME1	NME/NM23 nucleoside diphosphate kinase 1	x	x	x		
PAICS	phosphoribosylaminoimidazole carboxylase, phosphoribosylaminoimidazole succinocarboxamide synthetase	x	x	x		x
PRPS2	phosphoribosyl pyrophosphate synthetase 2	x	x			x
PSAT1	phosphoserine aminotransferase 1	x	x	x		x
RRM1	ribonucleotide reductase M1	x	x	x	x	x
RRM2	ribonucleotide reductase M2	x	x	x	x	x
SHMT2	serine hydroxymethyltransferase 2 (mitochondrial)	x	x			
TK1	thymidine kinase 1	x	x	x	x	x
TYMS	thymidylate synthetase	x	x	x	x	x
UMPS	uridine monophosphate synthetase	x	x	x		

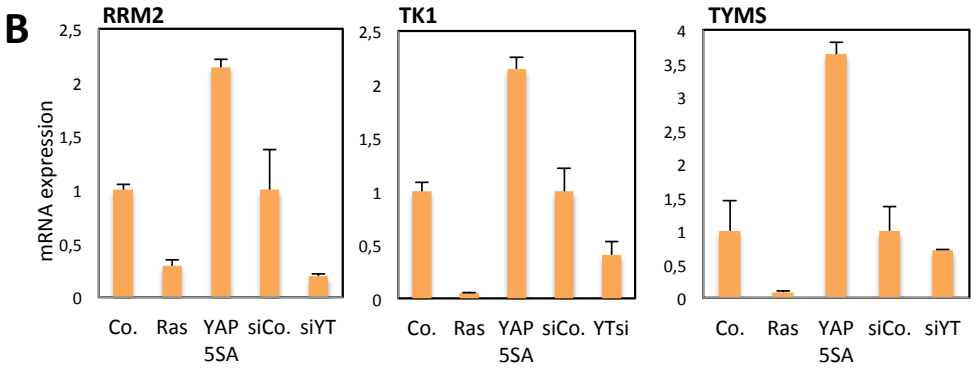

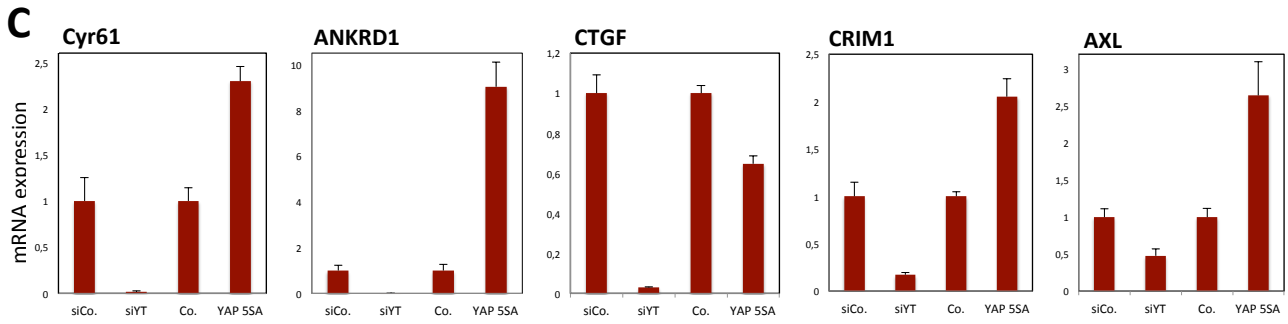

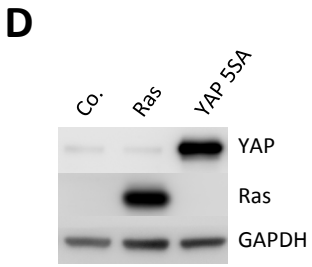

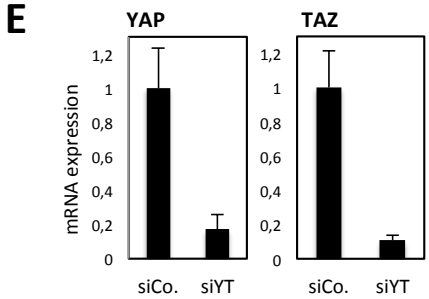

FIGURE 15

FIGURE 16. YAP overexpression is sufficient to overcome Ras-induced inhibition of genes involved in nucleotide metabolism

A) WI38 cells were infected with control (Co.), Ras-IRES-GFP or Ras-IRES-YAP 5SA-encoding retrovirus. We co-expressed both Ras and constitutive active YAP (YAP 5SA) from the same plasmid by using an internal ribosome entry site (IRES) sequence. 6 days from the beginning of the selection, cells were examined for RNA expression. qPCR for endogenous target genes related with nucleotide biosynthesis showed that YAP overexpression was sufficient to reestablish the expression of RRM2, TK1 and TYMS to levels comparable to control cells. Expression levels were calculated relative to *GAPDH*, and are given relative to Co. cells (arbitrarily set to 1). n=2 biological replicates from 3 independent experiments.

B) Same samples as in (A) but examined for mRNA expression of established YAP/TAZ target genes[32,53]. Ras activation inhibited YAP/TAZ target genes and YAP overexpression was able to rescue their levels. n=2 biological replicates from 3 independent experiments.

C) qPCR for endogenous YAP or TAZ mRNA levels. Oncogenic Ras activation did not induce a downregulation of YAP or TAZ mRNA expression.

D) Sizes of dATP, dGTP and dCTP pools in WI38 extracts infected as indicated. YAP overexpression rescued the levels of dATP, dGTP and dCTP. Results from one experiment (a new measurement is in progress).

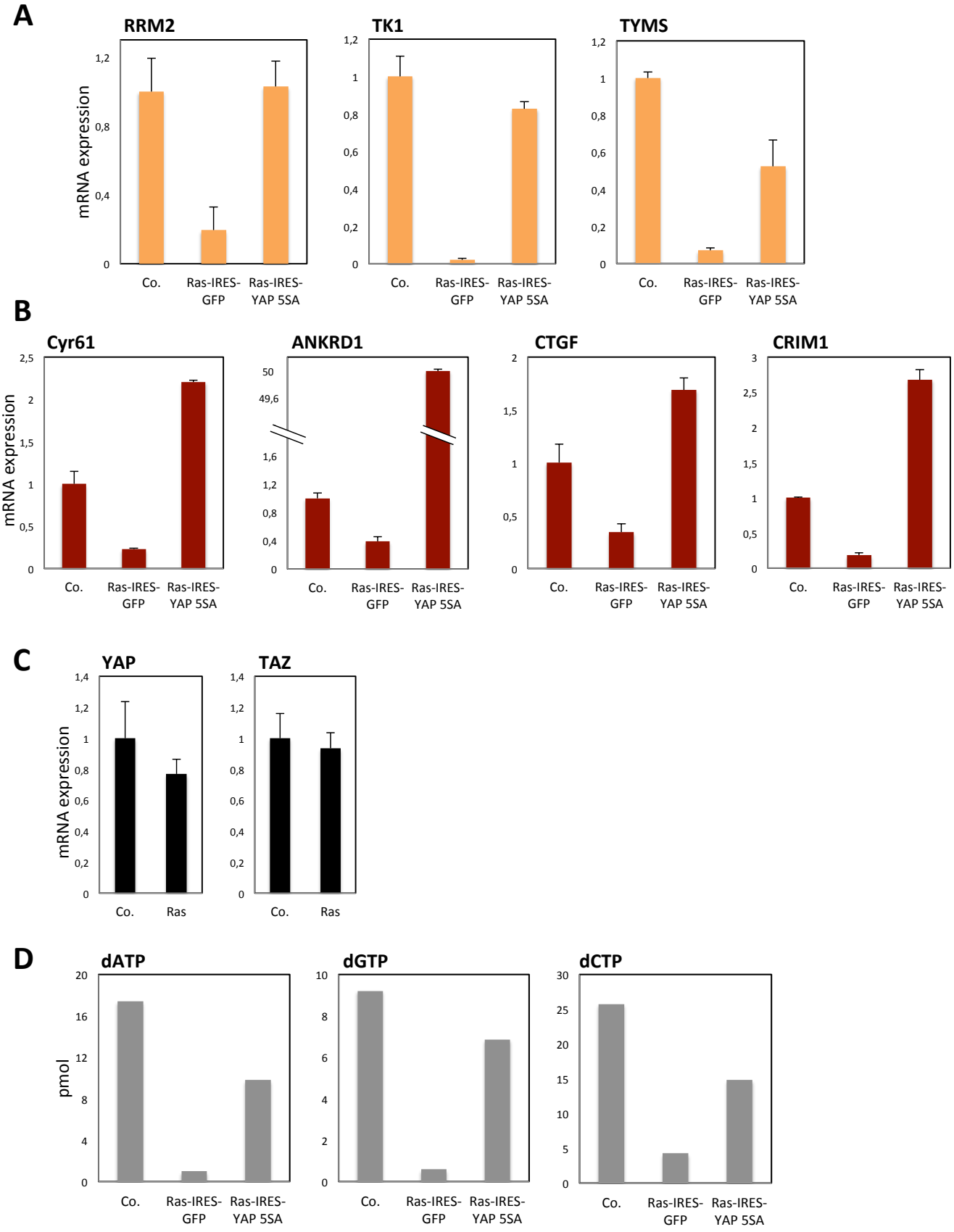
A
RRM2
TK1
TYMS
mRNA expression
Co.
Ras-IRES-GFP
Ras-IRES-YAP 5SA
B
Cyr61
ANKRD1
CTGF
CRIM1
C
YAP
TAZ
Co.
Ras
D
dATP
dGTP
dCTP
pmol

FIGURE 16

FIGURE 17. YAP overexpression is sufficient to overcome Ras-induced senescent phenotypes

A) WI38 cells were infected with control (Co.), Ras-IRES-GFP or Ras-IRES-YAP 5SA-encoding retrovirus. We co-expressed both Ras and constitutive active YAP (YAP 5SA) from the same plasmid by using an internal ribosome entry site (IRES) sequence. 6 days from the beginning of the selection, cells were examined for RNA expression. qPCR for endogenous genes that are either induced (*p21*, *p16* and *p15*) or inhibited (*cyclin A2*, *cyclin B1*, *CDCA7*) in senescent cells. YAP overexpression was sufficient to reestablish the expression of these markers to levels comparable to control cells, with the exception of p16. Expression levels were calculated relative to *GAPDH*, and are given relative to Co. cells (arbitrarily set to 1). n=2 biological replicates from 3 independent experiments.

B) Western blot analysis of cell extracts infected as in (A) and probed for YAP or Ras, to validate the overexpression, or for Lamin B, RRM2 or cyclin A2, to examine if YAP overcame the effects of Ras infection.

C) Quantification of proliferating cells, infected as in (A), measured by EdU incorporation (1h). YAP overexpression reestablished cell proliferation inhibited by Ras. Representative results of a single experiment (>350 cells per condition); 3 independent experiments were consistent.

D) Same as in (A) but cells were stained for SA-βgal activity. YAP expression counteracted the effects of Ras on SA-βgal activity. Representative results of a single experiment (>100 cells per condition); 3 independent experiments were consistent.

E) Same as in (A) but cells were examined for SAHF formation. YAP expression counteracted the effects of Ras on SAHF. Representative results of a single experiment (>100 cells per condition); 3 independent experiments were consistent.

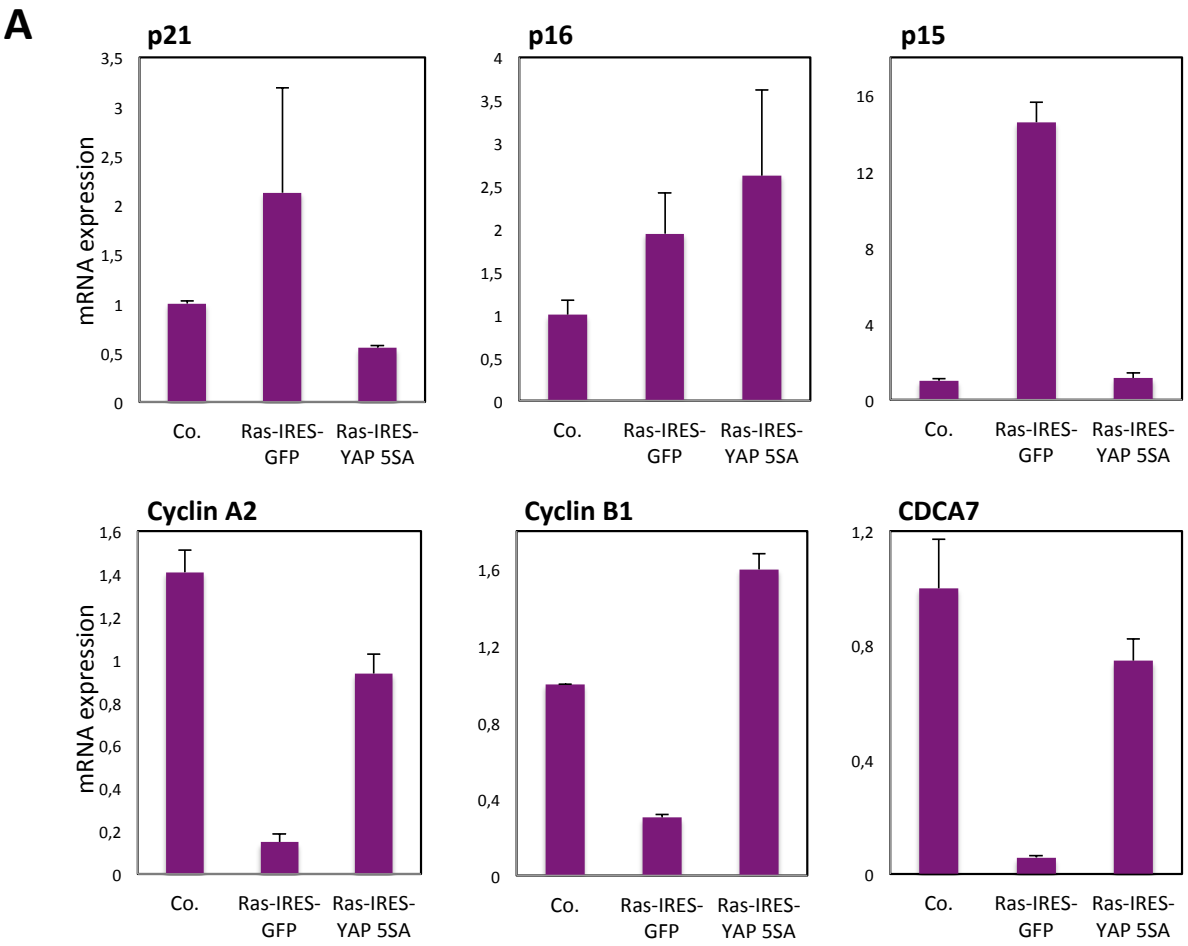
A
p21
p16
p15
mRNA expression
Co.
Ras-IRES-GFP
Ras-IRES-YAP 5SA
Cyclin A2
Cyclin B1
CDCA7

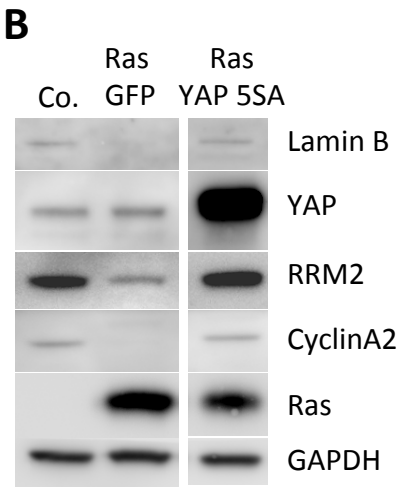
B
Co.
Ras GFP
Ras YAP 5SA
Lamin B
YAP
RRM2
CyclinA2
Ras
GAPDH

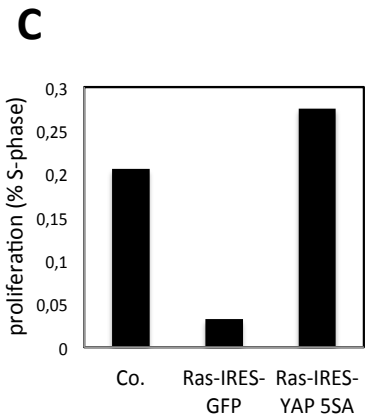
C
proliferation (% S-phase)
Co.
Ras-IRES-GFP
Ras-IRES-YAP 5SA

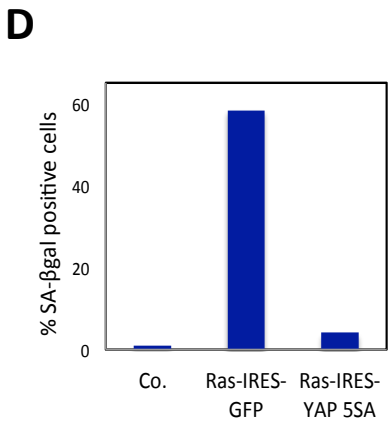
D
% SA-βgal positive cells
Co.
Ras-IRES-GFP
Ras-IRES-YAP 5SA

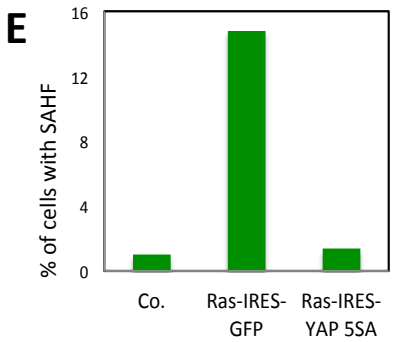
E
% of cells with SAHF
Co.
Ras-IRES-GFP
Ras-IRES-YAP 5SA

FIGURE 17

FIGURE 18. YAP depletion induces senescent phenotypes

A) Western blotting of WI38 cells transfected with the indicated siRNAs and probed with different antibodies. We monitored protein levels 5 days after cellular transfection. YAP or TAZ knockdown decreased the protein levels of RRM2, lamin B and cyclinA2, whose inhibitions are common in senescent cells[121,127]. As a control, YAP or TAZ were efficiently depleted from the cells.

B) WI38 cells were transfected with the indicated siRNAs: control (siCo.) or YAP (siYAP). On day 5, proliferating cells were measured by EdU incorporation (1h). In absence of YAP cell proliferation was impaired. Representative results of a single experiment (>600 cells per condition); 2 independent experiments were consistent.

C) Same as in (B) but cells were stained for SA-βgal activity. Representative result of a single experiment (>160 cells per condition); 2 independent experiments were consistent.

D) Same as in (B) but cells were examined for SAHF formation. Representative result of a single experiment (>160 cells per condition); 2 independent experiments were consistent.

E) WI38 cells were transfected with the indicated siRNAs, control (siCo.) or siYT (siYAP/TAZ), or infected with Ras as positive control. Ras-infected cells were analyzed 6 days after the selection start, whereas cells transfected with siRNAs were examined 48h after transfection because of the strong established effects of knockdown of both YAP and TAZ[31]. qPCR for endogenous genes that are either induced (*p21*, *p16*) or inhibited (*cyclin A2*) in senescent cells. YAP/TAZ depletion was sufficient to decrease the levels of cyclin A2 and to increase the CDKIs p21 and p16. Expression levels were calculated relative to *GAPDH*, and are given relative to Co. cells (arbitrarily set to 1). n=2 biological replicates from 2 independent experiments.

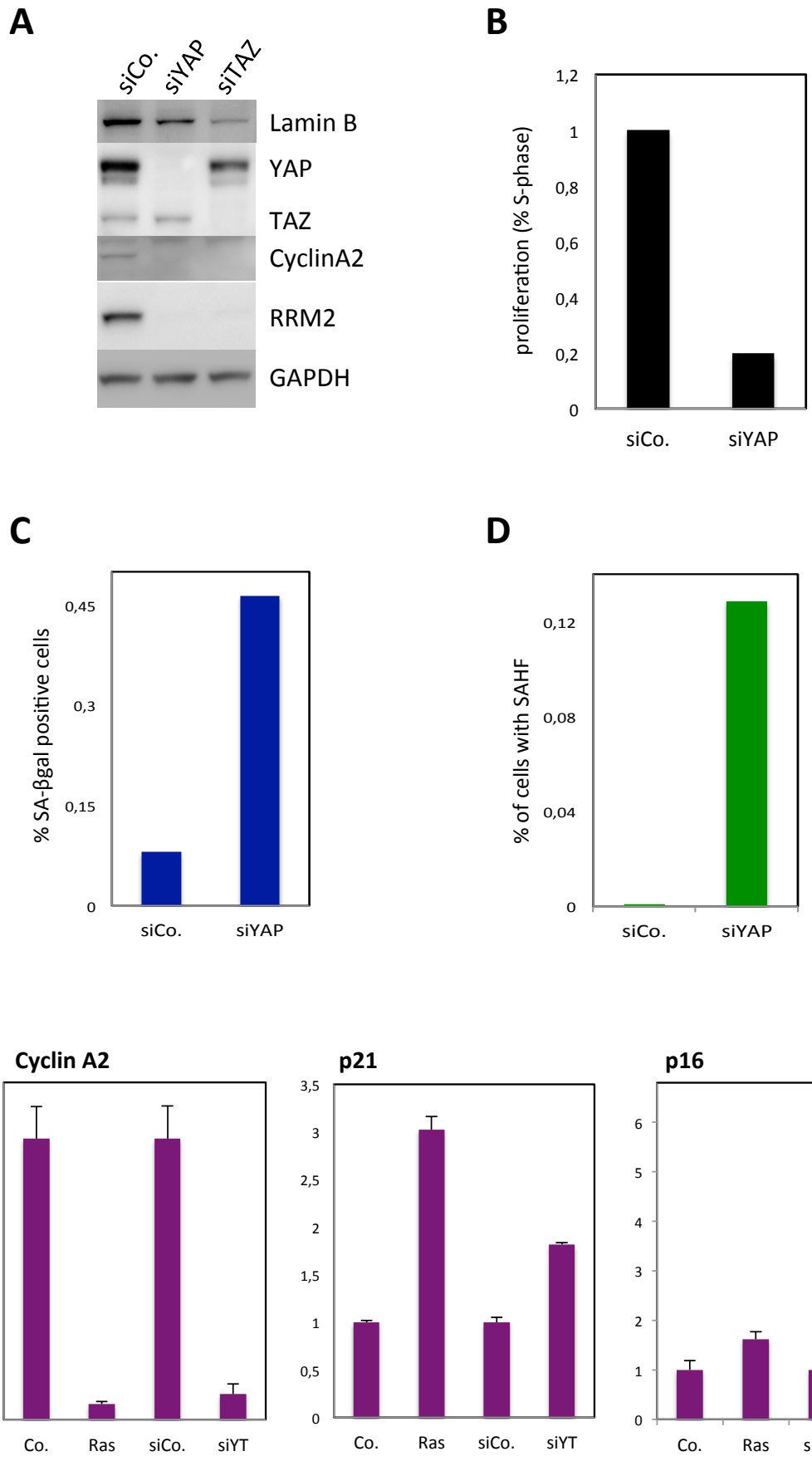
A
siCo.
siYAP
siTAZ
Lamin B
YAP
TAZ
CyclinA2
RRM2
GAPDH
B
proliferation (% S-phase)
1,2
1
0,8
0,6
0,4
0,2
0
siCo.
siYAP
C
% SA-βgal positive cells
0,45
0,3
0,15
0
siCo.
siYAP
D
% of cells with SAHF
0,12
0,08
0,04
0
siCo.
siYAP
E
Cyclin A2
p21
p16
mRNA expression
1,2
0,8
0,4
0
3,5
3
2,5
2
1,5
1
0,5
0
6
5
4
3
2
1
0
Co.
Ras
siCo.
siYT

FIGURE 18

Reference

1. Enzo, E. *et al.* Aerobic glycolysis tunes YAP/TAZ transcriptional activity. *EMBO J.* **34,** 1349–1370 (2015).

2. Santinon, G., Enzo, E. & Dupont, S. The sweet side of YAP/TAZ. *Cell Cycle* **14,** 2543–2544 (2015).

3. Santinon, G., Pocaterra, A. & Dupont, S. Control of YAP/TAZ Activity by Metabolic and Nutrient-Sensing Pathways. *Trends Cell Biol.* (2015). doi:10.1016/j.tcb.2015.11.004

4. Lunt, S. Y. & Vander Heiden, M. G. Aerobic Glycolysis: Meeting the Metabolic Requirements of Cell Proliferation. *Annu. Rev. Cell Dev. Biol.* **27,** 441–464 (2011).

5. Mor, I., Cheung, E. C. & Vousden, K. H. Control of Glycolysis through Regulation of PFK1: Old Friends and Recent Additions. *Cold Spring Harb. Symp. Quant. Biol.* **76,** 211–216 (2011).

6. Ochocki, J. D. & Simon, M. C. Nutrient-sensing pathways and metabolic regulation in stem cells. *J. Cell Biol.* **203,** 23–33 (2013).

7. Dang, C. V. Links between metabolism and cancer. *Genes Dev.* **26,** 877–890 (2012).

8. Yalcin, A., Telang, S., Clem, B. & Chesney, J. Regulation of glucose metabolism by 6-phosphofructo-2-kinase/fructose-2,6-bisphosphatases in cancer. *Exp. Mol. Pathol.* **86,** 174–179 (2009).

9. Efeyan, A., Comb, W. C. & Sabatini, D. M. Nutrient-sensing mechanisms and pathways. *Nature* **517,** 302–310 (2015).

10. O'Shea, J. M. & Ayer, D. E. Coordination of Nutrient Availability and Utilization by MAX- and MLX-Centered Transcription Networks. *Cold Spring Harb. Perspect. Med.* **3,** a014258–a014258 (2013).

11. Havula, E. & Hietakangas, V. Glucose sensing by ChREBP/MondoA–Mlx transcription factors. *Semin. Cell Dev. Biol.* **23,** 640–647 (2012).

12. Laplante, M. & Sabatini, D. M. mTOR Signaling in Growth Control and Disease. *Cell* **149,** 274–293 (2012).

13. Hanahan, D. & Weinberg, R. A. Hallmarks of Cancer: The Next Generation. *Cell* **144,** 646–674 (2011).

14. Otto Warburg. On the Origin of Carcer Cells. **123,** 309–314 (1956).

15. Kroemer, G. & Pouyssegur, J. Tumor Cell Metabolism: Cancer's Achilles'

Heel. *Cancer Cell* **13,** 472–482 (2008).

16. Ito, K. & Suda, T. Metabolic requirements for the maintenance of self-renewing stem cells. *Nat. Rev. Mol. Cell Biol.* **15,** 243–256 (2014).

17. Marroquin, L. D., Hynes, J., Dykens, J. A., Jamieson, J. D. & Will, Y. Circumventing the Crabtree Effect: Replacing Media Glucose with Galactose Increases Susceptibility of HepG2 Cells to Mitochondrial Toxicants. *Toxicol. Sci.* **97,** 539–547 (2007).

18. Hirschhaeuser, F., Sattler, U. G. A. & Mueller-Klieser, W. Lactate: A Metabolic Key Player in Cancer. *Cancer Res.* **71,** 6921–6925 (2011).

19. Wellen, K. E. & Thompson, C. B. A two-way street: reciprocal regulation of metabolism and signalling. *Nat. Rev. Mol. Cell Biol.* **13,** 270–276 (2012).

20. Gordan, J. D., Thompson, C. B. & Simon, M. C. HIF and c-Myc: Sibling Rivals for Control of Cancer Cell Metabolism and Proliferation. *Cancer Cell* **12,** 108–113 (2007).

21. Masson, N. & Ratcliffe, P. J. Hypoxia signaling pathways in cancer metabolism: the importance of co-selecting interconnected physiological pathways. *Cancer Metab* **2,** (2014).

22. Bensaad, K. *et al.* TIGAR, a p53-Inducible Regulator of Glycolysis and Apoptosis. *Cell* **126,** 107–120 (2006).

23. Gottlieb, E. & Tomlinson, I. P. M. Mitochondrial tumour suppressors: a genetic and biochemical update. *Nat. Rev. Cancer* **5,** 857–866 (2005).

24. King, A., Selak, M. A. & Gottlieb, E. Succinate dehydrogenase and fumarate hydratase: linking mitochondrial dysfunction and cancer. *Oncogene* **25,** 4675–4682 (2006).

25. Atsumi, T. *et al.* High expression of inducible 6-phosphofructo-2-kinase/fructose-2, 6-bisphosphatase (iPFK-2; PFKFB3) in human cancers. *Cancer Res.* **62,** 5881–5887 (2002).

26. Onodera, Y., Nam, J.-M. & Bissell, M. J. Increased sugar uptake promotes oncogenesis via EPAC/RAP1 and O-GlcNAc pathways. *J. Clin. Invest.* **124,** 367–384 (2014).

27. Zhao, B. *et al.* TEAD mediates YAP-dependent gene induction and growth control. *Genes Dev.* **22,** 1962–1971 (2008).

28. Pan, D. The Hippo Signaling Pathway in Development and Cancer. *Dev. Cell* **19,** 491–505 (2010).

29. Piccolo, S., Dupont, S. & Cordenonsi, M. The Biology of YAP/TAZ: Hippo Signaling and Beyond. *Physiol. Rev.* **94,** 1287–1312 (2014).

30. Zhao, B., Tumaneng, K. & Guan, K.-L. The Hippo pathway in organ size control, tissue regeneration and stem cell self-renewal. *Nat. Cell Biol.* **13,** 877–883 (2011).

31. Dupont, S. *et al.* Role of YAP/TAZ in mechanotransduction. *Nature* **474,** 179–183 (2011).

32. Aragona, M. *et al.* A Mechanical Checkpoint Controls Multicellular Growth through YAP/TAZ Regulation by Actin-Processing Factors. *Cell* **154,** 1047–1059 (2013).

33. Halder, G., Dupont, S. & Piccolo, S. Transduction of mechanical and cytoskeletal cues by YAP and TAZ. *Nat. Rev. Mol. Cell Biol.* **13,** 591–600 (2012).

34. Sorrentino, G. *et al.* Metabolic control of YAP and TAZ by the mevalonate pathway. *Nat. Cell Biol.* **16,** 357–366 (2014).

35. Camargo, F. D. *et al.* YAP1 Increases Organ Size and Expands Undifferentiated Progenitor Cells. *Curr. Biol.* **17,** 2054–2060 (2007).

36. Yang, Z. *et al.* Knockdown of YAP1 inhibits the proliferation of osteosarcoma cells inï¿½vitro and inï¿½vivo. *Oncol. Rep.* (2014). doi:10.3892/or.2014.3305

37. Chan, S. W. *et al.* A Role for TAZ in Migration, Invasion, and Tumorigenesis of Breast Cancer Cells. *Cancer Res.* **68,** 2592–2598 (2008).

38. Cai, J. *et al.* The Hippo signaling pathway restricts the oncogenic potential of an intestinal regeneration program. *Genes Dev.* **24,** 2383–2388 (2010).

39. Schlegelmilch, K. *et al.* Yap1 Acts Downstream of α-Catenin to Control Epidermal Proliferation. *Cell* **144,** 782–795 (2011).

40. Kapoor, A. *et al.* Yap1 Activation Enables Bypass of Oncogenic Kras Addiction in Pancreatic Cancer. *Cell* **158,** 185–197 (2014).

41. Liu-Chittenden, Y. *et al.* Genetic and pharmacological disruption of the TEAD-YAP complex suppresses the oncogenic activity of YAP. *Genes Dev.* **26,** 1300–1305 (2012).

42. Jiao, S. *et al.* A Peptide Mimicking VGLL4 Function Acts as a YAP Antagonist Therapy against Gastric Cancer. *Cancer Cell* **25,** 166–180 (2014).

43. Chaneton, B. & Gottlieb, E. Rocking cell metabolism: revised functions of the key glycolytic regulator PKM2 in cancer. *Trends Biochem. Sci.* **37,** 309–316 (2012).

44. Tennant, D. A., Durán, R. V. & Gottlieb, E. Targeting metabolic transformation for cancer therapy. *Nat. Rev. Cancer* **10,** 267–277 (2010).

45. Cordenonsi, M. *et al.* The Hippo Transducer TAZ Confers Cancer Stem

Cell-Related Traits on Breast Cancer Cells. *Cell* **147,** 759–772 (2011).

46. Ota, M. & Sasaki, H. Mammalian Tead proteins regulate cell proliferation and contact inhibition as transcriptional mediators of Hippo signaling. *Development* **135,** 4059–4069 (2008).

47. Zhang, H. *et al.* TEAD Transcription Factors Mediate the Function of TAZ in Cell Growth and Epithelial-Mesenchymal Transition. *J. Biol. Chem.* **284,** 13355–13362 (2009).

48. Kurtoglu, M. *et al.* Under normoxia, 2-deoxy-D-glucose elicits cell death in select tumor types not by inhibition of glycolysis but by interfering with N-linked glycosylation. *Mol. Cancer Ther.* **6,** 3049–3058 (2007).

49. Liu, C., Huang, W. & Lei, Q. Regulation and function of the TAZ transcription co-activator. *Int. J. Biochem. Mol. Biol.* **2,** 247 (2011).

50. Chen, H.-Z., Tsai, S.-Y. & Leone, G. Emerging roles of E2Fs in cancer: an exit from cell cycle control. *Nat. Rev. Cancer* **9,** 785–797 (2009).

51. Dick, F. A. & Rubin, S. M. Molecular mechanisms underlying RB protein function. *Nat. Rev. Mol. Cell Biol.* **14,** 297–306 (2013).

52. Wang, Z. *et al.* Interplay of mevalonate and Hippo pathways regulates RHAMM transcription via YAP to modulate breast cancer cell motility. *Proc. Natl. Acad. Sci.* **111,** E89–E98 (2014).

53. Zanconato, F. *et al.* Genome-wide association between YAP/TAZ/TEAD and AP-1 at enhancers drives oncogenic growth. *Nat. Cell Biol.* **17,** 1218–1227 (2015).

54. Wellen, K. E. *et al.* The hexosamine biosynthetic pathway couples growth factor-induced glutamine uptake to glucose metabolism. *Genes Dev.* **24,** 2784–2799 (2010).

55. Ostrowski, A. & van Aalten, D. M. F. Chemical tools to probe cellular *O* -GlcNAc signalling. *Biochem. J.* **456,** 1–12 (2013).

56. Chang, C.-H. *et al.* Posttranscriptional Control of T Cell Effector Function by Aerobic Glycolysis. *Cell* **153,** 1239–1251 (2013).

57. Bustamante, E. & Pedersen, P. L. High aerobic glycolysis of rat hepatoma cells in culture: role of mitochondrial hexokinase. *Proc. Natl. Acad. Sci.* **74,** 3735–3739 (1977).

58. Rossignol, R. *et al.* Energy substrate modulates mitochondrial structure and oxidative capacity in cancer cells. *Cancer Res.* **64,** 985–993 (2004).

59. Yang, Y. *et al.* Metabolic Reprogramming for Producing Energy and Reducing Power in Fumarate Hydratase Null Cells from Hereditary Leiomyomatosis Renal Cell Carcinoma. *PLoS ONE* **8,** e72179 (2013).

60. Sudarshan, S. *et al.* Fumarate Hydratase Deficiency in Renal Cancer Induces Glycolytic Addiction and Hypoxia-Inducible Transcription Factor 1 Stabilization by Glucose-Dependent Generation of Reactive Oxygen Species. *Mol. Cell. Biol.* **29,** 4080–4090 (2009).

61. Halder, G. & Johnson, R. L. Hippo signaling: growth control and beyond. *Development* **138,** 9–22 (2011).

62. Hardie, D. G., Ross, F. A. & Hawley, S. A. AMPK: a nutrient and energy sensor that maintains energy homeostasis. *Nat. Rev. Mol. Cell Biol.* **13,** 251–262 (2012).

63. Pike, K. G. *et al.* Optimization of potent and selective dual mTORC1 and mTORC2 inhibitors: The discovery of AZD8055 and AZD2014. *Bioorg. Med. Chem. Lett.* **23,** 1212–1216 (2013).

64. Zhang, Y.-J., Duan, Y. & Zheng, X. F. S. Targeting the mTOR kinase domain: the second generation of mTOR inhibitors. *Drug Discov. Today* **16,** 325–331 (2011).

65. Ribeiro, P. S. *et al.* Combined Functional Genomic and Proteomic Approaches Identify a PP2A Complex as a Negative Regulator of Hippo Signaling. *Mol. Cell* **39,** 521–534 (2010).

66. Yi, C. *et al.* A Tight Junction-Associated Merlin-Angiomotin Complex Mediates Merlin's Regulation of Mitogenic Signaling and Tumor Suppressive Functions. *Cancer Cell* **19,** 527–540 (2011).

67. Varelas, X. *et al.* The Hippo Pathway Regulates Wnt/β-Catenin Signaling. *Dev. Cell* **18,** 579–591 (2010).

68. Luo, W. & Semenza, G. L. Emerging roles of PKM2 in cell metabolism and cancer progression. *Trends Endocrinol. Metab.* **23,** 560–566 (2012).

69. Yi, W. *et al.* Phosphofructokinase 1 Glycosylation Regulates Cell Growth and Metabolism. *Science* **337,** 975–980 (2012).

70. Yin, F. *et al.* Spatial Organization of Hippo Signaling at the Plasma Membrane Mediated by the Tumor Suppressor Merlin/NF2. *Cell* **154,** 1342–1355 (2013).

71. Lai, D., Ho, K. C., Hao, Y. & Yang, X. Taxol Resistance in Breast Cancer Cells Is Mediated by the Hippo Pathway Component TAZ and Its Downstream Transcriptional Targets Cyr61 and CTGF. *Cancer Res.* **71,** 2728–2738 (2011).

72. Jarvius, M. *et al.* In situ detection of phosphorylated platelet-derived growth factor receptor β using a generalized proximity ligation method. *Mol. Cell. Proteomics* **6,** 1500–1509 (2007).

73. Banaszak, K. *et al.* The Crystal Structures of Eukaryotic Phosphofructokinases from Baker's Yeast and Rabbit Skeletal Muscle. *J. Mol.*

Biol. **407,** 284–297 (2011).

74. Ferreras, C., Hernandez, E. D., Martinez-Costa, O. H. & Aragon, J. J. Subunit Interactions and Composition of the Fructose 6-Phosphate Catalytic Site and the Fructose 2,6-Bisphosphate Allosteric Site of Mammalian Phosphofructokinase. *J. Biol. Chem.* **284,** 9124–9131 (2009).

75. De Bock, K. *et al.* Role of PFKFB3-Driven Glycolysis in Vessel Sprouting. *Cell* **154,** 651–663 (2013).

76. Herrero-Mendez, A. *et al.* The bioenergetic and antioxidant status of neurons is controlled by continuous degradation of a key glycolytic enzyme by APC/C–Cdh1. *Nat. Cell Biol.* **11,** 747–752 (2009).

77. Azzolin, L. *et al.* Role of TAZ as Mediator of Wnt Signaling. *Cell* **151,** 1443–1456 (2012).

78. Li, Z. *et al.* Structural insights into the YAP and TEAD complex. *Genes Dev.* **24,** 235–240 (2010).

79. Zhao, B. *et al.* Cell detachment activates the Hippo pathway via cytoskeleton reorganization to induce anoikis. *Genes Dev.* **26,** 54–68 (2012).

80. Zhao, B. *et al.* Inactivation of YAP oncoprotein by the Hippo pathway is involved in cell contact inhibition and tissue growth control. *Genes Dev.* **21,** 2747–2761 (2007).

81. Menendez, J., Perez-Garijo, A., Calleja, M. & Morata, G. A tumor-suppressing mechanism in Drosophila involving cell competition and the Hippo pathway. *Proc. Natl. Acad. Sci.* **107,** 14651–14656 (2010).

82. Khan, S. J. *et al.* Epithelial neoplasia in Drosophila entails switch to primitive cell states. *Proc. Natl. Acad. Sci.* **110,** E2163–E2172 (2013).

83. Grzeschik, N. A., Parsons, L. M., Allott, M. L., Harvey, K. F. & Richardson, H. E. Lgl, aPKC, and Crumbs Regulate the Salvador/Warts/Hippo Pathway through Two Distinct Mechanisms. *Curr. Biol.* **20,** 573–581 (2010).

84. Harvey, K. F., Zhang, X. & Thomas, D. M. The Hippo pathway and human cancer. *Nat. Rev. Cancer* **13,** 246–257 (2013).

85. Huang, J., Wu, S., Barrera, J., Matthews, K. & Pan, D. The Hippo Signaling Pathway Coordinately Regulates Cell Proliferation and Apoptosis by Inactivating Yorkie, the Drosophila Homolog of YAP. *Cell* **122,** 421–434 (2005).

86. Wu, S., Liu, Y., Zheng, Y., Dong, J. & Pan, D. The TEAD/TEF Family Protein Scalloped Mediates Transcriptional Output of the Hippo Growth-Regulatory Pathway. *Dev. Cell* **14,** 388–398 (2008).

87. Ziosi, M. *et al.* dMyc Functions Downstream of Yorkie to Promote the Supercompetitive Behavior of Hippo Pathway Mutant Cells. *PLoS Genet.* **6,**

e1001140 (2010).

88. Neto-Silva, R. M., de Beco, S. & Johnston, L. A. Evidence for a Growth-Stabilizing Regulatory Feedback Mechanism between Myc and Yorkie, the Drosophila Homolog of Yap. *Dev. Cell* **19,** 507–520 (2010).

89. Chen, J. *et al.* A restricted cell population propagates glioblastoma growth after chemotherapy. *Nature* **488,** 522–526 (2012).

90. Dong, C. *et al.* Loss of FBP1 by Snail-Mediated Repression Provides Metabolic Advantages in Basal-like Breast Cancer. *Cancer Cell* **23,** 316–331 (2013).

91. Feng, W. *et al.* Targeting Unique Metabolic Properties of Breast Tumor Initiating Cells: Metabolic Targeting of Tumor Initiating Cells. *STEM CELLS* **32,** 1734–1745 (2014).

92. Montagner, M. *et al.* SHARP1 suppresses breast cancer metastasis by promoting degradation of hypoxia-inducible factors. *Nature* **487,** 380–384 (2012).

93. Pece, S. *et al.* Biological and Molecular Heterogeneity of Breast Cancers Correlates with Their Cancer Stem Cell Content. *Cell* **140,** 62–73 (2010).

94. Liu, R. *et al.* The prognostic role of a gene signature from tumorigenic breast-cancer cells. *N. Engl. J. Med.* **356,** 217–226 (2007).

95. Clem, B. *et al.* Small-molecule inhibition of 6-phosphofructo-2-kinase activity suppresses glycolytic flux and tumor growth. *Mol. Cancer Ther.* **7,** 110–120 (2008).

96. DeRan, M. *et al.* Energy Stress Regulates Hippo-YAP Signaling Involving AMPK-Mediated Regulation of Angiomotin-like 1 Protein. *Cell Rep.* **9,** 495–503 (2014).

97. Wang, W. *et al.* AMPK modulates Hippo pathway activity to regulate energy homeostasis. *Nat. Cell Biol.* **17,** 490–499 (2015).

98. Mo, J.-S. *et al.* Cellular energy stress induces AMPK-mediated regulation of YAP and the Hippo pathway. *Nat. Cell Biol.* **17,** 500–510 (2015).

99. Mah, L. Y. & Ryan, K. M. Autophagy and Cancer. *Cold Spring Harb. Perspect. Biol.* **4,** a008821–a008821 (2012).

100. Qiu, B. & Simon, M. C. Oncogenes strike a balance between cellular growth and homeostasis. *Semin. Cell Dev. Biol.* **43,** 3–10 (2015).

101. Avivar-Valderas, A. *et al.* Regulation of autophagy during ECM detachment is linked to a selective inhibition of mTORC1 by PERK. *Oncogene* **32,** 4932–4940 (2013).

102. Hindupur, S. K. *et al.* Identification of a novel AMPK-PEA15 axis in the

anoikis-resistant growth of mammary cells. *Breast Cancer Res. BCR* **16,** 420–420 (2014).

103. Ng, T. L. *et al.* The AMPK stress response pathway mediates anoikis resistance through inhibition of mTOR and suppression of protein synthesis. *Cell Death Differ.* **19,** 501–510 (2012).

104. Koontz, L. M. *et al.* The Hippo Effector Yorkie Controls Normal Tissue Growth by Antagonizing Scalloped-Mediated Default Repression. *Dev. Cell* **25,** 388–401 (2013).

105. Pontarin, G., Ferraro, P., Reichard, P. & Bianchi, V. Out of S-phase: Shift of subunits for ribonucleotide reduction. *Cell Cycle* **11,** 4099–4100 (2012).

106. Rampazzo, C. *et al.* Regulation by degradation, a cellular defense against deoxyribonucleotide pool imbalances. *Mutat. Res. Toxicol. Environ. Mutagen.* **703,** 2–10 (2010).

107. Aye, Y., Li, M., Long, M. J. C. & Weiss, R. S. Ribonucleotide reductase and cancer: biological mechanisms and targeted therapies. *Oncogene.* **34,** 2011-2021 (2015).

108. Aird, K. M. & Zhang, R. Nucleotide metabolism, oncogene-induced senescence and cancer. *Cancer Lett.* **356,** 204–210 (2015).

109. L. Hayflick & P.S. Moorhead. The serial cultivation of human diploid cell strains. *Exp. Cell Res.* **25,** 585–621 (1961).

110. Campisi, J. & d'Adda di Fagagna, F. Cellular senescence: when bad things happen to good cells. *Nat. Rev. Mol. Cell Biol.* **8,** 729–740 (2007).

111. Rubin, H. The disparity between human cell senescence in vitro and lifelong replication in vivo. *Nat. Biotechnol.* **20,** 675–681 (2002).

112. DiMauro, T. & David, G. Ras-induced senescence and its physiological relevance in cancer. *Curr. Cancer Drug Targets* **10,** 869 (2010).

113. Kim, W. Y. & Sharpless, N. E. The Regulation of INK4/ARF in Cancer and Aging. *Cell* **127,** 265–275 (2006).

114. Mason, D. X., Jackson, T. J. & Lin, A. W. Molecular signature of oncogenic ras-induced senescence. *Oncogene* (2004). doi:10.1038/sj.onc.1208172

115. Dimri, G. P. *et al.* A biomarker that identifies senescent human cells in culture and in aging skin in vivo. *Proc. Natl. Acad. Sci.* **92,** 9363–9367 (1995).

116. Di Mitri, D. & Alimonti, A. Non-Cell-Autonomous Regulation of Cellular Senescence in Cancer. *Trends Cell Biol.* (2015). doi:10.1016/j.tcb.2015.10.005

117. Chang, Z. *et al.* Cooperativity of Oncogenic K-Ras and Downregulated p16/INK4A in Human Pancreatic Tumorigenesis. *PLoS ONE* **9,** e101452 (2014).

118. Vredeveld, L. C. W. *et al.* Abrogation of BRAFV600E-induced senescence by PI3K pathway activation contributes to melanomagenesis. *Genes Dev.* **26,** 1055–1069 (2012).

119. Gil, J. & Peters, G. Regulation of the INK4b–ARF–INK4a tumour suppressor locus: all for one or one for all. *Nat. Rev. Mol. Cell Biol.* **7,** 667–677 (2006).

120. Di Micco, R. *et al.* Oncogene-induced senescence is a DNA damage response triggered by DNA hyper-replication. *Nature* **444,** 638–642 (2006).

121. Aird, K. M. *et al.* Suppression of Nucleotide Metabolism Underlies the Establishment and Maintenance of Oncogene-Induced Senescence. *Cell Rep.* **3,** 1252–1265 (2013).

122. Mannava, S. *et al.* Depletion of Deoxyribonucleotide Pools Is an Endogenous Source of DNA Damage in Cells Undergoing Oncogene-Induced Senescence. *Am. J. Pathol.* **182,** 142–151 (2013).

123. Calvo, F. *et al.* Mechanotransduction and YAP-dependent matrix remodelling is required for the generation and maintenance of cancer-associated fibroblasts. *Nat. Cell Biol.* **15,** 637–646 (2013).

124. Mori, M. *et al.* Hippo Signaling Regulates Microprocessor and Links Cell-Density-Dependent miRNA Biogenesis to Cancer. *Cell* **156,** 893–906 (2014).

125. Li, W. *et al.* Merlin/NF2 Loss-Driven Tumorigenesis Linked to CRL4DCAF1-Mediated Inhibition of the Hippo Pathway Kinases Lats1 and 2 in the Nucleus. *Cancer Cell* **26,** 48–60 (2014).

126. Azzolin, L. *et al.* YAP/TAZ Incorporation in the β-Catenin Destruction Complex Orchestrates the Wnt Response. *Cell* **158,** 157–170 (2014).

127. Shimi, T. *et al.* The role of nuclear lamin B1 in cell proliferation and senescence. *Genes Dev.* **25,** 2579–2593 (2011).

128. Aird, K. M., Li, H., Xin, F., Konstantinopoulos, P. A. & Zhang, R. Identification of ribonucleotide reductase M2 as a potential target for pro-senescence therapy in epithelial ovarian cancer. *Cell Cycle* **13,** 199–207 (2014).

129. Ehmer, U. *et al.* Organ Size Control Is Dominant over Rb Family Inactivation to Restrict Proliferation In Vivo. *Cell Rep.* **8,** 371–381 (2014).

130. Frangini, M. *et al.* Synthesis of Mitochondrial DNA Precursors during Myogenesis, an Analysis in Purified C2C12 Myotubes. *J. Biol. Chem.* **288,** 5624–5635 (2013).

131. Ferraro, P., Franzolin, E., Pontarin, G., Reichard, P. & Bianchi, V. Quantitation of cellular deoxynucleoside triphosphates. *Nucleic Acids Res.* **38,** e85–e85 (2010).

132. Rustighi, A. *et al.* Prolyl-isomerase Pin1 controls normal and cancer stem cells of the breast. *EMBO Mol. Med.* **6,** 99–119 (2014).

133. Adorno, M. *et al.* A Mutant-p53/Smad Complex Opposes p63 to Empower TGFβ-Induced Metastasis. *Cell* **137,** 87–98 (2009).

134. Sola-Penna, M., Da Silva, D., Coelho, W. S., Marinho-Carvalho, M. M. & Zancan, P. Regulation of mammalian muscle type 6-phosphofructo-1-kinase and its implication for the control of the metabolism. *IUBMB Life* **62,** 791–796 (2010).

135. Lee, T. & Luo, L. Mosaic analysis with a repressible cell marker (MARCM) for Drosophila neural development. *Trends Neurosci.* **24,** 251–254 (2001).